Organic & Biomolecular Chemistry RSCPublishing

COMMUNICATION

Electronic Supporting Information for:

Two step access to bis-*meso*-perfluoroalkyl-corroles, precursors of *meso*-perfluoroacyl-ABC-corroles

Paul-Gabriel Julliard,[a] Simon Pascal,[a,b] Olivier Siri,[a] Michel Giorgi,[c] Diego Cortés-Arriagada,[d] Luis Sanhueza*[e,f] and Gabriel Canard*[a]

[a] *Aix Marseille Univ, CNRS, CINaM, UMR 7325, 13288, Marseille, France. E-mails: gabriel.canard@univ-amu.fr.*

[b] *Present adress : Laboratoire CEISAM, CNRS UMR 6230, Université de Nantes, 2, rue de la Houssinière, 44322 Nantes, France.*

[c] *Aix Marseille Univ, CNRS, Centrale Marseille, FSCM, Spectropole, Marseille, France.*

[d] *Instituto Universitario de Investigación y Desarrollo Tecnologico, Universidad Tecnológica Metropolitana, Ignacio Valdivieso 2409, San Joaquín, Santiago, Chile.*

[e] *Departamento de Ciencias Biológicas y Químicas, Facultad de Recursos Naturales, Universidad Católica de Temuco, Temuco, Chile.*

[f] *Núcleo de Investigación en Bioproductos y Materiales Avanzados (BioMA), Universidad Católica de Temuco, Av. Rudecindo Ortega 02950, Temuco, Chile.*

E-mail: luis.sanhueza@uct.cl.

Table S1: Optimization of experimental conditions leading to the bilane **6a**.

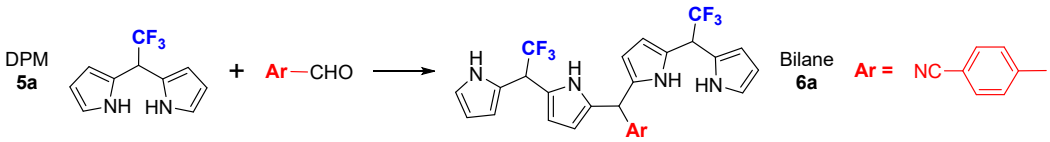

5a (mmol)	aldehyde (mmol)	acid (mmol)	solvents, reaction times, temperatures	Yields (%)
1	0.5	benzoic acid (0.5)	i) neat, 5 min, 120 °C; ii) DCM, 17 h, RT	23
1	0.5	benzoic acid (0.5)	neat, 5 min, 120 °C	3
1	0.5	benzoic acid (0.5)	i) neat, 5 min, 120 °C; ii) DCM, 1 h, RT	8
1	0.5	benzoic acid (0.5)	i) neat, 5 min, 140 °C; ii) DCM, 17 h, RT	Ø
1	0.5	propionic acid (0.5)	i) neat, 5 min, 120 °C; ii) DCM, 17 h, RT	7
2	0.5	benzoic acid (0.5)	i) neat, 5 min, 120 °C; ii) DCM, 17 h, RT	23
1	0.5	propionic acid (1)	i) neat, 5 min, 120 °C; ii) DCM, 6 h, RT	6
1	0.5	propionic acid (0.5)	neat, 24 h, 120 °C	Ø
1	0.5	propionic acid (2.5)	neat, 17 h, RT	30
1	0.75	propionic acid (2.5)	neat, 17 h, RT	11
1	0.5	propionic acid (5)	neat, 17 h, RT	20
1	0.5	propionic acid (7.5)	neat, 17 h, RT	23
15	0.5	propionic acid (2.5)	neat, 8 h, RT	29
1	0.5	acetic acid (2.5)	neat, 17 h, RT	22
1	0.75	acetic acid (2.5)	neat, 17 h, RT	10
1	0.5	MSA (0.5)	neat, 5 min, RT	25
1	0.5	TFA (0.5)	neat, 5 min, RT	27
10	5	TFA (0.5)	neat, 5 min, RT	26

a) **b)**

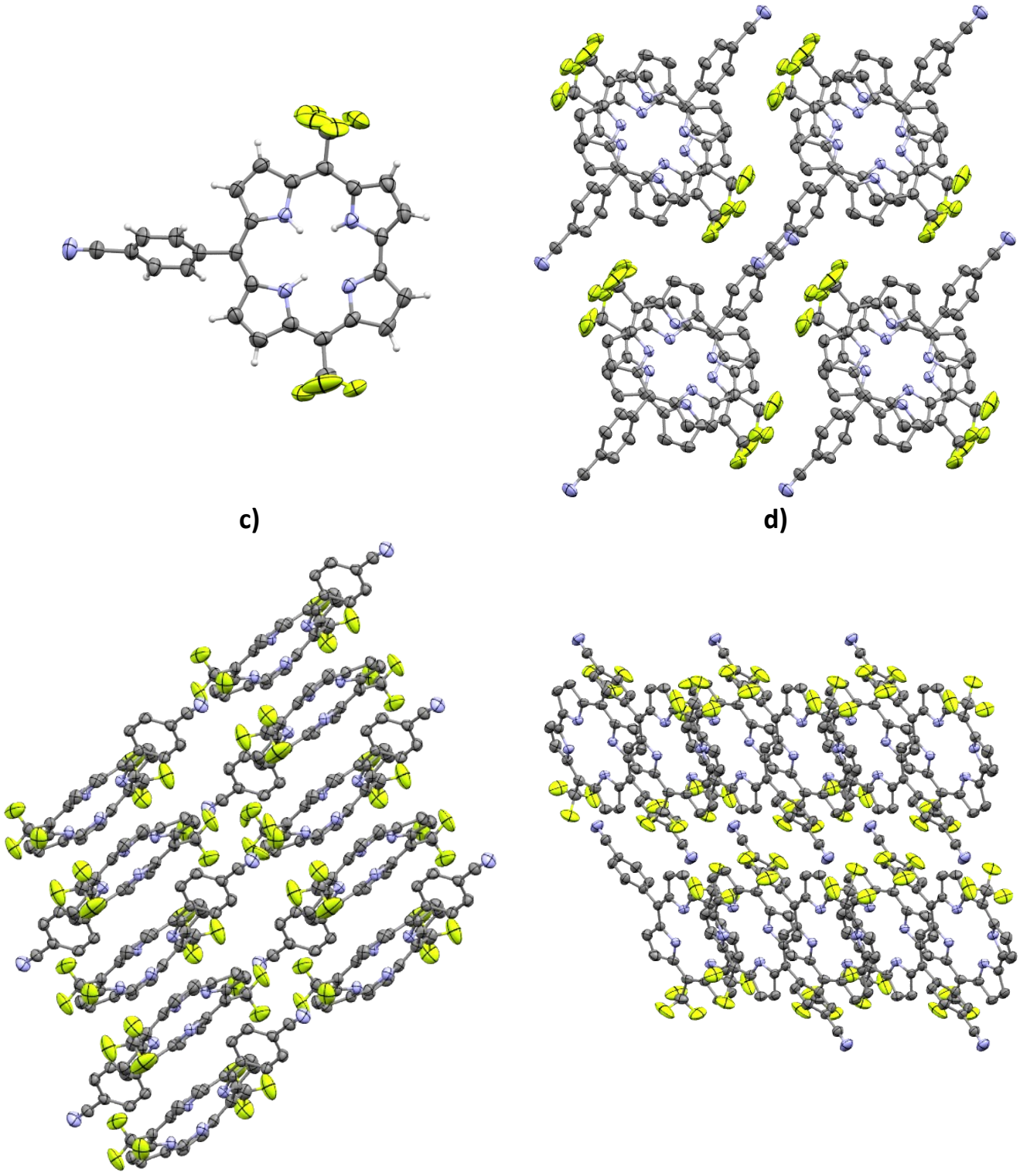

Figure S1: Views of the single crystal X-ray diffraction structures of corrole **7a**: a) side view. b) crystal packing along the a-axis. c) crystal packing along the b-axis. d) crystal packing along the c-axis.

.

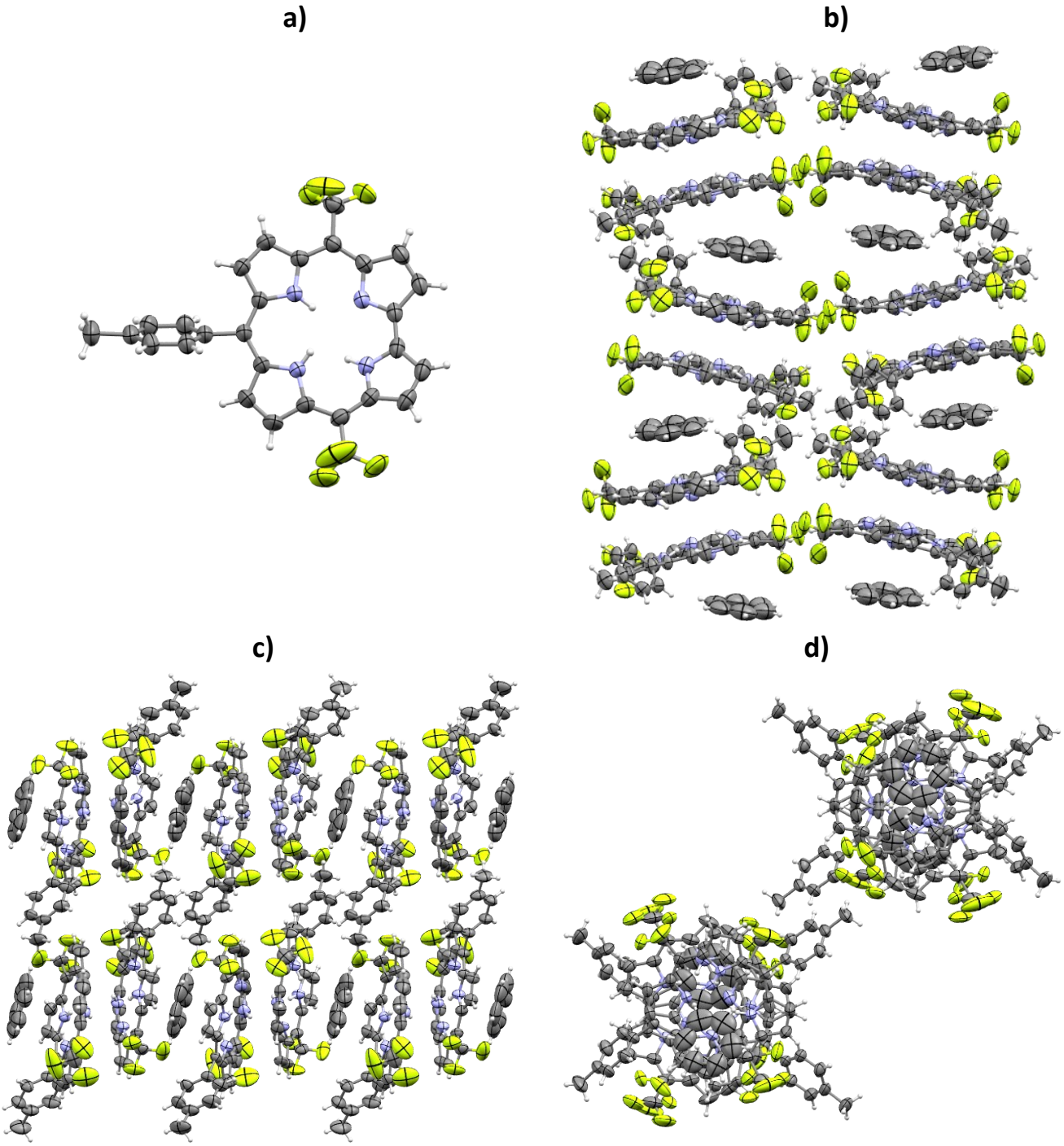

Figure S2: Views of the single crystal X-ray diffraction structures of corrole **7b**: a) side view. b) crystal packing along the a-axis. c) crystal packing along the b-axis. d) crystal packing along the c-axis.

.

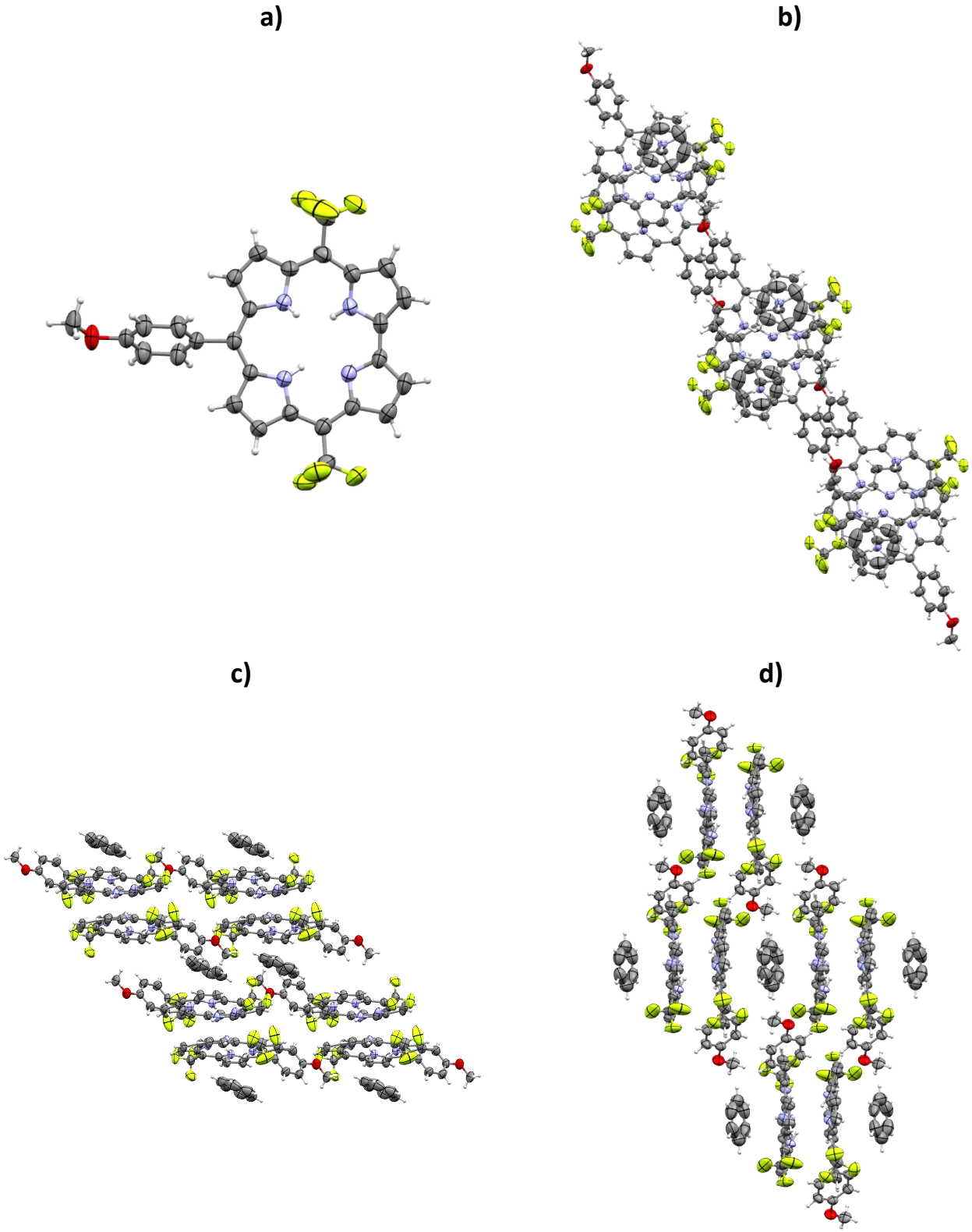

Figure S3: Views of the single crystal X-ray diffraction structures of corrole **7c** : a) side view. b) crystal packing along the a-axis. c) crystal packing along the b-axis. d) crystal packing along the c-axis.

.

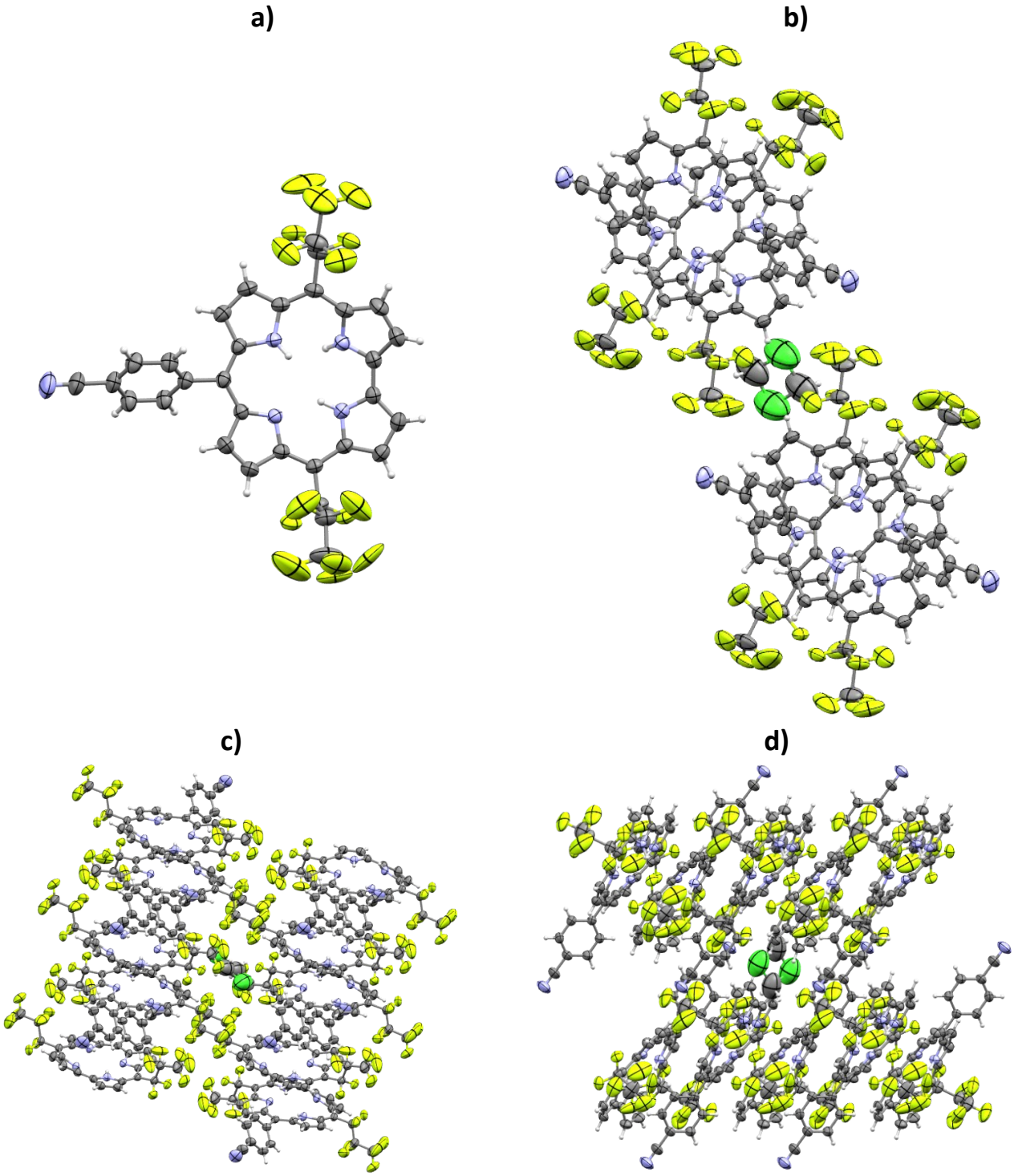

Figure S4: Views of the single crystal X-ray diffraction structures of corrole **7d**: a) side view. b) crystal packing along the a-axis. c) crystal packing along the b-axis. d) crystal packing along the c-axis.

.

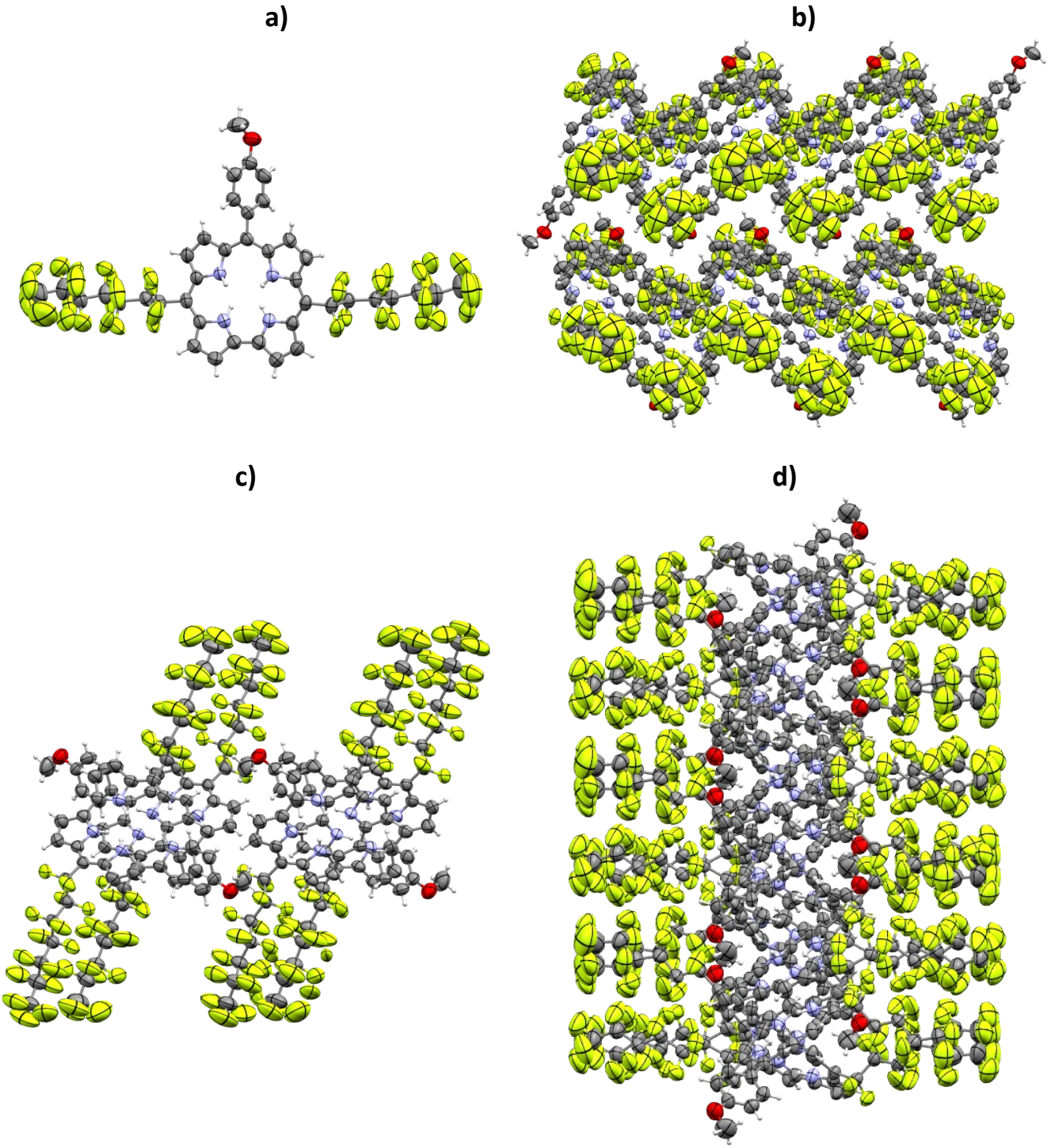

Figure S5: Views of the single crystal X-ray diffraction structures of corrole **7i**: a) side view. b) crystal packing along the a-axis. c) crystal packing along the b-axis. d) crystal packing along the c-axis.

.

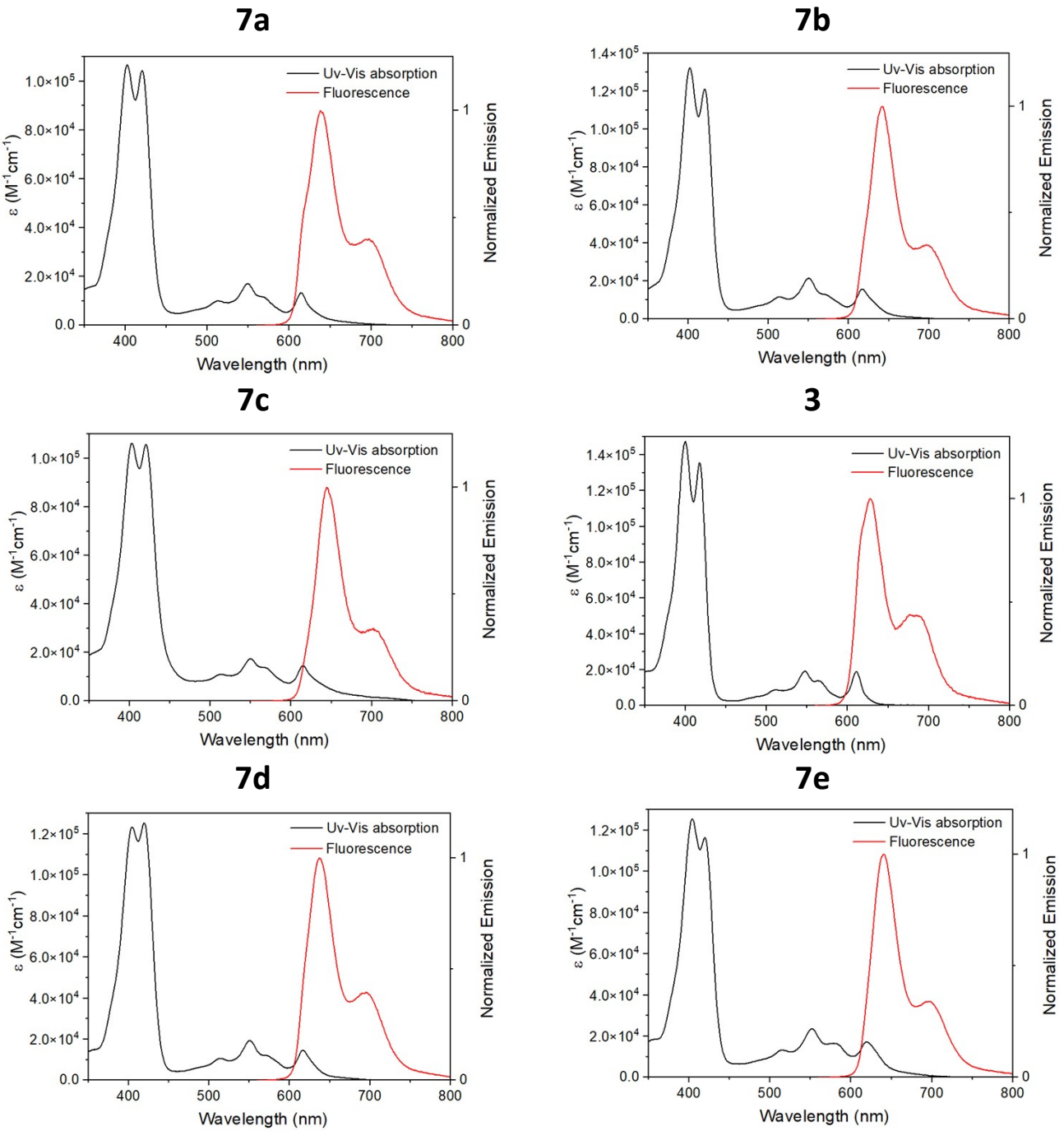

Figure S6: Absorption (black line) and normalized corrected emission (red line) spectra of corroles **3** and **7a-e** in aerated DCM solutions at room temperature (excitation at 550 nm).

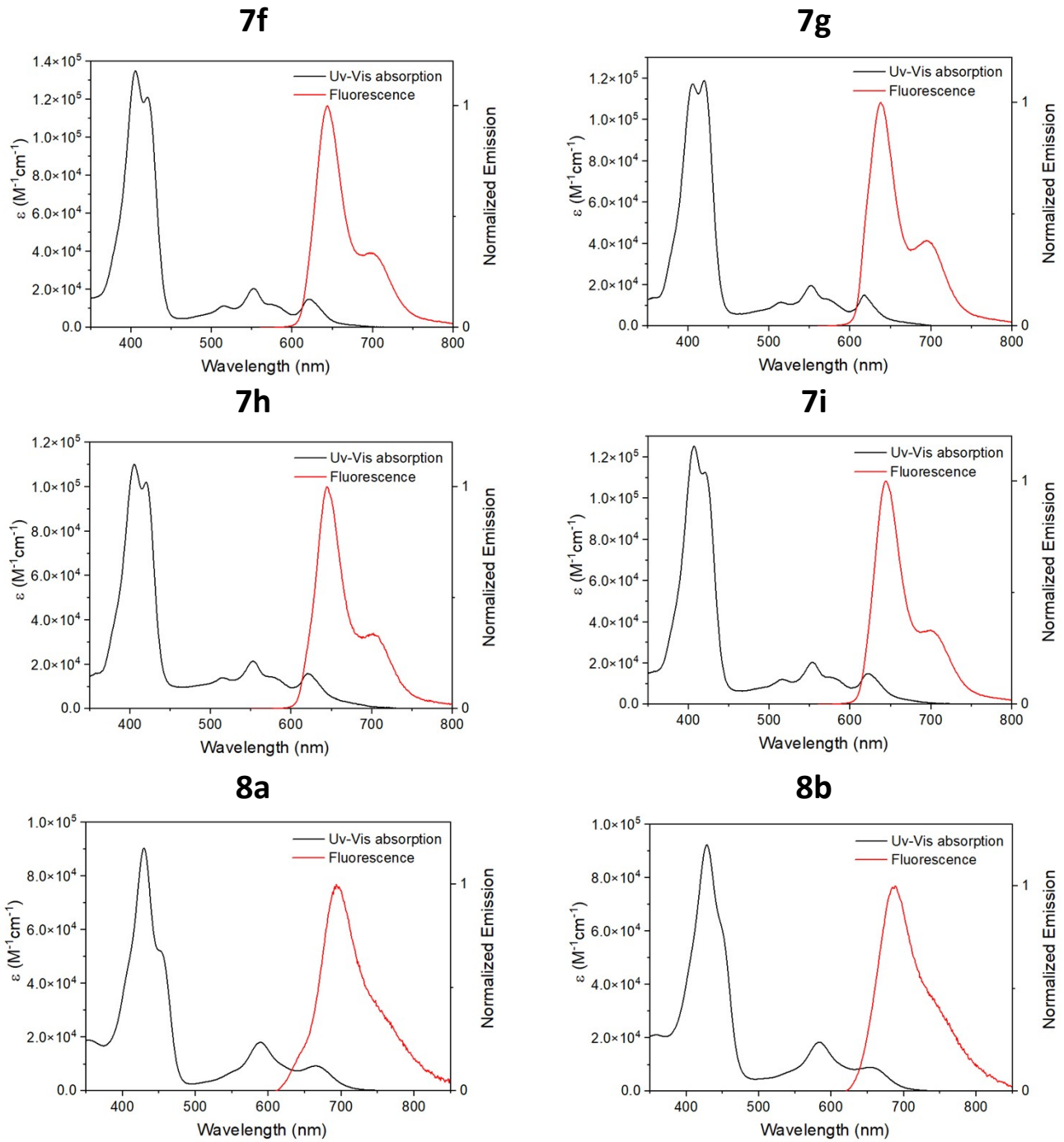

Figure S7: Absorption (black line) and normalized corrected emission (red line) spectra of corroles **7f-i** (excitation at 550 nm) and **8a-b** in aerated DCM solutions at room temperature (excitation at 590 nm).

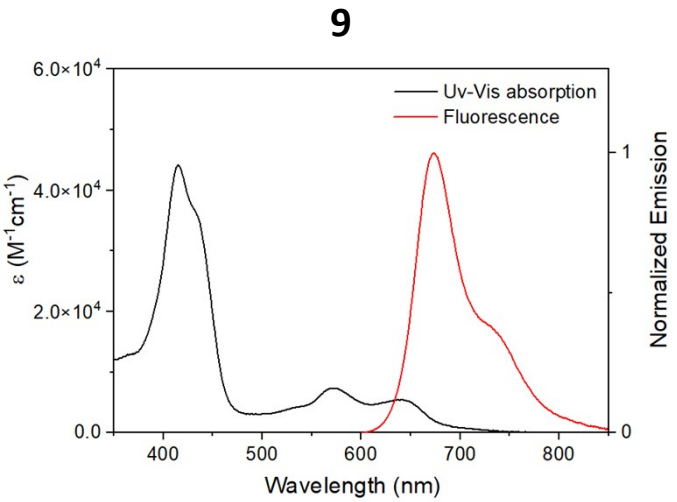

Figure S8: Absorption (black line) and normalized corrected emission (red line) spectra of corrole **9** in aerated methanol at room temperature (excitation at 585 nm).

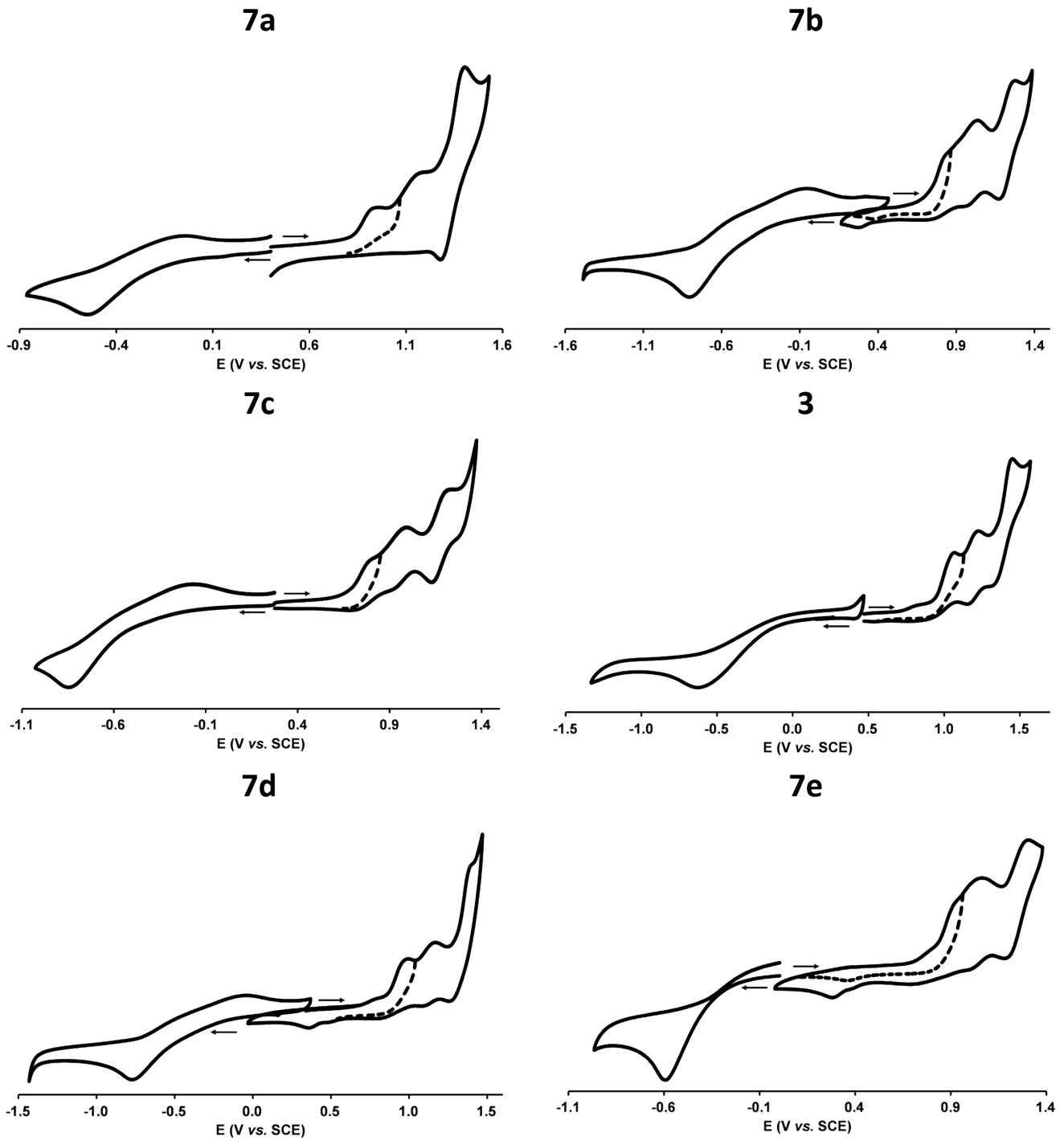

Figure S9: Cyclic voltammograms of corroles **3** and **7a-e** in DCM containing 0.1 M of $^{n}Bu_4NPF_6$ at room temperature (scan rate of 100 mV/s).

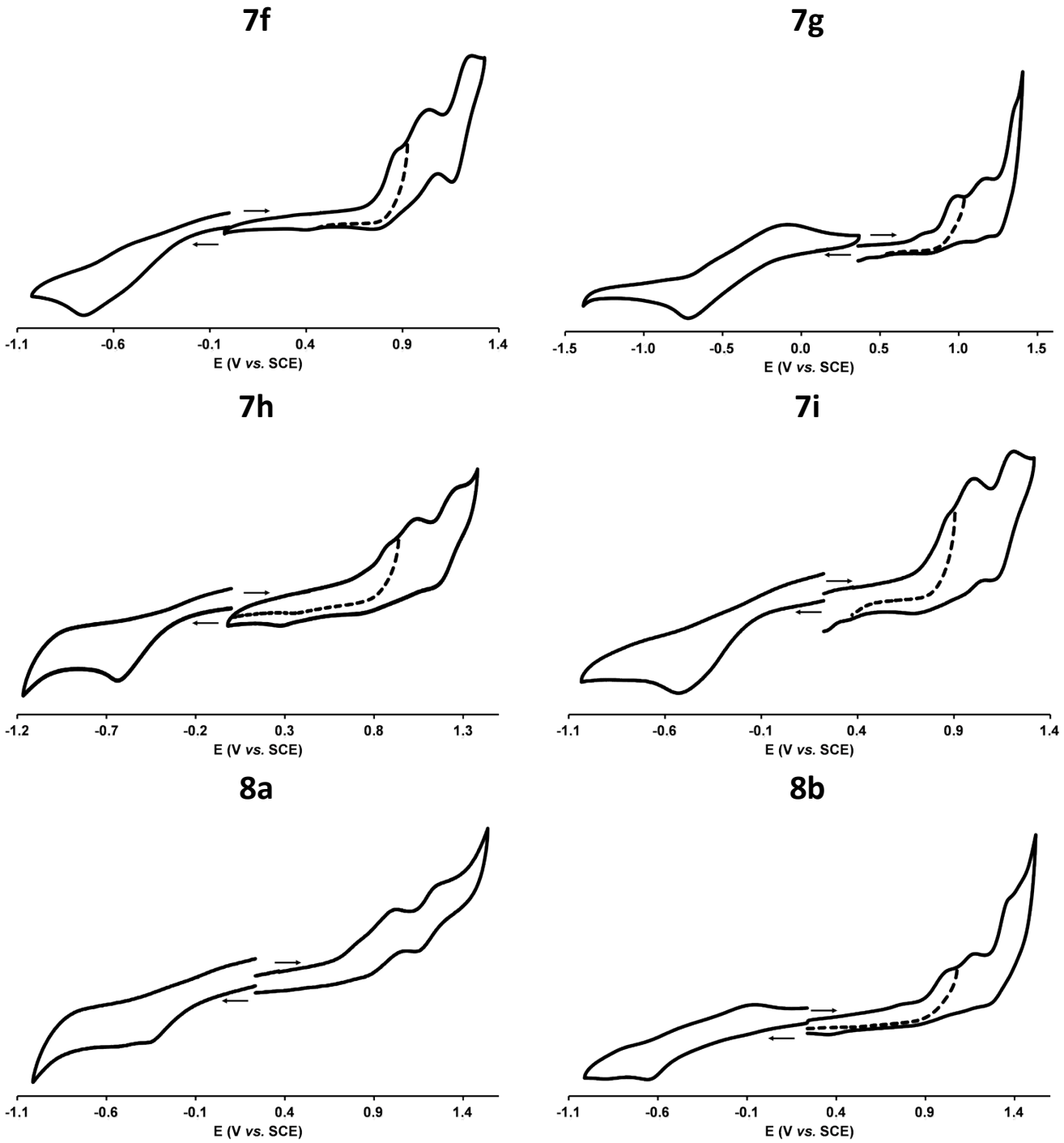

Figure S10: Cyclic voltammograms of corroles **7f-i** and **8a-b** in DCM containing 0.1 M of $^{n}Bu_4NPF_6$ at room temperature (scan rate of 100 mV/s).

Theoretical analyses

1. Computational Details

Calculations were performed at the Density Functional Theory (DFT) level in Gaussian 16,[1] and using the B3LYP/6-31G(d,p) methodology. The geometry optimizations were carried out without symmetry constraints to ensure the minimum energy followed by frequency calculations to corroborate the real optimized structure, obtaining only positive values. Only one tautomeric species was considered for compounds, according to the X-ray crystal structure of **7a**; note that tautomeric species have been reported to coexist in solution.[2] Time-Dependent DFT (TD-DFT) calculations were performed in dichloromethane (DCM) as the solvent, using the Conductor-like Polarizable Continuum Model (CPCM) for the first 80 vertical singlet-singlet electron excitations. Wavefunction analyses were performed in MultiWfn 3.8.[3]

2. Optimized geometries and Frontier Molecular Orbitals (FMOs).

The structures of corroles **7a**, **7d**, **7g**, **8a** and **8b** bearing an identical *p*-cyanophenyl group on the *meso* position 10 were fully optimized by B3LYP/6-31G(d,p) calculations. Figure S11 shows the main structural parameters of **7a** as a representative system (bond distances, angles and saddled structure) and displays the dihedral angles for corroles **7a**, **7d**, **7g**, **8a** and **8b**. Bond distances and angles values of the core center show comparable values among all the structures with respect to the different 5 and 15 *meso*-perfluoroalkyl substituents (Figure S11, Figure S12 and Figure S13 for all systems). The C-N bonds in the pyrrole rings display lengths of ~1.4 Å, and for the direct bond between both pyrrole rings (C_1-C_{19}), a bond length of *ca.* 1.42 Å is observed. Similarly, the 5, 15 and 10 *meso* positions show angle values in the core center in the order of 123-127°. The external dihedral angles (χ_1, χ_2, and χ_3, Figure S11b) show a typical saddled structure, which agrees with reported compounds and for the experimental observations.[2] Here, lower χ_1 values of ~10° are observed, compared to the χ_2 and χ_3 values (~35° and ~74°, respectively). The latter is associated with the presence of N-H···N hydrogen bonding between both adjacent pyrrole rings,

that participate in the χ_1 torsion angle. Specifically, for corroles **8a** and **8b**, the presence of the acyl moiety modulates the χ_1 torsion angle, increasing the corresponding values up to 28°, without a clear distinction of the acyl substituent. This enhanced value, observed in the acyl-based corroles seems to be related to the structural nature of the acyl moiety, increasing the saddling structure in the core region of the macrocycle.

a)

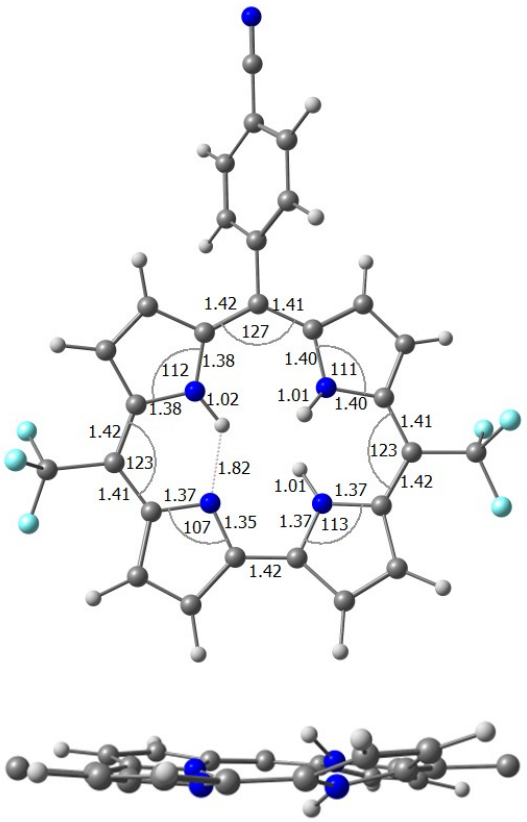

b)

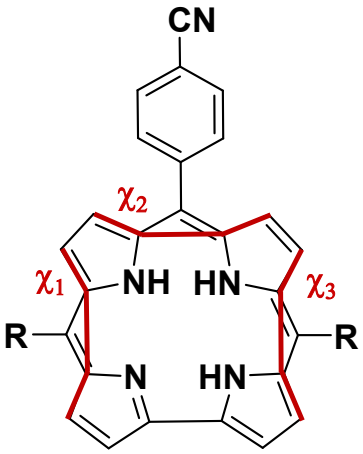

Compound/R	Computed dihedral angles		
	χ_1	χ_2	χ_3
7a/CF_3	11.5°	35.7°	72.4°
7d/C_3F_7	10.6°	38.0°	74.4°
7g/C_7F_{15}	10.5°	37.7°	74.0°
8a/ C_3F_7, COC_2F_5	27.9°	33.3°	73.8°
8b/ C_7F_{15}, COC_6F_{13}	28.5°	32.7°	73.2°

Figure S11: Main geometrical parameters and saddled conformation of corrole **7a** as a representative molecule. b) External dihedral angles of the core center for the studied compounds.

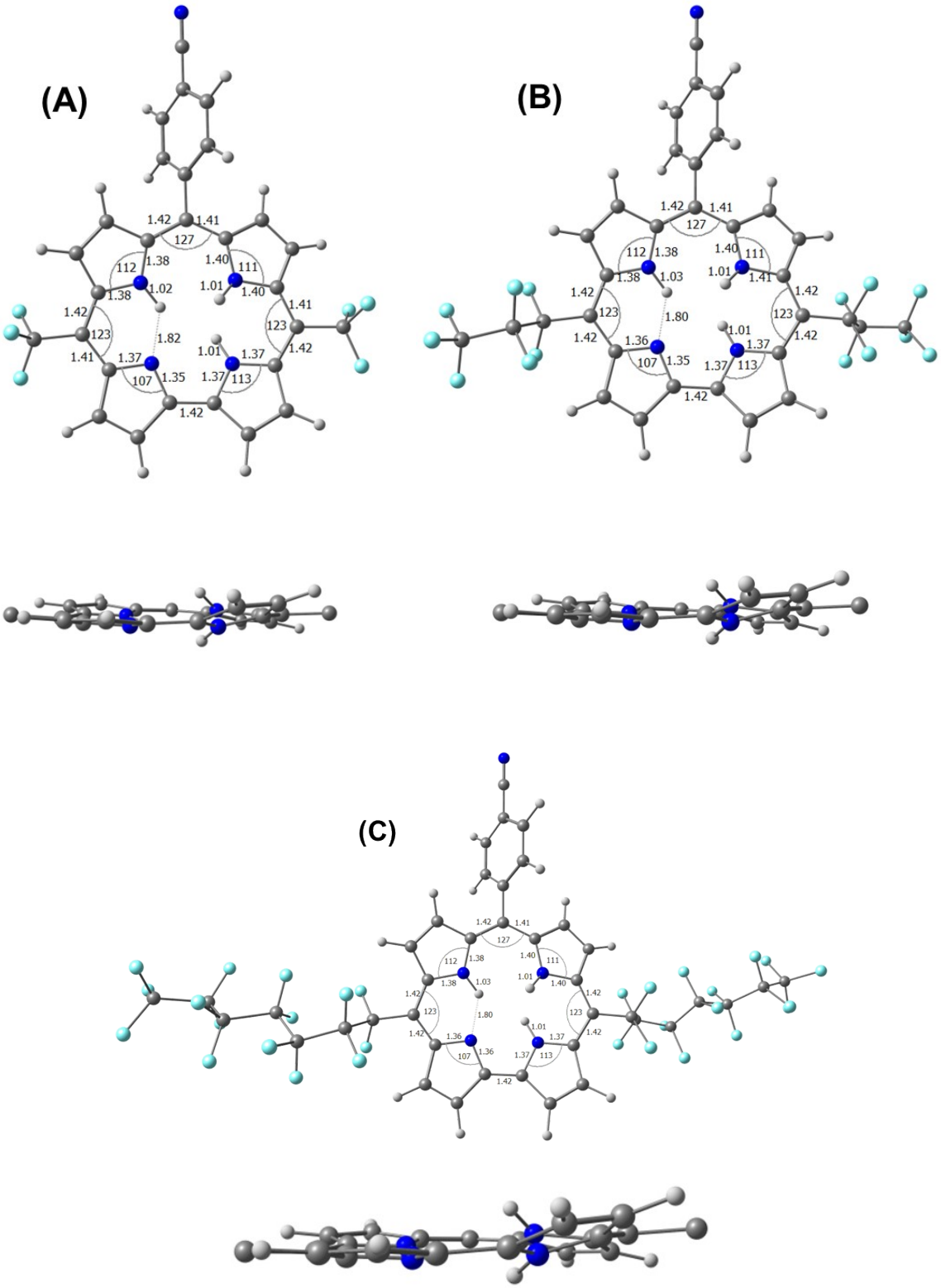

Figure S12: Geometrical parameters for the optimized structures of corroles **7a** (A), **7d** (B) and **7g** (C); The *meso* substituent was replaced by a carbon atom in the saddled structures for clarity.

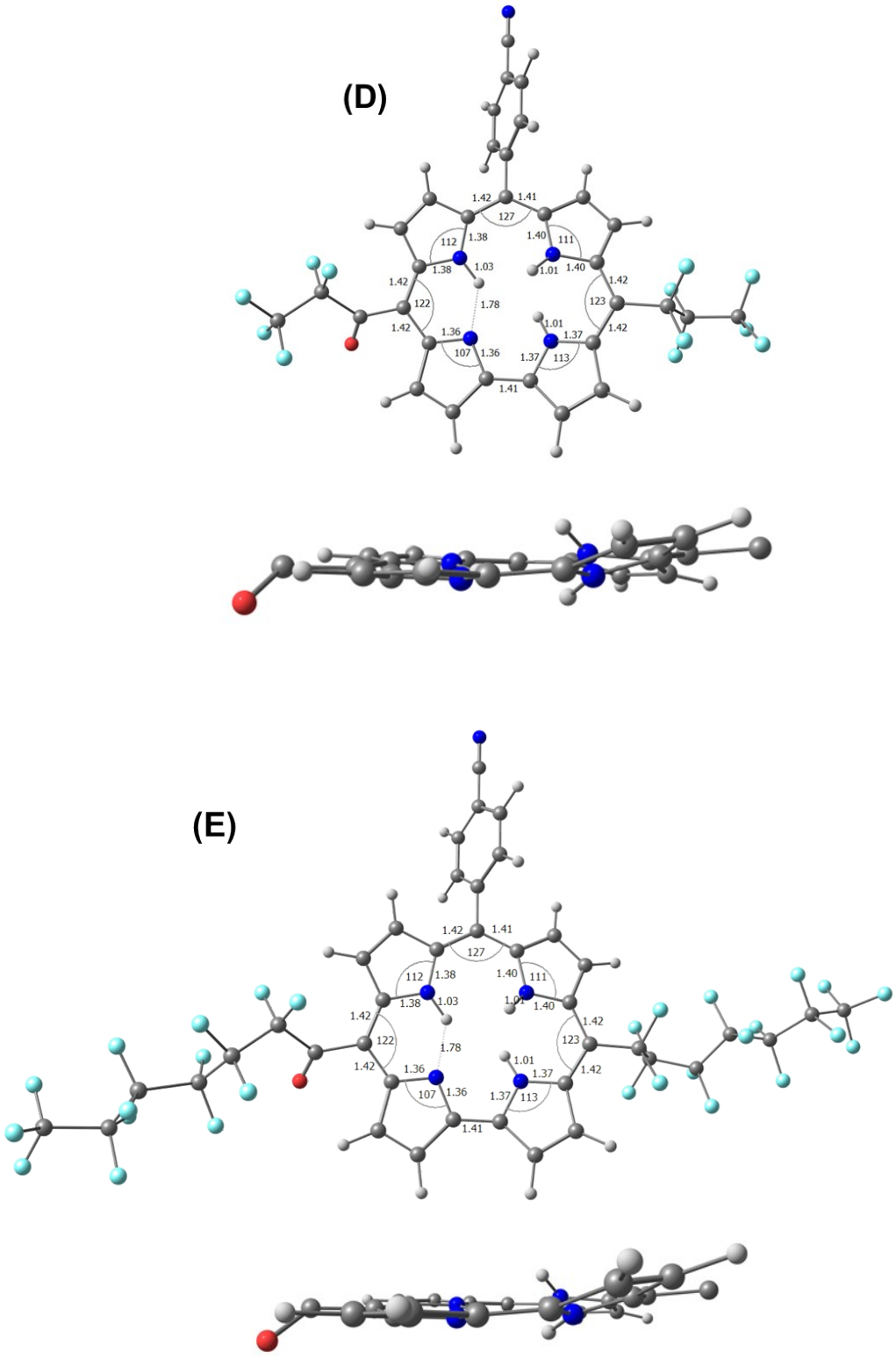

Figure S13: Geometrical parameters for the optimized structures of corroles **8a** (D) and **8b** (E); The *meso* substituent was replaced by a carbon atom in the saddled structures for clarity.

Figure S14 and Figure S15 show the isosurface plots of the frontier molecular orbitals (FMOs) of all the computed of corroles **7a**, **7d**, **7g**, **8a** and **8b**, obtained from the TD-DFT calculations. Table S2 includes the energy of the highest occupied molecular orbital (HOMO) and lowest unoccupied molecular orbital (LUMO), and the HOMO-LUMO energy difference (ΔH-L). Considering the electron-withdrawing character of the *meso* substituents, the HOMO and HOMO-1 (Figure S14, Figure S15 and Table S2) appears located at the core region of the corrole structure in almost all the studied compounds (aromatic systems and N atoms), with slight differences with respect to the exchange of the *meso* substituents. The HOMO of the fluoroalkyl *meso*-substituted $–C_nF_{2n+1}$ compounds **7a**, **7d** and **7g** appears at 5.31 to 5.36 eV, which is then stabilized by the *meso*-substitution of the acyl group up to 5.43 and 5.45 eV for **8a** and **8b**, respectively. Otherwise, the LUMO is located at the aromatic core of the corrole in all cases, with energy values in the range of 2.70 to 2.75 eV, while LUMO+1 shows a larger contribution on the benzonitrile group at the 10 position. For **8a** and **8b**, a stabilization energy of up to ~3.0 eV is observed *via* the acyl functionalization. This stabilizing energy can be assumed due to the direct presence of the electron-withdrawing acyl fragment at the LUMO isosurface, stabilizing the energy of this orbital. Therefore, the above results highlight the HOMO-LUMO energy modulation *via* functionalization. Although similar GAP values are observed in the case of **7a**, **7d** and **7g**, with values equal to 2.61 eV, lower values are evidenced in the case of the acyl-based corroles **8a** and **8b**, up to 2.48 eV. These last values confirm the stabilizing effect of the acyl moiety on the frontier molecular orbitals for the latter compounds.

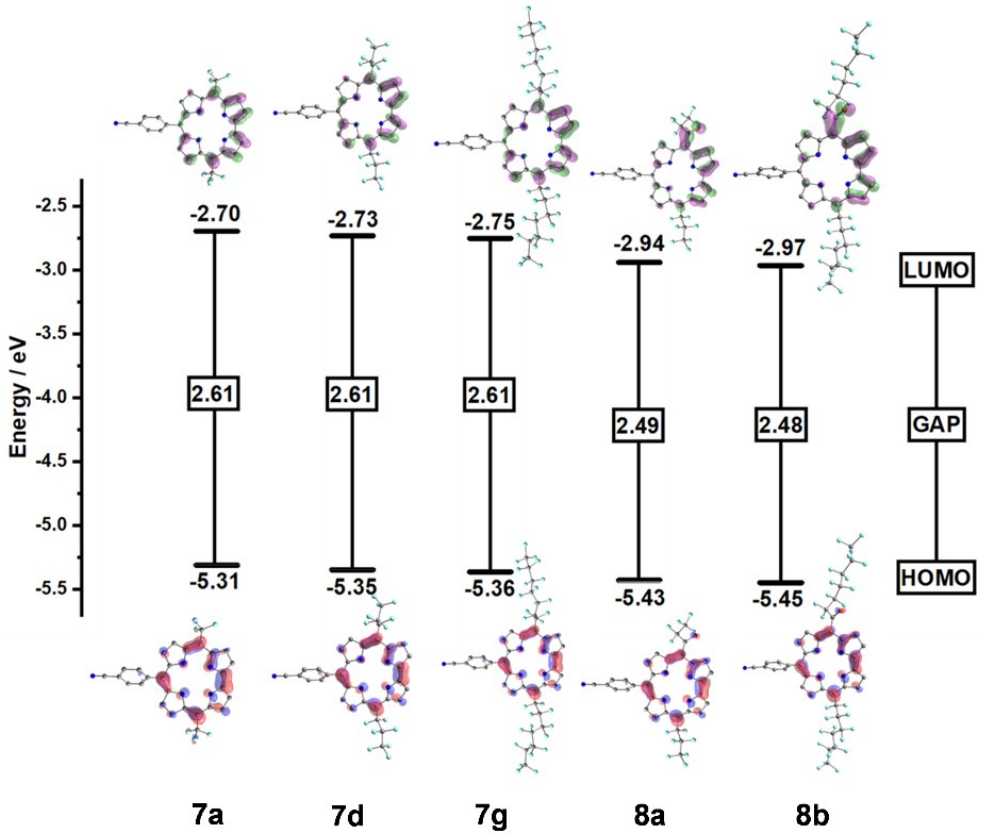

Figure S14: Energies of the FMOs and the LUMO-HOMO energy differences (GAP, Δ_{HL}) in eV units for corroles **7a**, **7d**, **7g**, **8a** and **8b**.

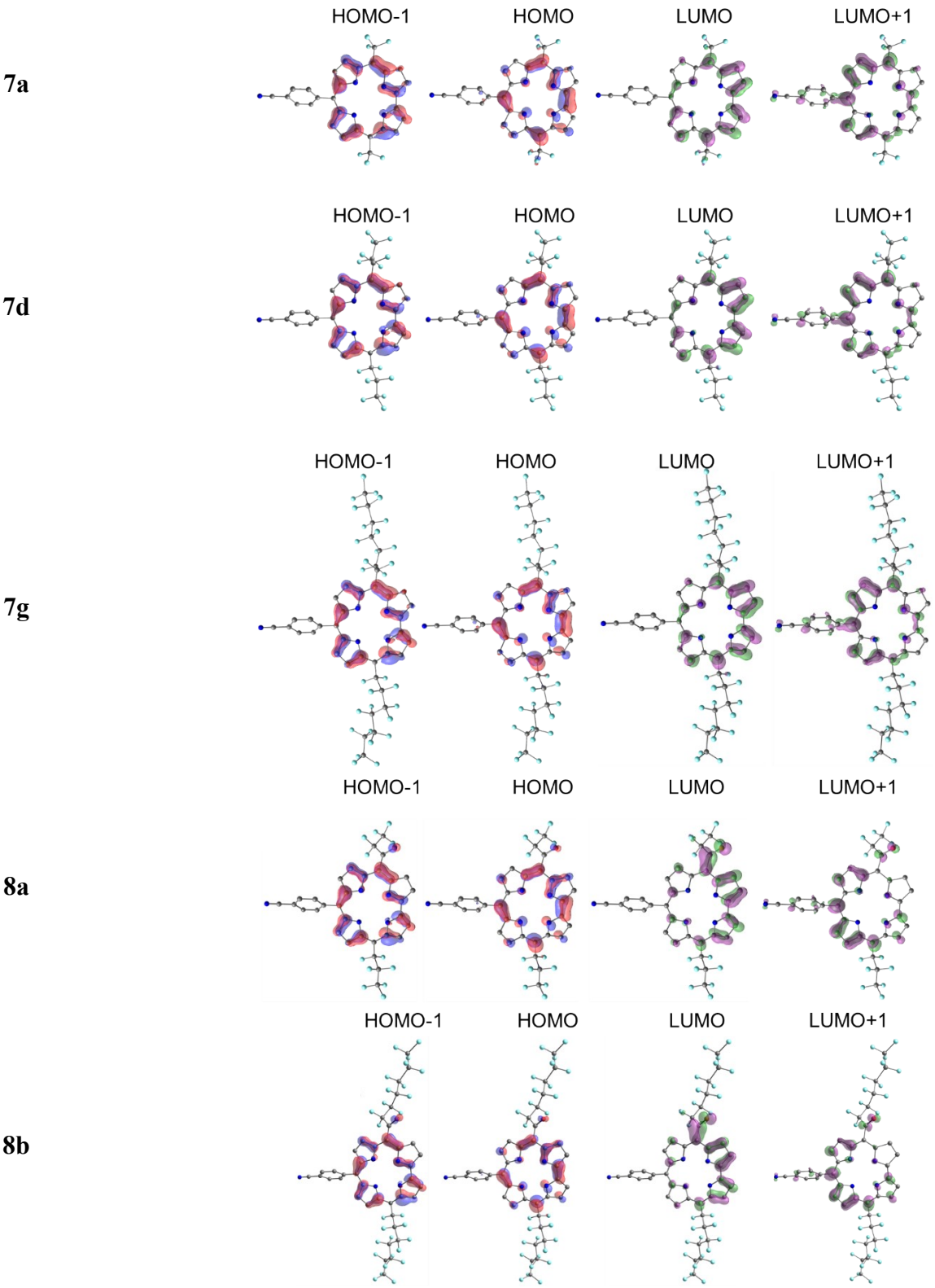

Figure S15: TD-DFT computed plots of the frontier molecular orbitals HOMO-1 to LUMO+1 for corroles **7a**, **7d**, **7g**, **8a** and **8b**, obtained from the TD-DFT calculations.

Table S2: Energy of the Highest Occupied Molecular Orbital (HOMO), the Lowest Unoccupied Molecular Orbital (LUMO), the energy difference between the LUMO – HOMO (Gap) and the global reactivity indexes, including the molecular hardness (η), chemical potential (μ), and electrophilicity (ω) calculated according to the Koopman´s theorem. All values are in electron-volt units.

Corrole	HOMO-1	HOMO	LUMO	LUMO+1	Gap	η	μ	ω
7a	-5.52	-5.31	-2.70	-2.38	2.61	2.61	-4.00	3.07
7d	-5.51	-5.35	-2.73	-2.39	2.62	2.62	-4.04	3.11
7g	-5.52	-5.36	-2.75	-2.40	2.61	2.61	-4.06	3.15
8a	-5.58	-5.43	-2.94	-2.57	2.49	2.49	-4.19	3.52
8b	-5.59	-5.45	-2.97	-2.58	2.48	2.48	-4.21	3.57

3. Computed electronic transitions

TD-DFT calculations were performed to study the contribution of the FMO on the electronic transitions. The simulated UV-Vis absorption spectra of **7a**, **7d**, **7g**, **8a,** and **8b** are depicted in Figures S16 and include the hole (red) and electron (yellow) distribution surfaces of the highest allowed excited states responsible for Soret and Q-bands of **7a** and **8a** as representative molecules.

Table S3 and Table S4 gather additional TD-DFT data for the 5 computed corroles whereas Figure S17 to Figure S21 show the Hole-Electron distributions of all the systems. As observed in Figure S16, Soret and Q bands appear at similar maxima energies (about 420 and 550-600 nm, respectively). For **7a**, **7d,** and **7g**, Q bands appear around 530- 560 nm, and are characterized by a low allowed electron promotion with a f_{osc} = 0.37-0.62 a.u as a result of the non-degeneracy FMOs. The Q-bands are mainly a mixture of $\pi \rightarrow \pi^*$ and $n \rightarrow \pi^*$ transitions involving the occupied HOMO/HOMO+1 and/or virtual LUMO/LUMO+1 FMOs, without a dependence on the nature of the *meso*-substituents. In the particular case of the acyl-based corroles **8a** and **8b**, the Q-bands are characterized by red-shifted absorption maxima (560 and 588 nm) and increased oscillator strengths of the S_1 state (f_{osc}=0.07-0.11 a.u.). This electronic modulation could be related to an enhanced geometrical distortion exerted by the acyl group. The latter increases the non-degeneracy of the

stabilized FMOs, in conjunction with an enhanced polarizing electron promotion compared to the corroles **7a**, **7d** and **7g** (see $\Delta\mu$ values within the participating S_1 and S_2 excited states in Tables S3 and S4).

Otherwise, the Soret band is found between 400 to 420 nm for **7a**, **7d,** and **7g,** and is mainly attributed to the S_3 and S_4 excited states. As observed, the hole-electron distribution of this band presents an enhanced participation towards the CN-phenyl moiety, thus increasing the polarizing effect on the observed transitions. For **8a** and **8b**, a red-shifted electronic transition appears at the Soret region until ~450 nm. Here, electron promotions involve the S_5 excited state; however, the oscillator strength decreases, which is confirmed by the hole-electron isosurfaces where an increased contribution of the acyl fragment takes place instead of the CN-phenyl fragment.

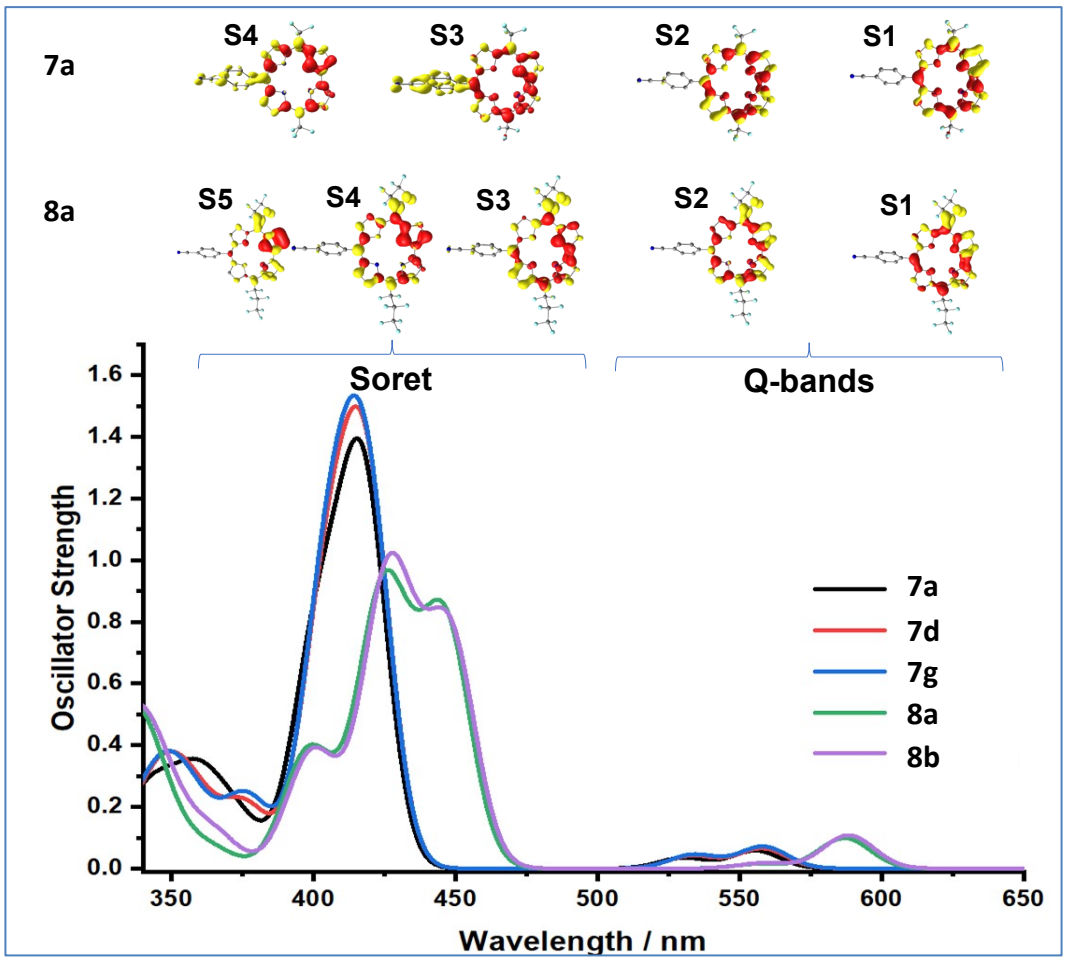

Figure S16: Simulated UV-visible absorption spectra of corroles **7a**, **7d**, **7g**, **8a** and **8b** in dichloromethane as solvent. Hole (red) and electron (yellow) surface distribution of the highest allowed excited states responsible for Soret and Q-bands are displayed for **7a** and **8a** as representative compounds. Hydrogen atoms are omitted for clarity.

Table S3: Properties of the Singlet (S_i) excites states of corroles **7a** and **7d**: calculated transition energies (λ_{calc}, in nm); oscillator strength (f_{osc}); mono-excitations with the percentage of contribution to the excited state wavefunction; and dipole moment difference $\Delta\mu$.

Corrole	State	λ_{calc}	f_{osc}	Monoexcitations	$\Delta\mu eg$ (a.u.)
7a	S1	556	0.0579	HOMO → LUMO (51 %) HOMO-1 → LUMO+1 (19 %) HOMO-1 → LUMO (16 %) HOMO → LUMO+1 (13 %)	0.615
	S2	530	0.0343	HOMO-1 → LUMO (37 %) HOMO → LUMO+1 (32 %) HOMO → LUMO (22 %)	0.606
	S3	417	1.257	HOMO → LUMO+1 (49 %) HOMO-1 → LUMO (38 %)	3.565
	S4	401	0.7072	HOMO-1 → LUMO+1 (62 %) HOMO → LUMO (20 %) HOMO-2 → LUMO (11 %)	3.538
7d	S1	558	0.0651	HOMO → LUMO (46 %) HOMO-1 → LUMO (21 %) HOMO-1 → LUMO+1 (17 %) HOMO → LUMO+1 (15 %)	0.53
	S2	533	0.0414	HOMO-1 → LUMO (37 %) HOMO → LUMO (26 %) HOMO → LUMO+1 (26 %) HOMO-1 → LUMO+1 (10 %)	0.42
	S3	419	1.2191	HOMO → LUMO+1 (54 %) HOMO-1 → LUMO (35 %)	3.555
		404	0.8265	HOMO-1 → LUMO +1 (63 %) HOMO → LUMO (21 %) HOMO-2 → LUMO (10 %)	3.583

Table S4: Properties of the Singlet (S_i) excites states of corroles **7g**, **8a** and **8b**: calculated transition energies (λ_{calc}, in nm); oscillator strength (f_{osc}); monoexcitations with the percentage of contribution to the excited state wavefunction; and dipole moment difference $\Delta\mu$.

Corrole	State	λ_{calc}	f_{osc}	Monoexcitations	$\Delta\mu eg$ (a.u.)
7g	S1	558	0.0709	HOMO → LUMO (45 %) HOMO-1 → LUMO (22 %) HOMO-1 → LUMO+1 (17 %) HOMO → LUMO+1 (15 %)	0.537
	S2	534	0.0449	HOMO-1 → LUMO (37 %), HOMO → LUMO (27 %) HOMO → LUMO+1 (26 %) HOMO-1 → LUMO+1 (10 %)	0.373
	S3	419	1.1989	HOMO-1 → LUMO (34 %), HOMO → LUMO+1 (55 %)	3.493
	S4	405	0.8803	HOMO-1 → LUMO+1 (63 %) HOMO → LUMO (21 %) HOMO-2 → LUMO (10 %)	3.527
8a	S1	587	0.0985	HOMO → LUMO (70 %) HOMO-1 → LUMO+1 (23 %)	1.903
	S2	557	0.0152	HOMO-1 → LUMO (65 %) HOMO → LUMO+1 (29 %)	0.976
	S3	446	0.8018	HOMO → LUMO+1 (58 %) HOMO-1 → LUMO (26 %)	1.448
	S4	425	0.9071	HOMO-1 → LUMO+1 (59 %) HOMO → LUMO (20 %) HOMO-2 → LUMO (15 %)	1.627
	S5	399	0.3869	HOMO-2 → LUMO (77 %)	1.518
8b	S1	588	0.1074	HOMO → LUMO (71 %) HOMO-1 → LUMO+1 (23 %)	2.275
	S2	559	0.0178	HOMO-1 → LUMO (66 %) HOMO → LUMO+1 (28 %)	1.09
	S3	448	0.7627	HOMO → LUMO+1 (58 %) HOMO-1 → LUMO (24 %)	1.566
	S4	427	0.9651	HOMO-1 → LUMO+1 (60 %) HOMO → LUMO (19 %) HOMO-2 → LUMO (14 %)	1.595
	S5	400	0.3797	HOMO-2 → LUMO (79 %)	1.445

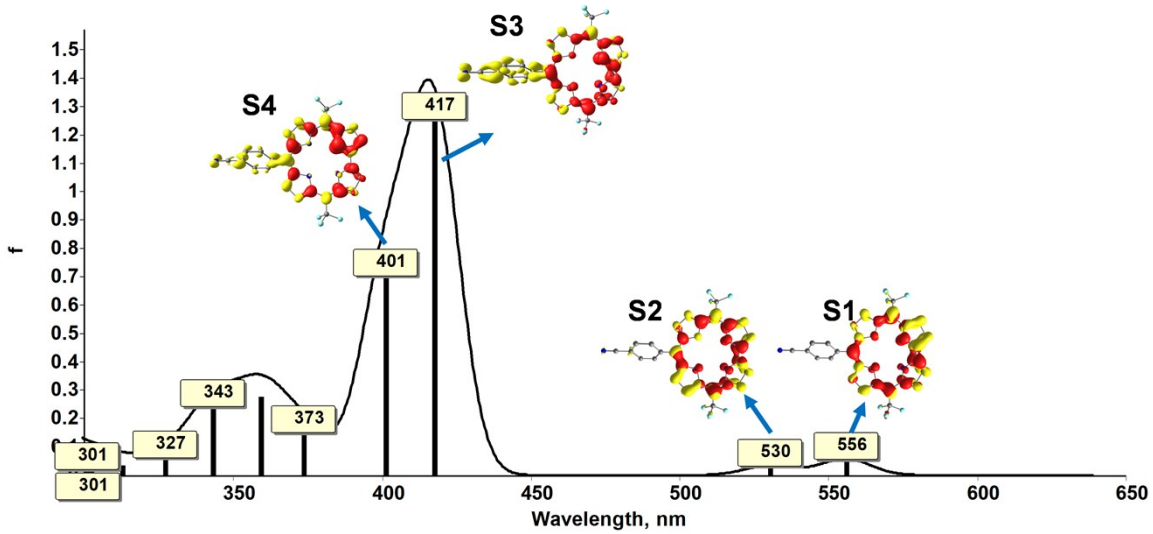

Figure S17: Simulated UV-visible absorption spectra and hole (red) and electron (yellow) surface distribution of main excited states responsible for Soret and Q-bands for **7a**.

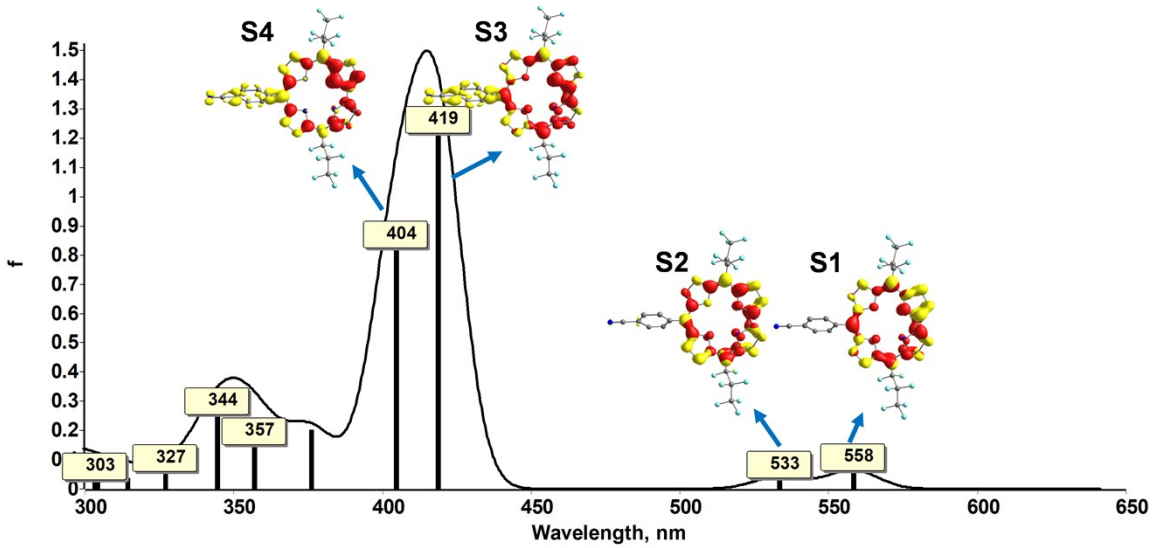

Figure S18: Simulated UV-visible absorption spectra and hole (red) and electron (yellow) surface distribution of main excited states responsible for Soret and Q-bands for **7d**.

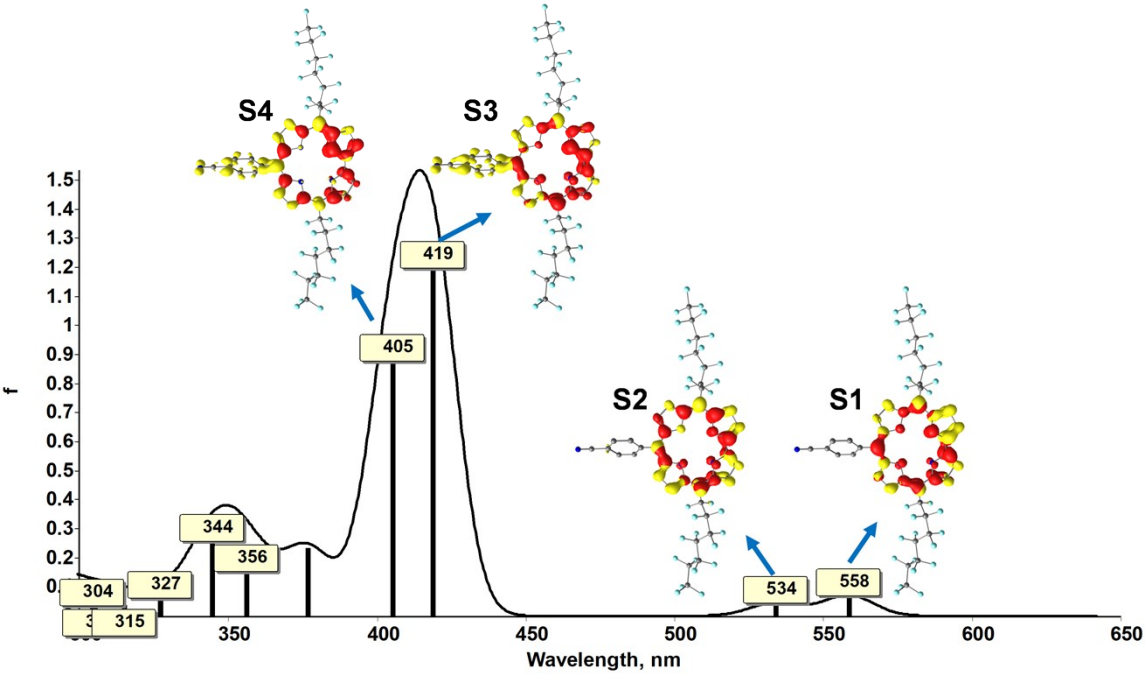

Figure S19: Simulated UV-visible absorption spectra and hole (red) and electron (yellow) surface distribution of main excited states responsible for Soret and Q-bands for **7g**.

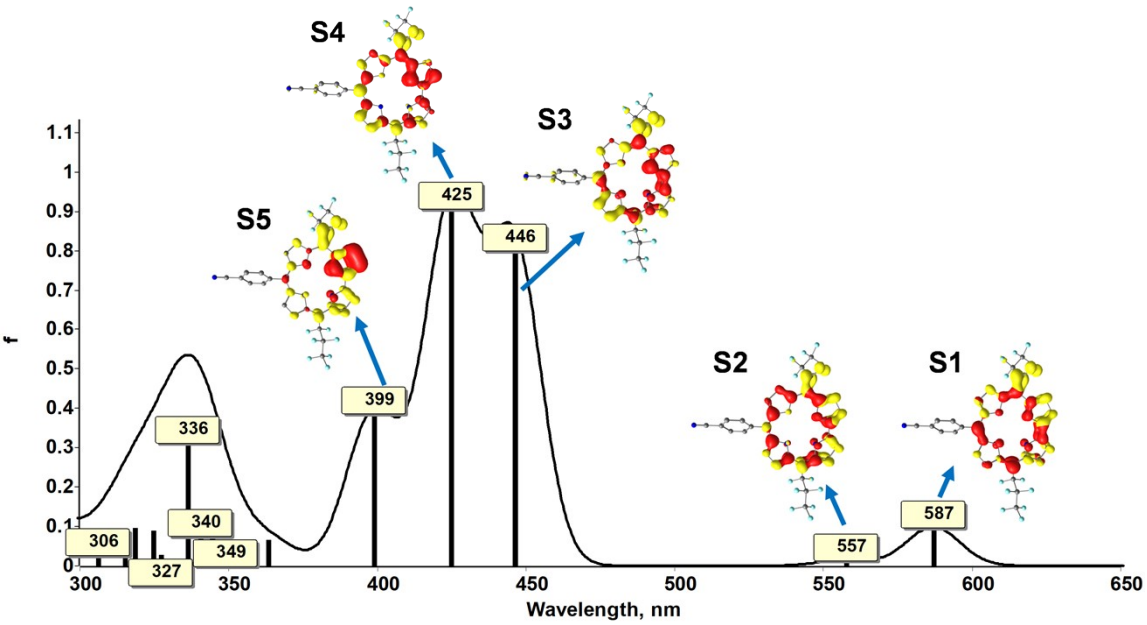

Figure S20: Simulated UV-visible absorption spectra and hole (red) and electron (yellow) surface distribution of main excited states responsible for Soret and Q-bands for **8a**.

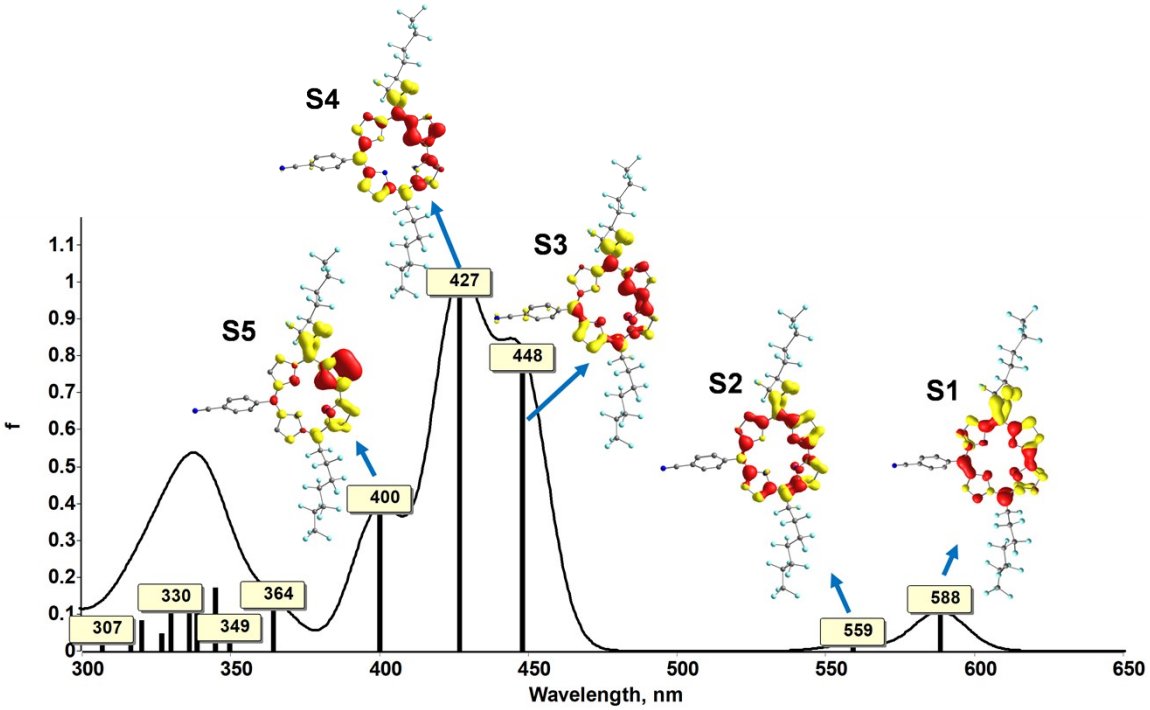

Figure S21: Simulated UV-visible absorption spectra and hole (red) and electron (yellow) surface distribution of main excited states responsible for Soret and Q-bands for **8b**.

Synthetic protocols and characterizations

Reagents. All reagents were purchased from Alfa-Aesar and or from Sigma-Aldrich and used as received. Column chromatography was performed using Silica 60M (0.04-0.063 mm) purchased from Macherey-Nagel. Optical properties were recorded in spectrophotochemical grade solvents. Dipyrromethanes **5a**[4,5] and **5b-c**[6] were prepared following previously reported protocols.

NMR and Mass spectrometry. NMR spectra were recorded on a JEOL ECS400 NMR spectrometer at room temperature. NMR chemical shifts are given in ppm (δ) relative to Me_4Si with solvent resonances used as internal standards ($CDCl_3$: 7.26 ppm for ^1H and 77.16 for ^{13}C; Benzene-d_6: 7.16 ppm for ^1H; Acetone-d_6: 2.05 ppm for ^1H and 29.84 for ^{13}C; Methanol-d_4: 3.31 ppm for ^1H; DMSO-d_6: 2.50 ppm for ^1H; D_2O: 4.79 ppm for ^1H). HRMS (ESI) and MS (ESI) analyses were performed on a QStar Elite (Applied Biosystems SCIEX) spectrometer or a SYNAPT G2 HDMS (Waters) spectrometer by the "*Spectropole*" of Aix Marseille University. These two instruments are equipped with an ESI or MALDI source spectrometer.

Electrochemistry. Cyclic voltammetry (CV) data were recorded using a BAS 100 (Bioanalytical Systems) potentiostat and the BAS100W software (v2.3). All the experiments were conducted under an argon atmosphere in a standard one-compartment using a three electrodes setup: a Pt working electrode (Ø = 1.6 mm), a Pt wire as counter electrode and an Ag/AgCl reference electrode (filled with a 3 M NaCl solution). Tetra-*n*-butylammonium hexafluorophosphate ([TBA][PF_6]) was used as a supporting electrolyte (10^{-1} M), with a concentration of the electro-active compound *ca*. 10^{-3} M. The reference electrode was calibrated using ferrocene ($E°(Fc^+/Fc)$ = 0.46V/SCE in DCM).[7] The scan rate was 100 mV/S. The solution was degassed using argon before recording each reductive scan, and the working electrode (Pt) was polished before each scan recording.

Electronic absorption and fluorescence: UV-vis absorption spectra were recorded in spectrophotometric grade solvents (*ca.* 10^{-6} M) on a Varian Cary 50 SCAN spectrophotometer. Emission spectra were obtained using a Horiba-Jobin Yvon Fluorolog-3 spectrofluorimeter equipped with a three-slit double-grating excitation and a spectrograph emission mono-chromator with dispersions of 2.1 $nm.mm^{-1}$ (1200 grooves per mm). A 450 W xenon continuous wave lamp provided excitation. Fluorescence of diluted solutions was detected at the right angle using 10 mm quartz cuvettes. Fluorescence quantum yields Φ were measured in diluted aerated dichloromethane or methanol solutions with an optical density lower than 0.1 using the following equation:

$$\frac{\Phi_x}{\Phi_r} = \left(\frac{A_r(\lambda)}{A_x(\lambda)}\right)\left(\frac{n_x^2}{n_r^2}\right)\left(\frac{D_x}{D_r}\right)$$

where A is the absorbance at the excitation wavelength (λ), *n* is the refractive index and D is the integrated intensity. "r" and "x" stand for reference and sample. The fluorescence quantum yields were measured relative to tetraphenylporphyrin (TPP) in acetonitrile (Φ = 0.15).[8] Excitation of reference and sample compounds was performed at the same wavelength (550 nm for **3** and **7a-i**, 590 nm for **8a-b** and 585 nm for **9**).

Single Crystal X-ray Diffraction: Crystals suitable for single crystal X-ray diffraction analysis of corroles **7a**, **7b**, **7c**, **7d** and **7i** were obtained by slow diffusion of *n*-hexane in concentrated dichloromethane solutions for **7a**, **7b**, **7c** and **7i** and in a C_6D_6 solution for **7d**. They were measured on a Rigaku Oxford Diffraction SuperNova diffractometer at room temperature at the CuKα radiation (λ=1.54184 Å). Data collection reduction and multiscan ABSPACK correction were performed with CrysAlisPro (Rigaku Oxford Diffraction). Using Olex2[9] the structures were solved by intrinsic phasing methods with SHELXT[10] and SHELXL[11] was used for full matrix least squares refinement. H-atoms were found experimentally but re-introduced at geometrical positions and refined as riding atoms with their Uiso parameters constrained to 1.2Ueq(parent atom) for the CH, CH_2 and NH groups and to 1.5Ueq(parent atom) for the CH_3.

Synthesis of bilanes 6a-j

5,15-bis-trifluoromethyl-10-(4-cyanophenyl)-bilane 6a

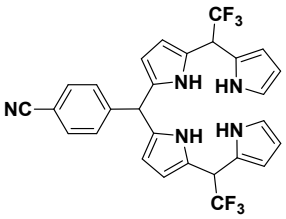

5-(trifluoromethyl)dipyrromethane **5a** (214 mg, 1.0 mmol, 1 equiv.) and 4-cyanobenzaldehyde (66 mg, 0.50 mmol, 0.5 equiv.) were heated to *ca.* 70 °C under stirring to homogenize the medium. TFA (38 µL, 0.50 mmol, 0.5 equiv.) was then added and the stirring was maintained for 5 min at room temperature. A saturated aqueous $NaHCO_3$ solution and dichloromethane were added. The organic phase was extracted with DCM, washed with water, dried over Na_2SO_4 and evaporated to dryness. The residue was purified by flash chromatography (DCM then DCM/EtOAc 95:5) to afford **6a** as a brown foam-like solid (73 mg, 0.13 mmol, 27%). Scale up from **5a** (2.14 g, 10 mmol) afforded **6a** (715 mg, 1.3 mmol, 26%).

R_F: 0.40 (silica, DCM/EtOAc 95:5); **^{1}H NMR (Acetone-d_6):** δ = 9.93 (br s, 2H, NH), 9.87 (br s, 2H, NH), 7.58 (d, $^3J_{H\text{-}H}$ = 7.7 Hz, 2H, Ar-H), 7.26 (d, $^3J_{H\text{-}H}$ = 7.7 Hz, 2H, Ar-H), 6.65 (s, 2H, α-H), 6.02 (s, 4H, β-H), 5.94 (s, 2H, β-H), 5.56 (dd, $^3J_{H\text{-}H}$ = 7.3 Hz, $^4J_{H\text{-}H}$ = 2.6 Hz, 2H, β-H), 5.45 (s, 1H, *meso*-10-H), 4.87 (q, $^3J_{H\text{-}F}$ = 9.6 Hz, 2H, *meso*-5,15-H) ppm; **^{19}F NMR (Acetone-d_6):** δ = -69.57 ppm; **^{13}C {^{1}H} NMR (Acetone-d_6):** δ = 149.6 (t , $^3J_{C\text{-}F}$ = 2.6 Hz, C), 133.3 (t, $^3J_{C\text{-}F}$ = 2.8 Hz, C), 132.9 (CH), 130.3 (t, $^4J_{C\text{-}F}$ = 1.6 Hz, CH), 126.6 (d, $^1J_{C\text{-}F}$ = 279.2 Hz, C), 124.7 (C), 124.4 (C), 119.4 (C), 119.1 (d, $^3J_{C\text{-}F}$ = 2.5 Hz, CH), 111.0 (C), 109.1 (d, $^3J_{C\text{-}F}$ = 4.1 Hz, CH), 108.9 (CH), 108.7 (CH), 108.5 (CH), 44.6 (CH), 43.6 (q, $^2J_{C\text{-}F}$ = 29.8 Hz, CH) ppm; **HRMS-ESI:** calculated for $C_{28}H_{22}F_6N_5^+$ $[M+H^+]^+$: 542.1774, found 542.1774.

5,15-bis-trifluoromethyl-10-(*p*-tolyl)-bilane 6b

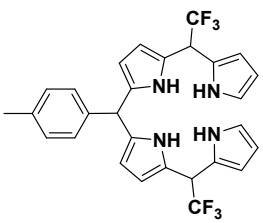

5-(trifluoromethyl)dipyrromethane **5a** (2.14 g, 10 mmol, 1 equiv.) and *p*-tolualdehyde (0.59 mL, 5.0 mmol, 0.5 equiv.) were heated to *ca.* 70 °C under stirring to homogenize the medium. TFA (0.38 mL, 5.0 mmol, 0.5 equiv.) was then added and the stirring was maintained for 5 min at room temperature. A saturated aqueous $NaHCO_3$ solution and dichloromethane were added. The organic phase was extracted with DCM, washed with water, dried over Na_2SO_4 and evaporated to dryness. The residue was purified by flash chromatography (DCM/petroleum ether 2:1 then DCM) to afford **6b** as a brown foam-like solid (503 mg, 0.95 mmol, 19%).

R_F: 0.45 (silica, DCM); **^{1}H NMR (Acetone-d_6):** δ = 9.91 (br s, 2H, NH), 9.67 (br s, 2H, NH), 6.93 (s, 4H, Ar-H and α-H), 6.60 (s, 2H, Ar-H), 5.96 (d, $^3J_{H\text{-}H}$ = 11.3 Hz, 4H, β-H), 5.89 (m, 2H, β-H), 5.52 (m, 2H, β-H), 5.22 (s, 1H, *meso*-10-H), 4.83 (q, $^3J_{H\text{-}F}$ = 9.6 Hz, 2H, *meso*-5,15-H), 2.14 (s, 3H, CH_3) ppm; **^{19}F NMR (Acetone-d_6):** δ = -69.56 ppm; **^{13}C {^{1}H} NMR (Acetone-d_6):** δ = 141.0 (C), 136.6 (C), 134.7 (d, $^3J_{C\text{-}F}$ = 5.5

Hz, C), 129.6 (CH), 129.2 (t, $^{4}J_{C\text{-}F}$ = 2.0 Hz, CH), 126.7 (d, $^{1}J_{C\text{-}F}$ = 279.3 Hz, C), 124.6 (C), 124.1 (C), 119.0 (d, $^{3}J_{C\text{-}F}$ = 2.7 Hz, CH), 109.0 (d, $^{3}J_{C\text{-}F}$ = 4.5 Hz, CH), 108.7 (CH), 108.5 (CH), 108.0 (CH), 44.3 (t, $^{4}J_{C\text{-}F}$ = 1.8 Hz, CH), 43.7 (q, $^{2}J_{C\text{-}F}$ = 29.8 Hz, CH), 20.1 (CH_3) ppm; **HRMS-ESI:** calculated for $C_{28}H_{23}F_6N_4^-$ [M-H$^+$]$^-$: 529.1832, found 529.1824.

5,15-bis-trifluoromethyl-10-(*p*-anisyl)-bilane 6c

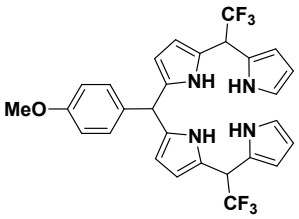

5-(trifluoromethyl)dipyrromethane **5a** (1.07 g, 5.0 mmol, 1 equiv.) and *p*-anisaldehyde (0.31 mL, 2.5 mmol, 0.5 equiv.) were heated to *ca.* 70 °C under stirring to homogenize the medium. TFA (0.19 mL, 0.25 mmol, 0.5 equiv.) was then added and the stirring was maintained for 5 min at room temperature. A saturated aqueous $NaHCO_3$ solution and dichloromethane were added. The organic phase was extracted with DCM, washed with water, dried over Na_2SO_4 and evaporated to dryness. The residue was purified by flash chromatography (DCM then DCM/EtOAc 95:5) to afford **6c** as a brown foam-like solid (550 mg, 1.0 mmol, 40%).

R_F: 0.30 (silica, DCM/EtOAc 95:5); **^{1}H NMR (Acetone-d_6):** δ = 9.91 (br s, 2H, NH), 9.67 (br s, 2H, NH), 6.98 (d, $^{3}J_{H\text{-}H}$ = 8.0 Hz, 2H, Ar-H), 6.73 (d, $^{3}J_{H\text{-}H}$ = 8.0 Hz, 2H, Ar-H), 6.65 (s, 2H, α-H), 6.01 (d, $^{3}J_{H\text{-}H}$ = 11.2 Hz, 4H, β-H), 5.94 (s, 2H, β-H), 5.55 (m, 2H, β-H), 5.25 (s, 1H, *meso*-10-H), 4.88 (q, $^{3}J_{H\text{-}F}$ = 9.5 Hz, 2H, *meso*-5,15-H), 3.66 (s, 3H, O-Me) ppm; **^{19}F NMR (Acetone-d_6):** δ = -69.57 ppm; **^{13}C {^{1}H} NMR (Acetone-d_6):** δ = 159.3 (C), 135.8 (t, $^{3}J_{C\text{-}F}$ = 2.8 Hz, C), 134.9 (dd, $^{3}J_{C\text{-}F}$ = 5.0 Hz, $^{4}J_{C\text{-}F}$ = 1.6 Hz, C), 130.2 (t, $^{4}J_{C\text{-}F}$ = 1.9 Hz CH), 126.6 (d, $^{1}J_{C\text{-}F}$ = 279.2 Hz, C), 124.6 (C), 124.1 (C), 119.0 (d, $^{3}J_{C\text{-}F}$ = 2.5 Hz, CH), 114.3 (CH), 109.0 (d, $^{3}J_{C\text{-}F}$ = 3.5 Hz, CH), 108.8 (CH), 108.5 (CH), 107.9 (CH), 55.4 (CH_3), 43.8 (t, $^{4}J_{C\text{-}F}$ = 1.6 Hz, CH), 43.6 (q, $^{2}J_{C\text{-}F}$ = 29.7 Hz, CH) ppm; **HRMS-ESI:** calculated for $C_{28}H_{24}F_6N_4Cl^-$ [M+Cl$^-$]$^-$: 581.1548, found 581.1548.

5,15-bis-trifluoromethyl-10-(pentafluorophenyl)-bilane 6j

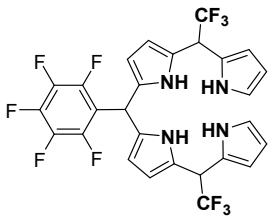

5-(trifluoromethyl)dipyrromethane **5a** (2.14 g, 10 mmol, 1 equiv.) and 2,3,4,5,6-pentafluoro benzaldehyde (0.62 mL, 5.0 mmol, 0.5 equiv.) were heated to *ca.* 70 °C under stirring to homogenize the medium. TFA (0,38 mL, 5.0 mmol, 0.5 equiv.) was then added and the stirring was maintained for 5 min at room temperature. A saturated aqueous $NaHCO_3$ solution and dichloromethane were added. The organic phase was extracted with DCM, washed with water, dried over Na_2SO_4 and evaporated to dryness. The residue was purified by flash chromatography (DCM then DCM/EtOAc 95:5) to afford **6j** as a yellow foam-like solid (410 mg, 0.07 mmol, 13%).

R_F: 0.50 (silica, DCM/EtOAc 95:5); **^{1}H NMR (Acetone-d_6):** δ = 10.00 (br s, 4H, NH), 6.72 (m, 2H, α-H), 6.11 (m, 4H, β-H), 6.02 (q, $^3J_{H\text{-}H}$ = 2.8 Hz, 2H, β-H), 5.86 (t + s, $^3J_{H\text{-}H}$ = 3.0 Hz 3H, β-H and *meso*-10-H), 4.98 (q, $^3J_{H\text{-}F}$ = 9.6 Hz, 2H, *meso*-5,15-H) ppm; **^{19}F NMR (Acetone-d_6):** δ = -69.54, -142.94 (d, $^3J_{F\text{-}F}$ = 19.3 Hz), -158.99 (t, $^3J_{F\text{-}F}$ = 19.6 Hz), -164.48 (m) ppm; **^{13}C {^{1}H} NMR (Acetone-d_6):** δ = 142.3 (quint., $^1J_{C\text{-}F}$ = 250.3 Hz, C), 130.1 (m, C), 126.6 (q, $^1J_{C\text{-}F}$ = 279.1 Hz, C), 124.9 (m, C), 124.3 (dm, $^3J_{C\text{-}F}$ = 7.7 Hz, C), 119.1 (d, $^3J_{C\text{-}F}$ = 3.8 Hz, CH) , 117.5 (m, C), 115.2 (C), 109.1 (d, $^4J_{C\text{-}F}$ = 3.1 Hz, CH), 109.0 (d, $^2J_{C\text{-}F}$ = 11.4 Hz, CH), 108.8 (CH), 108.4 (m, CH), 54.9 (C), 43.6 (q, $^2J_{C\text{-}F}$ = 29.9 Hz, CH), 33.95 (CH) ppm; **HRMS-ESI:** calculated for $C_{27}H_{16}F_{11}N_4$ [M-H$^+$]$^-$: 605.1205, found 605.1205.

5,15-bis-perfluoropropyl-10-(4-cyanophenyl)-bilane 6d

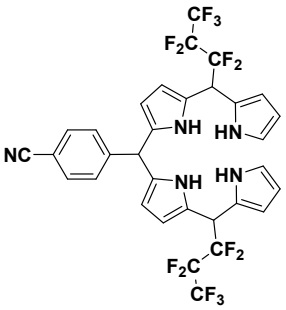

5-(heptafluoropropyl)dipyrromethane **5b** (157 mg, 0.50 mmol, 1 equiv.) and 4-cyanobenzaldehyde (33 mg, 0.25 mmol, 0.5 equiv.) were heated to *ca.* 70 °C under stirring to homogenize the medium. TFA (19 µL, 0.25 mmol, 0.5 equiv.) was then added and the stirring was maintained for 5 min at room temperature. A saturated aqueous $NaHCO_3$ solution and dichloromethane were added. The organic phase was extracted with DCM, washed with water, dried over Na_2SO_4 and evaporated to dryness. The residue was purified by flash chromatography (DCM then DCM/EtOAc 95:5) to afford **6d** as brown foam-like solid (51 mg, 0.07 mmol, 28%). Scale up from **5b** (3.14 g, 10 mmol) afforded **6d** (931 mg, 1.2 mmol, 25%).

R_F: 0.60 (silica, DCM/EtOAc 95:5); **^{1}H NMR (Acetone-d_6):** δ = 10.05 (br s, 2H, NH), 9.97-9.94 (br s, 2H, NH), 7.62 (d, $^3J_{H\text{-}H}$ = 7.8 Hz, 2H, Ar-H), 7.28 (d, $^3J_{H\text{-}H}$ = 7.8 Hz, 2H, Ar-H), 6.70 (s, 2H, α-H), 6.12 (s, 4H, β-H), 5.98 (s, 2H, β-H), 5.55 (m, 2H, β-H), 5.49 (s, 1H, *meso*-10-H), 5.05 (dt, $^3J_{H\text{-}F}$ = 17.8 Hz, $^4J_{H\text{-}F}$ = 6.1 Hz, 2H, *meso*-5,15-H) ppm; **^{19}F NMR (Acetone-d_6):** δ = -81.54 (CF_3), -113.37, -125.28 ppm; **^{13}C {^{1}H} NMR (Acetone-d_6):** δ = 149.5 (C), 133.5 (d, $^4J_{C\text{-}F}$ = 2.0 Hz, C), 133.3 (C), 132.9 (CH), 130.3 (t, $^4J_{C\text{-}F}$ = 1.3 Hz, CH), 124.0 (C), 123.6 (C), 119.4 (C), 119.3 (d, $^3J_{C\text{-}F}$ = 5.6 Hz, CH), 111.1 (C), 109.8 (d, $^3J_{C\text{-}F}$ = 6.7 Hz, CH), 109.6 (d, $^2J_{C\text{-}F}$ = 10.1 Hz, CH), 108.7 (d, $^4J_{C\text{-}F}$ = 2.4 Hz, CH), 108.7 (CH), 44.5 (CH), 41.3 (t, $^2J_{C\text{-}F}$ = 23.0 Hz, CH) ppm (carbon signals of the perfluoroalkyl chains could not be observed); **HRMS-ESI:** calculated for $C_{32}H_{22}F_{14}N_5^+$ [M+H$^+$]$^+$: 742.1646, found 742.1648.

5,15-bis-perfluoropropyl-10-(*p*-tolyl)-bilane 6e

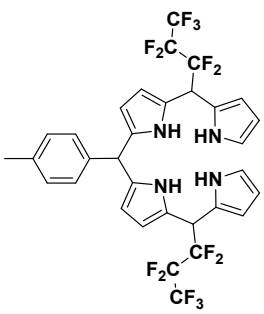

5-(heptafluoropropyl)dipyrromethane **5b** (157 mg, 0.50 mmol, 1 equiv.) and *p*-tolualdehyde (30 µL, 0.25 mmol, 0.5 equiv.) were heated to *ca.* 70 °C under stirring to homogenize the medium. TFA (19 µL, 5 mmol, 0.5 equiv.) was then added and the stirring was maintained for 5 min at room temperature. A saturated aqueous $NaHCO_3$ solution and dichloromethane were added. The organic phase was extracted with DCM, washed with water, dried over Na_2SO_4 and evaporated to dryness. The residue was purified by flash chromatography (DCM/petroleum ether 2:1 then DCM) to afford **6e** as a brown foam-like solid (29 mg, 0.04 mmol, 16%). Scale up from **5b** (3.14 g, 10 mmol) afforded **6e** (619 mg, 0.85 mmol, 17%).

R_F: 0.60 (silica, DCM/petroleum ether 2:1); **^{1}H NMR (Acetone-d_6):** δ = 10.04 (br s, 2H, NH), 9.78 (br s, 2H, NH), 7.02 (d, $^3J_{H\text{-}H}$ = 6.8 Hz, 2H, Ar-H), 6.98 (d, $^3J_{H\text{-}H}$ = 6.8 Hz, 2H, Ar-H), 6.72 (s, 2H, α-H), 6.13 (s, 4H, β-H), 6.00 (s, 2H, β-H), 5.57 (m, 2H, β-H), 5.32 (s, 1H, *meso*-10-H), 5.07 (t, $^3J_{H\text{-}F}$ = 17.8 Hz, 2H, *meso*-5,15-H), 2.25 (s, 3H, CH_3) ppm; **^{19}F NMR (Acetone-d_6):** δ = -81.55 (CF_3), -113.33, -125.24 ppm; **^{13}C {^{1}H} NMR (Acetone-d_6):** δ =140.9 (C), 136.6 (C), 134.9 (C), 134.8 (CH), 129.4 (d, $^2J_{C\text{-}F}$ = 33.6 Hz, CH), 123.9 (C), 123.5 (C), 119.2 (d, $^3J_{C\text{-}F}$ = 7.3 Hz, C), 119.2 (d, $^3J_{C\text{-}F}$ = 5.2 Hz, CH), 109.8 (d, $^3J_{C\text{-}F}$ = 5.4 Hz, CH), 109.4 (d, $^3J_{C\text{-}F}$ = 8.2 Hz, CH), 108.8 (CH), 108.3 (CH), 44.3 (CH), 41.7 (t, $^2J_{C\text{-}F}$ = 22.9 Hz, CH), 21.0 (CH_3) ppm (carbon atom signals of the perfluoroalkyl chains could not be observed); **HRMS-ESI:** calculated for $C_{32}H_{25}F_{14}N_4^+$ $[M+H^+]^+$: 731.1850, found 731.1853.

5,15-bis-perfluoropropyl-10-(*p*-anisyl)-bilane 6f

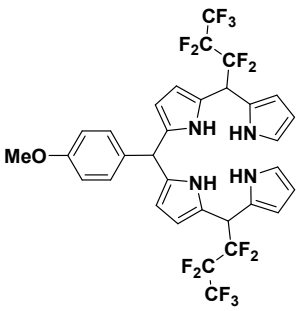

5-(heptafluoropropyl)dipyrromethane **5b** (157 mg, 0.50 mmol, 1 equiv.) and *p*-anisaldehyde (30 µL, 0.25 mmol, 0.5 equiv.) were heated to *ca.* 70 °C under stirring to homogenize the medium. TFA (19 µL, 0.25 mmol, 0.5 equiv.) was then added and the stirring was maintained for 5 min at room temperature. A saturated aqueous $NaHCO_3$ solution and dichloromethane were added. The organic phase was extracted with DCM, washed with water, dried over Na_2SO_4 and evaporated to dryness. The residue was purified by flash chromatography (DCM/petroleum ether 2:1 then DCM) to afford **6f** as a brown foam-like solid (24 mg, 0.03 mmol, 13%). Scale up from **5b** (3.14 g, 10 mmol) afforded **6f** (422 mg, 0.56 mmol, 11%).

R_F: 0.50 (silica, DCM); **^{1}H NMR (Acetone-d_6):** δ = 10.06 (br s, 2H, NH), 9.79-9.77 (br s, 2H, NH), 7.04 (d, $^3J_{H\text{-}H}$ = 7.8 Hz, 2H, Ar-H), 6.80 (d, $^3J_{H\text{-}H}$ = 7.8 Hz, 2H, Ar-H), 6.75 (s, 2H, α-H), 6.15 (s, 4H, β-H), 6.02 (s, 2H, β-H), 5.60 (m, 2H, β-H), 5.33 (s, 1H, *meso*-10-H), 5.10 (t, $^3J_{H\text{-}F}$ = 17.9 Hz, 2H, *meso*-5,15-H), 3.75 (s, 3H, O-Me) ppm; **^{19}F NMR (Acetone-d_6):** δ = -81.54 (CF_3), -113.31, -125.23 ppm; **^{13}C {^{1}H} NMR (Acetone-d_6):** δ = 159.3 (C), 135.8 (C), 135.1 (d, $^4J_{C\text{-}F}$ = 1.7 Hz, C), 134.9 (d, $^4J_{C\text{-}F}$ = 1.4 Hz, C), 130.2 (m, CH), 123.8 (C), 123.3 (C), 119.2 (d, $^3J_{C\text{-}F}$ = 4.6 Hz, CH), 114.3 (CH), 109.7 (d, $^3J_{C\text{-}F}$ = 4.3 Hz, CH), 109.3 (d, $^2J_{C\text{-}F}$ = 11.7 Hz, CH), 108.7 (d, $^3J_{C\text{-}F}$ = 2.8 Hz, CH), 109.1 (d, $^3J_{C\text{-}F}$ = 2.2 Hz, CH), 55.4 (CH_3), 43.8 (CH), 41.3 (t, $^2J_{C\text{-}F}$ = 22.7 Hz, CH) ppm (carbon atom signals of the perfluoroalkyl chains could not be observed); **HRMS-ESI:** calculated for $C_{32}H_{24}F_{14}N_4OCl^-$ $[M+Cl^-]^-$: 742.1421, found 781.1415.

5,15-bis-perfluoroheptyl-10-(4-cyanophenyl)-bilane 6g

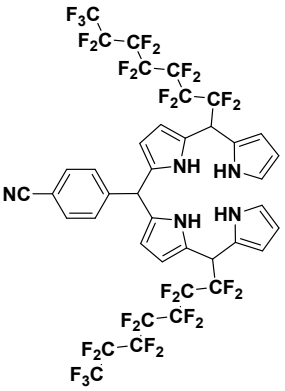

5-(pentadecafluoroheptyl)dipyrromethane **5c** (257 mg, 0.50 mmol, 1 equiv.) and 4-cyanobenzaldehyde (33 mg, 0.25 mmol, 0.5 equiv.) were heated to *ca.* 70 °C under stirring to homogenize the medium. TFA (19 µL, 0.25 mmol, 0.5 equiv.) was then added and the stirring was maintained for 5 min at room temperature. A saturated aqueous $NaHCO_3$ solution and dichloromethane were added. The organic phase was extracted with DCM, washed with water, dried over Na_2SO_4 and evaporated to dryness. The residue was purified by flash chromatography (DCM/petroleum ether 2:1 then 4:1) to afford **6g** as a brown foam-like solid (37 mg, 0.03 mmol, 13%). Scale up from **5c** (5.14 g, 10 mmol) afforded **6g** (720 mg, 0.63 mmol, 13%).

R_F: 0.50 (silica, DCM/petroleum ether 4:1); **^{1}H NMR (Acetone-d_6):** δ = 10.09 (br s, 2H, NH), 10.00-9.97 (br s, 2H, NH), 7.63 (d, $^3J_{H\text{-}H}$ = 7.8 Hz, 2H, Ar-H), 7.30 (d, $^3J_{H\text{-}H}$ = 7.8 Hz, 2H, Ar-H), 6.73 (s, 2H, α-H), 6.15 (s, 4H, β-H), 6.01 (s, 2H, β-H), 5.59 (m, 2H, β-H), 5.52 (s, 1H, *meso*-10-H), 5.05 (dt, $^3J_{H\text{-}F}$ = 17.5 Hz, $^4J_{H\text{-}F}$ = 5.8 Hz, 2H, *meso*-5,15-H) ppm; **^{19}F NMR (Acetone-d_6):** δ = -81.60 (CF_3), -112.66, -120.74, -122.15, -122.49, -123.24, -126.71 ppm; **^{13}C {^{1}H} NMR (Acetone-d_6):** δ = 149.5 (C), 133.5 (d, $^4J_{C\text{-}F}$ = 3.2 Hz, C), 133.3 (d, $^4J_{C\text{-}F}$ = 2.3 Hz, C), 131.6 (m, CH), 130.3 (m, CH), 123.6 (C), 119.4 (C), 119.3 (d, $^3J_{C\text{-}F}$ = 4.8 Hz, CH), 111.1 (C), 109.8 (d, $^3J_{C\text{-}F}$ = 6.3 Hz, CH), 109.6 (d, $^3J_{C\text{-}F}$ = 5.9 Hz, CH), 108.8 (d, $^4J_{C\text{-}F}$ = 2.4 Hz, CH), 108.7 (CH), 44.6 (CH), 41.6 (t, $^2J_{C\text{-}F}$ = 23.2 Hz, CH) ppm (carbon atom signals of the perfluoroalkyl chains could not be observed); **HRMS-ESI:** calculated for $C_{40}H_{22}F_{30}N_5^+$ $[M+H^+]^+$: 1142.1391, found 1142.1389.

5,15-bis-perfluoroheptyl-10-(*p*-tolyl)-bilane 6h

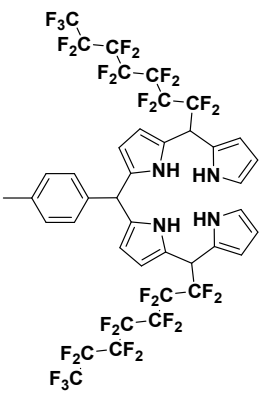

5-(pentadecafluoroheptyl)dipyrromethane **5c** (5.14 g, 10 mmol, 1 equiv.) and *p*-tolualdehyde (0.59 mL, 5.0 mmol, 0.5 equiv.) were heated to *ca.* 70 °C under stirring to homogenize the medium. TFA (0.38 mL, 5.0 mmol, 0.5 equiv.) was then added and the stirring was maintained for 5 min at room temperature. A saturated aqueous $NaHCO_3$ solution and dichloromethane were added. The organic phase was extracted with DCM, washed with water, dried over Na_2SO_4 and evaporated to dryness. The residue was purified by flash chromatography (DCM/petroleum ether 1:1 then 2:1) to afford **6h** as a brown foam-like solid (1.05 g, 0.93 mmol, 18%).

R_F: 0.40 (silica, DCM/petroleum ether 2:1); **^{1}H NMR (Acetone-d_6):** δ = 10.05 (br s, 2H, NH), 9.79-9.76 (br s, 2H, NH), 7.01 (d, $^3J_{H-H}$ = 6.6 Hz, 2H, Ar-H), 6.98 (d, $^3J_{H-H}$ = 6.6 Hz, 2H, Ar-H), 6.72 (s, 2H, α-H), 6.14 (s, 4H, β-H), 6.00 (s, 2H, β-H), 5.58 (m, 2H, β-H), 5.32 (s, 1H, *meso*-10-H), 5.10 (t, $^3J_{H-F}$ = 18.1 Hz, 2H, *meso*-5,15-H), 2.24 (s, 3H, CH_3) ppm; **^{19}F NMR (Acetone-d_6):** δ = -81.64 (CF_3), -112.56, -120.67, -122.10, -122.45, -123.21, -126.69 ppm; **^{13}C {^{1}H} NMR (Acetone-d_6):** 140.9 (C), 136.6 (C), 134.9 (m, C), 134.8 (CH), 129.4 (d, $^2J_{C-F}$ = 33.6 Hz, CH), 123.9 (C), 123.5 (C), 119.2 (d, $^3J_{C-F}$ = 3.9 Hz, C), 109.8 (m, CH), 109.4 (d, $^3J_{C-F}$ = 8.2 Hz, CH), 108.8 (CH), 108.3 (CH), 44.3 (CH), 41.7 (t, $^2J_{C-F}$ = 22.9 Hz, CH), 21.0 (CH_3) ppm (carbon atom signals of the perfluoroalkyl chains could not be observed); **HRMS-ESI:** calculated for $C_{40}H_{24}F_{30}N_4Cl^-$ [M+Cl^-]$^-$: 1165.1216, found 1165.1215.

5,15-bis-perfluoroheptyl-10-(*p*-anisyl)-bilane 6i

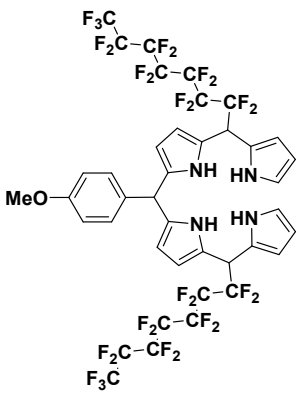

5-(pentadecafluoroheptyl)dipyrromethane **5c** (257 mg, 0.50 mmol, 1 equiv.) and *p*-anisaldehyde (30 µL, 0.25 mmol, 0.5 equiv.) were heated to *ca.* 70 °C under stirring to homogenize the medium. TFA (19 µL, 0.25 mmol, 0.5 equiv.) was then added and the stirring was maintained for 5 min at room temperature. A saturated aqueous $NaHCO_3$ solution and dichloromethane were added. The organic phase was extracted with DCM, washed with water, dried over Na_2SO_4 and evaporated to dryness. The residue was purified by flash chromatography (DCM/petroleum ether 2:1 then 4:1) to afford **6i** as a brown foam-like solid (41 mg, 0.04 mmol, 14%). Scale up from **5c** (5.14 g, 10 mmol) afforded **6i** (850 mg, 0.74 mmol, 15%).

R_F: 0.40 (silica, DCM/petroleum ether 4:1); **^{1}H NMR (Acetone-d_6):** δ = 10.05 (br s, 2H, NH), 9.78-9.75 (br s, 2H, NH), 6.97 (d, $^3J_{H-H}$ = 7.8 Hz, 2H, Ar-H), 6.73 (d, $^3J_{H-H}$ = 7.8 Hz, 2H, Ar-H), 6.69 (s, 2H, α-H), 6.11 (s, 4H, β-H), 5.96 (s, 2H, β-H), 5.53 (m, 2H, β-H), 5.27 (s, 1H, *meso*-10-H), 5.07 (t, $^3J_{H-F}$ = 18.0 Hz, 2H, *meso*-5,15-H), 3.68 (s, 3H, O-Me) ppm; **^{19}F NMR (Acetone-d_6):** δ = -81.16 (CF_3), -112.19, -120.28, -121.70, -122.05, -122.80, -126.27 ppm; **^{13}C {^{1}H} NMR (Acetone-d_6):** 159.3 (C), 135.9 (C), 135.1 (C), 134.9 (C), 130.2 (CH), 123.8 (C), 123.4 (C), 119.2 (CH), 114.3 (CH), 109.7 (CH), 109.4 (d, $^3J_{C-F}$ = 7.4 Hz, CH), 108.7 (CH), 108.2 (CH), 55.5 (CH), 43.7 (CH), 41.6 (t, $^2J_{C-F}$ = 22.7 Hz, CH) ppm (carbon atom signals

of the perfluoroalkyl chains could not be observed); **HRMS-ESI:** calculated for $C_{40}H_{24}F_{30}N_4OCl^-$ $[M+Cl^-]^-$: 1181.1165, found 1181.1166.

Synthesis of the bis-perfluoroalkyl-corroles

5,15-bistrifluoromethyl-10-(4-cyanophenyl)-corrole 7a

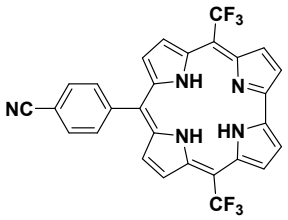

5,15-bistrifluoromethyl-10-(4-cyanophenyl)bilane **6a** (270 mg, 0.50 mmol, 1 equiv.) was dissolved in DCM (7.5 mL) before a solution of DDQ (160 mg, 0.75 mmol, 1.5 equiv.) in THF (1.5 mL) was added while stirring. The reaction mixture was stirred for a further 5 min. After evaporation, the crude product was purified by flash chromatography (DCM/petroleum ether 2:1) followed by precipitation in heptane to afford **7a** (49 mg, 0.09 mmol, 18%). Starting from a solution of **6a** (100 mg, 0.18 mmol, 1 equiv.) and PIFA (202 mg, 0.45 mmol, 2.6 equiv.) in DCM (40 mL), the oxidation produced after evaporation and chromatographic purification almost the same yield of **7a** (17%).

R_F: 0.55 (silica, DCM/petroleum ether 2:1); **^{1}H NMR (DMSO-d_6):** δ = 9.38 (d, $^3J_{H\text{-}H}$ = 4.1 Hz, 2H, β-H), 9.20 (m, 2H, β-H), 9.09 (br s, 2H, β-H), 8.55 (d, $^3J_{H\text{-}H}$ = 4.8 Hz, 2H, β-H), 8.31 (d, $^3J_{H\text{-}H}$ = 8.2 Hz, 2H, Ar-H), 8.25 (d, $^3J_{H\text{-}H}$ = 8.2 Hz, 2H, Ar-H) ppm; **^{19}F NMR (DMSO-d_6):** δ = -43.76 (br s) ppm; **UV-Vis (DCM):** λ_{max} (ε x 10^{-4}) = 402 (10.67), 420 (10.43), 513 (1.00), 549 (1.71), 614 (1.34) nm (10^4 $M^{-1}.cm^{-1}$); **Fluorescence (DCM):** λ_{ex} = 550 nm, λ_{max} = 639, 697 nm, Φ_{fl} = 9%; **HRMS-ESI:** calculated for $C_{28}H_{14}F_6N_5^-$ $[M\text{-}H^+]^-$: 534.1159, found 534.1163.

5,15-bis-trifluoromethyl-10-(*p*-tolyl)-corrole 7b

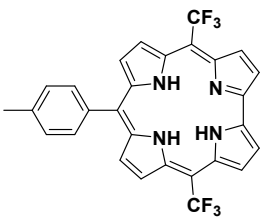

5,15-bis-trifluoromethyl-10-(*p*-tolyl)-bilane **6b** (212 mg, 0.50 mmol, 1 equiv.) was dissolved in DCM (7.5 mL) before a solution of DDQ (160 mg, 0.75 mmol, 1.5 equiv.) in THF (1.5 mL) was added while stirring. The reaction mixture was stirred for a further 5 min. After evaporation, the crude product was purified by flash chromatography (DCM/petroleum ether 1:1) followed by precipitation in heptane to afford **7b** (33 mg, 0.06 mmol, 13%).

R_F: 0.50 (silica, DCM/petroleum ether 1:1); **^{1}H NMR (Benzene-d_6, 60 °C):** δ = 9.30 (s, 2H, β-H), 9.15 (br s, 2H, β-H), 8.80 (s, 2H, β-H), 8.63 (d, $^3J_{H\text{-}H}$ = 4.1 Hz, 2H, β-H), 8.02 (d, $^3J_{H\text{-}H}$ = 7.3 Hz, 2H, Ar-H), 7.44 (d, $^3J_{H\text{-}H}$ = 7.3 Hz, 2H, Ar-H), 2.52 (s, 3H, CH_3), 0.40 (br s, 3H, NH) ppm; **^{19}F NMR (Benzene-d_6):** δ = -41.58, -45.89 ppm; **UV-Vis (DCM):** λ_{max} (ε x 10^{-4}) = 402 (13.25), 420 (12.12), 516 (1.16), 550 (2.16), 617 (1.58) nm (10^4 $M^{-1}.cm^{-1}$); **Fluorescence (DCM):** λ_{ex} = 550 nm, λ_{max} = 642, 696 nm, Φ_{fl} = 9%; **HRMS-ESI:** calculated for $C_{28}H_{17}F_6N_4^-$ $[M\text{-}H^+]^-$: 523.1363, found 523.1362.

5,15-bis-trifluoromethyl-10-(*p*-anisyl)-corrole 7c

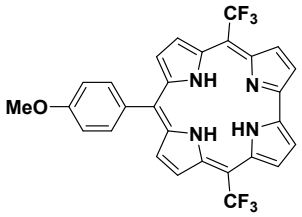

5,15-bis-trifluoromethyl-10-(*p*-anisyl)-bilane **6c** (273 mg, 0.50 mmol, 1 equiv.) was dissolved in DCM (7.5 mL) before a solution of DDQ (160 mg, 0.75 mmol, 1.5 equiv.) in THF (1.5 mL) was added while stirring. The reaction mixture was stirred for a further 5 min. After evaporation, the crude product was purified by flash chromatography (DCM/petroleum ether 1:1) followed by precipitation in heptane to afford **7c** (45 mg, 0.08 mmol, 17%).

R_F: 0.60 (silica, DCM/petroleum ether 1:1); **^{1}H NMR (Benzene-d_6, 60 °C and RT):** δ = 9.31 (s, 2H, β-H), 9.15 (br s, 2H, β-H), 8.81 (s, 2H, β-H), 8.64 (s, 2H, β-H), 8.01 (t, $^3J_{H\text{-}H}$ = 7.4 Hz, 2H, Ar-H), 7.22 (t, $^3J_{H\text{-}H}$ = 7.5 Hz, 2H, Ar-H, partially hidden by the solvent peak), 3.67 (d, $^3J_{H\text{-}H}$ = 7.3 Hz, 3H, O-Me), 0.41 (br s, 3H, NH) ppm (there is no coupling between the Ar-H and the O-Me at room temperature, the first appearing as doublets with $^3J_{H\text{-}H}$ = 7.4 Hz, and the later as a singlet); **^{19}F NMR (Benzene-d_6):** δ = -41.54, -45.90 ppm; **UV-Vis (DCM):** λ_{max} (ε $_x$ 10^{-4}) = 403 (10.62), 420 (10.57), 513 (1.10), 550 (1.74), 615 (1.45) nm (10^4 $M^{-1}.cm^{-1}$); **Fluorescence (DCM):** λ_{ex} = 550 nm, λ_{max} = 644, 691 nm, Φ_{fl} = 9%; **HRMS-ESI:** calculated for $C_{28}H_{17}F_6N_4O^-$ $[M\text{-}H^+]^-$: 539.1312, found 539.1306.

5,15-bis-trifluoromethyl-10-pentafluorophenyl-corrole 3

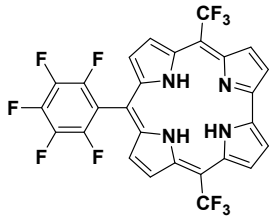

5,15-bis-trifluoromethyl-10-pentafluorophenyl-bilane **6j** (150 mg, 0.25 mmol, 1 equiv.) was dissolved in DCM (3.75 mL) before a solution of DDQ (80 mg, 0.4 mmol, 1.5 equiv.) in THF (0.75 mL) was added while stirring. The reaction mixture was stirred for a further 5 min. After evaporation, the crude product was purified by flash chromatography (DCM/petroleum ether 2:1) to afford **3** (13 mg, 0.02 mmol, 9%). Characterizations are in accordance with the ones reported in the literature.[12]

R_F: 0.70 (silica, DCM/petroleum ether 2:1); **^{1}H NMR (Benzene-d_6):** δ = 9.41 (s, 2H, β-H), 9.07 (br s, 2H, β-H), 8.68 (s, 2H, β-H), 8.28 (d, $^3J_{H\text{-}H}$ = 4.6 Hz, 2H, β-H) ppm; **^{19}F NMR (Benzene-d_6):** δ = -43.57 (br s), -138.23 (d, $^3J_{F\text{-}F}$ = 21 Hz), -151.95 (t, $^3J_{F\text{-}F}$ = 21 Hz), -161.69 (t, $^3J_{F\text{-}F}$ = 21 Hz) ppm; **UV-Vis (DCM):** λ_{max} (ε $_x$ 10^{-4}) = 400 (14.74), 417 (13.55), 547 (1.92), 563 (1.39), 611 (1.91) nm (10^{-4} $M^{-1}.cm^{-1}$); **Fluorescence (DCM):** λ_{ex} = 550 nm, λ_{max} = 628, 681 nm, Φ_{fl} = 9.3%; **HRMS-ESI:** calculated for $C_{27}H_{10}F_{11}N_4^-$ $[M\text{-}H^+]^-$: 599.0735, found 599.0735.

5,15-perfluoropropyl-10-(4-cyanophenyl)-corrole 7d

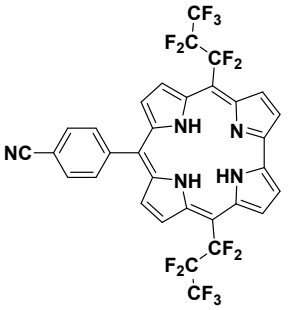

5,15-bis-perfluoropropyl-10-(4-cyanophenyl)-bilane **6d** (530 mg, 0.71 mmol, 1 equiv.) was dissolved in DCM (10.5 mL) before a solution of DDQ (247 mg, 1.1 mmol, 1.5 equiv.) in THF (2 mL) was added while stirring. The reaction mixture was stirred for a further 5 min. After evaporation, the crude product was purified by flash chromatography (DCM/petroleum ether 2:1) followed by precipitation in heptane to afford **7d** (175 mg, 0.24 mmol, 33%).

R_F: 0.70 (silica, DCM/petroleum ether 2:1); **^{1}H NMR (DMSO-d_6):** δ = 9.34 (s, 2H, β-H), 9.06 (s, 2H, β-H), 8.93 (s, 2H, β-H), 8.49 (d, $^3J_{H\text{-}H}$ = 4.1 Hz, 2H, β-H), 8.27 (d, $^3J_{H\text{-}H}$ = 7.6 Hz, 2H, Ar-H), 8.21 (d, $^3J_{H\text{-}H}$ = 7.6 Hz, 2H, Ar-H) ppm; **^{19}F NMR (DMSO-d_6):** δ = -78.65 (CF_3), -90.02 (br s), -94.32 (br s), -122.12 ppm; **UV-Vis (DCM):** λ_{max} (ε x 10^{-4}) = 404 (12.34), 420 (12.53), 514 (1.07), 551 (1.94), 617 (1.47) nm (10^4 $M^{-1}.cm^{-1}$); **Fluorescence (DCM):** λ_{ex} = 550 nm, λ_{max} = 637, 695 nm, Φ_{fl} = 12%; **HRMS-ESI:** calculated for $C_{32}H_{14}F_{14}N_5^-$ $[M\text{-}H^+]^-$: 734.1031, found 734.1024.

5,15-perfluoropropyl-10-(*p*-tolyl)-corrole 7e

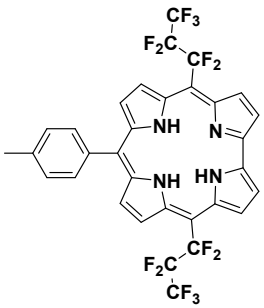

5,15-bis-perfluoropropyl-10-(*p*-tolyl)-bilane **6e** (300 mg, 0.41 mmol, 1 equiv.) was dissolved in DCM (6 mL) before a solution of DDQ (139 mg, 0.61 mmol, 1.5 equiv.) in THF (1.5 mL) was added while stirring. The reaction mixture was stirred for a further 5 min. After evaporation, the crude product was purified by flash chromatography (DCM/petroleum ether 2:1) followed by precipitation in heptane to afford **7e** (17 mg, 0.02 mmol, 6%).

R_F: 0.50 (silica, DCM/petroleum ether 2:1); **^{1}H NMR (Benzene-d_6, 60 °C):** δ = 9.23 (s, 2H, β-H), 9.13 (br s, 2H, β-H), 8.87 (s, 2H, β-H), 8.63 (s, 2H, β-H), 8.01 (d, $^3J_{H\text{-}H}$ = 7.3 Hz, 2H, Ar-H), 7.45 (d, $^3J_{H\text{-}H}$ = 7.3 Hz, 2H, Ar-H), 2.51 (s, 3H, CH_3) ppm; **^{19}F NMR (Benzene-d_6):** δ = -79.13 (CF_3), -89.88, -95.41, -121.87, -122.38 ppm; **UV-Vis (DCM):** λ_{max} (ε x 10^{-4}) = 404 (12.54), 419 (11.63), 515 (1.33), 552 (2.36), 620 (1.73) nm (10^4 $M^{-1}.cm^{-1}$); **Fluorescence (DCM):** λ_{ex} = 550 nm, λ_{max} = 641, 696 nm, Φ_{fl} = 14%; **HRMS-ESI:** calculated for $C_{32}H_{19}F_{14}N_4^+$ $[M+H^+]^+$: 725.1381, found 725.1381.

5,15-perfluoropropyl-10-(*p*-anisyl)-corrole 7f

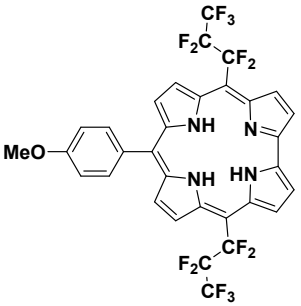

5,15-bisperfluoropropyl-10-(*p*-anisyl)bilane **6f** (212 mg, 0.28 mmol, 1 equiv.) was dissolved in DCM (3.5 mL) before a solution of DDQ (97 mg, 0.43 mmol, 1.5 equiv.) in THF (1 mL) was added while stirring. The reaction mixture was stirred for a further 5 min. After evaporation, the crude product was purified by flash chromatography (DCM/petroleum ether 2:1) followed by precipitation in heptane to afford **7f** (51 mg, 0.07 mmol, 24%).

R_F: 0.50 (silica, DCM/petroleum ether 2:1); **^{1}H NMR (DMSO-d_6):** δ = 9.37 (s, 2H, β-H), 9.07 (s, 2H, β-H), 8.96 (br s, 2H, β-H), 8.56 (s, 2H, β-H), 8.04 (d, $^3J_{H\text{-}H}$ = 7.6 Hz, 2H, Ar-H), 7.36 (d, $^3J_{H\text{-}H}$ = 7.6 Hz, 2H, Ar-H), 4.02 (s, 3H, O-Me) ppm; **^{19}F NMR (DMSO-d_6):** δ = -78.65 (CF_3), -88.98, -95.45, -121.70, -122.60 ppm; **UV-Vis (DCM):** λ_{max} (ε_x 10^{-4}) = 405 (13.50), 420 (12.10), 514 (1.14), 552 (2.07), 620 (1.50) nm (10^4 $M^{-1}.cm^{-1}$); **Fluorescence (DCM)**: λ_{ex} = 550 nm, λ_{max} = 644, 699 nm, Φ_{fl} = 14%; **HRMS-ESI:** calculated for $C_{32}H_{17}F_{14}N_4O^-$ [M-H$^+$]$^-$: 739.1184, found 739.1185.

5,15-perfluoroheptyl-10-(4-cyanophenyl)-corrole 7g

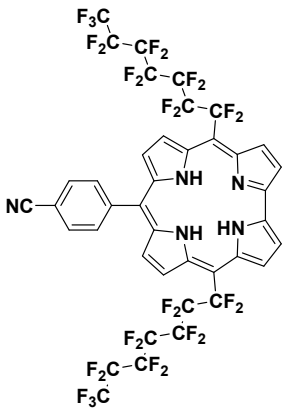

5,15-bis-perfluoroheptyl-10-(5-cyanophenyl)-bilane **6g** (360 mg, 0.31 mmol, 1 equiv.) was dissolved in DCM (4.5 mL) before a solution of DDQ (107 mg, 0.47 mmol, 1.5 equiv.) in THF (1 mL) was added while stirring. The reaction mixture was stirred for a further 5 min. After evaporation, the crude product was purified by flash chromatography (DCM/petroleum ether 1:1) to afford **7g** (23 mg, 0.02 mmol, 7%).

R_F: 0.60 (silica, DCM/petroleum ether 1:1); **^{1}H NMR (Benzene-d_6):** δ = 9.28 (s, 2H, β-H), 9.11 (br s, 2H, β-H), 8.83 (s, 2H, β-H), 8.28 (s, 2H, β-H), 7.74 (d, $^3J_{H\text{-}H}$ = 7.5 Hz, 2H, Ar-H), 7.49 (d, $^3J_{H\text{-}H}$ = 7.5 Hz, 2H, Ar-H), 0.37 (s, 3H, NH) ppm; **^{19}F NMR (Benzene-d_6):** δ = -80.81 (CF_3), -89.25, -94.39, -117.30, -120.48, -121.42, -122.39, -125.90 ppm; **UV-Vis (DCM):** λ_{max} (ε_x 10^{-4}) = 406 (11.73), 420 (11.89), 515 (1.16), 552 (1.96), 618 (1.50) nm (10^4 $M^{-1}.cm^{-1}$); **Fluorescence (DCM):** λ_{ex} = 550 nm, λ_{max} = 637, 695 nm, Φ_{fl} = 12%; **HRMS-ESI:** calculated for $C_{40}H_{14}F_{30}N_5^-$ [M-H$^+$]$^-$: 1134.0776, found 1134.0780.

5,15-perfluoroheptyl-10-(*p*-tolyl)-corrole 7h

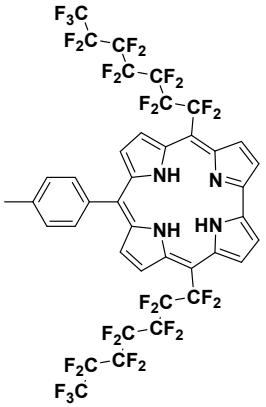

5,15-bis-perfluoroheptyl-10-(*p*-tolyl)-bilane **6h** (450 mg, 0.40 mmol, 1 equiv.) was dissolved in DCM (6 mL) before a solution of DDQ (136 mg, 0.60 mmol, 1.5 equiv.) in THF (1.5 mL) was added while stirring. The reaction mixture was stirred for a further 5 min. After evaporation, the crude product was purified by flash chromatography (DCM/petroleum ether 1:1) to afford **7h** (51 mg, 0.05 mmol, 11%).

R_F: 0.65 (silica, DCM/petroleum ether 1:1); **^{1}H NMR (Benzene-d_6, 60 °C):** δ = 9.25 (s, 2H, β-H), 9.14 (br s, 2H, β-H), 8.89 (s, 2H, β-H), 8.64 (s, 2H, β-H), 8.02 (d, $^3J_{H\text{-}H}$ = 6.4 Hz, 2H, Ar-H), 7.45 (d, $^3J_{H\text{-}H}$ = 6.4 Hz, 2H, Ar-H), 2.52 (s, 3H, CH_3), 0.48 (br s, 3H, NH) ppm; **^{19}F NMR (Benzene-d_6):** δ = -80.82 (CF_3), -89.02, -94.51, -117.29, -120.50, -121.43, -122.40, -125.91 ppm; **UV-Vis (DCM):** λ_{max} (ε x 10^{-4}) = 405 (11.01), 420 (10.20), 516 (1.40), 553 (2.15), 621 (1.59) nm (10^4 $M^{-1}.cm^{-1}$); **Fluorescence (DCM):** λ_{ex} = 550 nm, λ_{max} = 641, 695 nm, Φ_{fl} = 13%; **HRMS-ESI:** calculated for $C_{40}H_{17}F_{30}N_4^-$ [M-H$^+$]$^-$: 1123.0980, found 1123.0977.

5,15-perfluoroheptyl-10-(*p*-anisyl)-corrole 7i

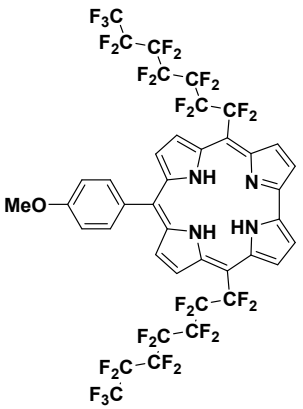

5,15-bis-perfluoroheptyl-10-(*p*-anisyl)-bilane **6i** (425 mg, 0.37 mmol, 1 equiv.) was dissolved in DCM (5.5 mL) before a solution of DDQ (126 mg, 0.56 mmol, 1.5 equiv.) in THF (1.5 mL) was added while stirring. The reaction mixture was stirred for a further 5 min. After evaporation, the crude product was purified by flash chromatography (DCM/petroleum ether 1:1) to afford **7i** (60 mg, 0.05 mmol, 14%).

R_F: 0.40 (silica, DCM/petroleum ether 1:1); **^{1}H NMR (Benzene-d_6, 60 °C):** δ = 9.27 (s, 2H, β-H), 9.17 (br s, 2H, β-H), 8.91 (s, 2H, β-H), 8.65 (s, 2H, β-H), 8.01 (d, $^3J_{H\text{-}H}$ = 8.0 Hz, 2H, Ar-H), 7.24 (d, $^3J_{H\text{-}H}$ = 8.0 Hz, 2H, Ar-H), 3.69 (s, 3H, O-Me) ppm; **^{19}F NMR (Benzene-d_6):** δ = -80.82 (CF_3), -88.95, -94.56, -116.88, -117.66, -120.48, -121.41, -122.39, -125.90 ppm; **UV-Vis (DCM):** λ_{max} (ε x 10^{-4}) = 407 (12.53), 420 (11.26),

517 (1.21), 554 (2.04), 622 (1.49) nm (10^4 $M^{-1}.cm^{-1}$); **Fluorescence (DCM):** λ_{ex} = 550 nm, λ_{max} = 644, 698 nm, Φ_{fl} = 15%; **HRMS-ESI:** calculated for $C_{40}H_{17}F_{30}N_4O^-$ $[M\text{-}H^+]^-$: 1139.0929, found 1139.0927.

Hydrolysis of the *meso*-perfluoroalkyl-corroles

5-perfluoropropyl-10-(4-cyanophenyl)-15-perfluoropropionyl-corrole 8a

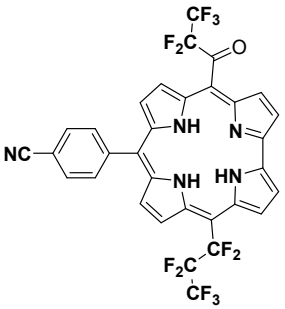

5,15-bis-(heptafluoropropyl)-10-(4-cyanophenyl)-corrole **7d** (22 mg, 30 µmol, 1 equiv.) was dissolved in THF (1 mL) before aqueous NaOH (20 mM, 20 mL) was added while stirring. The reaction mixture was stirred overnight at room temperature before acidification by aqueous HCl (1 M, 2 mL) causing the precipitation of the product(s). The solid was then filtered on a Büchner funnel equipped with sintered glass, washed with water, dissolved in DCM and dried with Na_2SO_4. The crude product was finally purified by flash chromatography (DCM/petroleum ether 1:1) to afford **8a** (8 mg, 0.05 mmol, 36%).

R_F: 0.70 (silica, DCM/petroleum ether 2:1); **^{1}H NMR ($CDCl_3$):** δ = 9.16 (m, 4H, β-H), 9.07 (s, 1H, β-H), 8.93 (s, 1H, β-H), 8.57 (s, 2H, β-H), 8.29 (d, $^3J_{H\text{-}H}$ = 7.7 Hz, 2H, Ar-H), 8.12 (d, $^3J_{H\text{-}H}$ = 7.7 Hz, 2H, Ar-H) ppm; **^{19}F NMR ($CDCl_3$):** δ = -79.18 (CF_3), -80.26 (CF_3), -92.11, -111.61, -122.29 ppm; **UV-Vis (DCM):** λ_{max} (ε x 10^{-4}) = 429 (9.37), 589 (1.81), 665 (0.93) nm (10^4 $M^{-1}.cm^{-1}$); **Fluorescence (DCM):** λ_{ex} = 590 nm, λ_{max} = 688 nm, Φ_{fl} = 2%; **HRMS-ESI:** calculated for $C_{32}H_{14}F_{12}N_5O^-$ $[M\text{-}H^+]^-$: 712.1012, found 712.1011.

5-perfluoroheptyl-10-(4-cyanophenyl)-15-perfluoroheptanoyl-corrole 8b

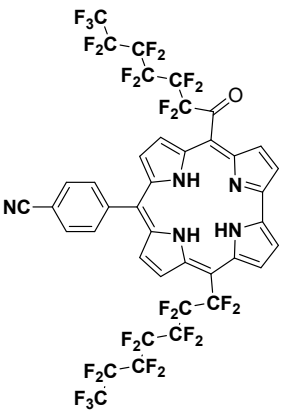

5,15-bis-(pentadecafluoroheptyl)-10-(4-cyanophenyl)-corrole **7g** (34 mg, 30 µmol, 1 equiv.) was dissolved in THF (1 mL) before aqueous NaOH (20 mM, 20 mL) was added while stirring. The reaction mixture was stirred overnight at room temperature before acidification by aqueous HCl (1 M, 2mL) causing the precipitation of the product(s). The solid was then filtered on a Büchner funnel equipped with sintered glass, washed with H_2O, dissolved in DCM and dried with Na_2SO_4. The crude product was finally purified by flash chromatography (DCM/petroleum ether 1:1) to afford **8b** (11 mg, 10 µmol, 33%).

R_F: 0.60 (silica, DCM/petroleum ether 2:1); **^{1}H NMR ($CDCl_3$):** δ = 9.21-914 (br s, 5H, β-H), 8.93 (br s, 1H, β-H), 8.58 (s, 2H, β-H), 8.30 (d, $^3J_{H\text{-}H}$ = 7.7 Hz, 2H, Ar-H), 8.12 (d, $^3J_{H\text{-}H}$ = 7.3 Hz, 2H, Ar-H) ppm;

^{19}F NMR ($CDCl_3$): δ = -80.59 (CF_3), -90.16, -108.38, -117.38, -119.44, -120.52, -120.73, -121.56, -122.54, -125.88 ppm; **UV-Vis (DCM):** λ_{max} (ε x 10^{-4}) = 428 (9.24), 583 (1.84), 653 (0.90) nm (10^4 $M^{-1}.cm^{-1}$); **Fluorescence (DCM):** λ_{ex} = 590 nm, λ_{max} = 693 nm, Φ_{fl} = 3%; **HRMS-ESI:** calculated for $C_{40}H_{14}F_{28}N_5O^-$ [M-H^+]$^-$: 1112.0757, found 1112.0730.

5,15-carboxy-10-(4-carboxyphenyl)-corrole 9

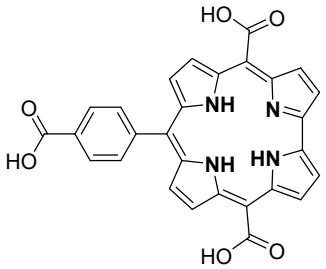

5,15-bis(trifluoromethyl)-10-(4-cyanophenyl)corrole **7a** (32 mg, 60 µmol, 1 equiv.) was dissolved in THF (0.5 mL) before a saturated aqueous NaOH solution (6 mL) was added while stirring. The reaction mixture was stirred at reflux overnight before acidification by aqueous HCl (1 M) causing the precipitation of the product(s). The precipitate formed was then filtered on a Büchner funnel equipped with sintered glass and washed with H_2O several times to afford **9** as a dark solid (19 mg, 19 µmol, 32%). Alternative procedure, starting from **7d** (22 mg, 30 µmol) in the same conditions afforded **9** (18 mg, 36 µmol, 60%).

^{1}H NMR (Methanol-d_4): δ = 9.67 (d, $^3J_{H-H}$ = 4.5 Hz, 2H, β-H), 9.38 (d, $^3J_{H-H}$ = 4.5 Hz, 2H, β-H), 9.19 (d, $^3J_{H-H}$ = 3.7 Hz, 2H, β-H), 8.55 (d, $^3J_{H-H}$ = 4.8 Hz, 2H, β-H), 8.48 (d, $^3J_{H-H}$ = 8.2 Hz, 2H, Ar-H), 8.31 (d, $^3J_{H-H}$ = 7.7 Hz, 2H, Ar-H) ppm; **^{1}H NMR (D_2O+NaOD):** δ = 9.11 (d, $^3J_{H-H}$ = 3.6 Hz, 2H, β-H), 9.01 (d, $^3J_{H-H}$ = 4.5 Hz, 2H, β-H), 8.95 (d, $^3J_{H-H}$ = 4.5 Hz, 2H, β-H), 8.42 (d, $^3J_{H-H}$ = 3.6 Hz, 2H, β-H), 8.03 (s, 4H, Ar-H), 8.29 ppm (d, $^3J_{H-H}$ = 7.9 Hz, 2H, Ar-H); **UV-Vis (MeOH):** λ_{max} (ε x 10^{-4}) = 414 (4.41) 574 (0.74), 639 (0.54) nm (10^4 $M^{-1}.cm^{-1}$); **Fluorescence (MeOH):** λ_{ex} = 585 nm, λ_{max} = 669 nm, Φ_{fl} = 2%; **HRMS-ESI:** calculated for $C_{28}H_{17}N_4O_6^-$ [M-H^+]$^-$: 505.1154, found 505.1156.

Mass, ^{1}H and ^{13}C NMR spectra

Bilanes

5,15-bis-trifluoromethyl-10-(4-cyanophenyl)-bilane 6a

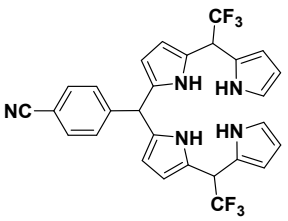

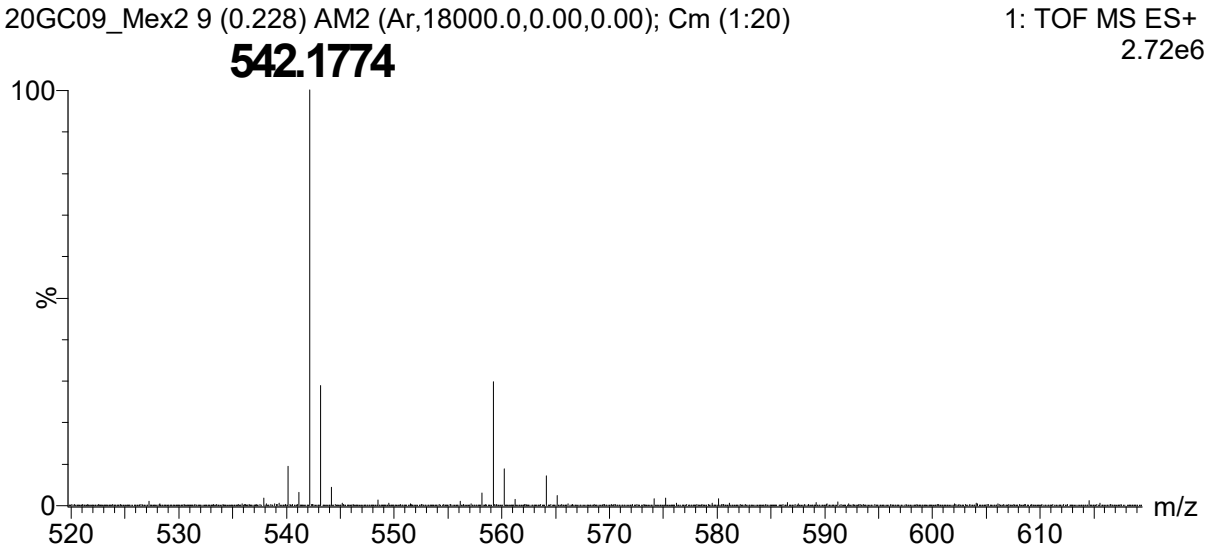

Figure S22: HRMS spectrum of bilane **6a**.

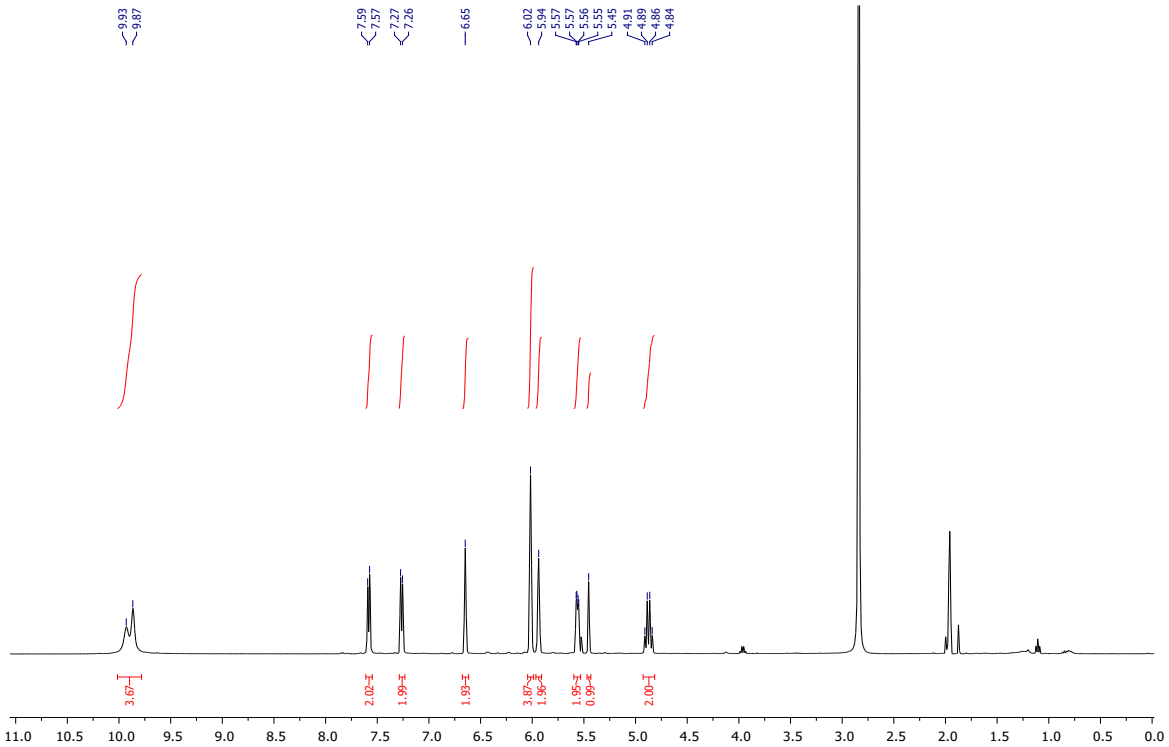

Figure S23: ^{1}H NMR spectrum of bilane **6a** (acetone-d_6, 298 K).

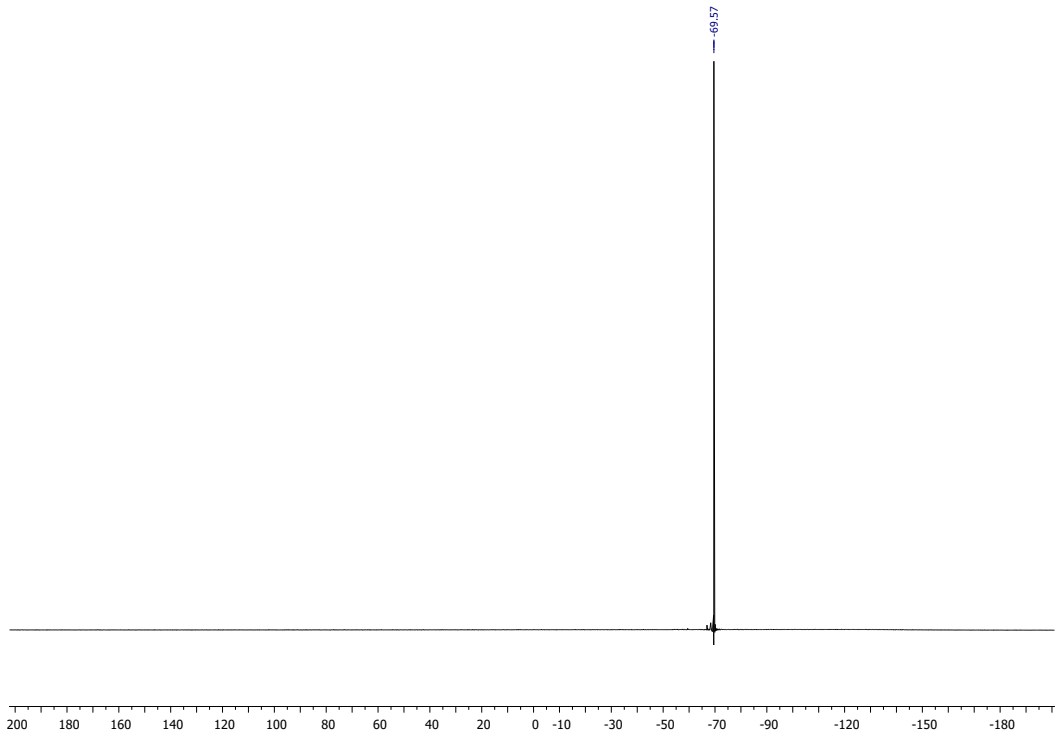

Figure S24: ^{19}F NMR spectrum of bilane **6a** (acetone-d_6, 298 K).

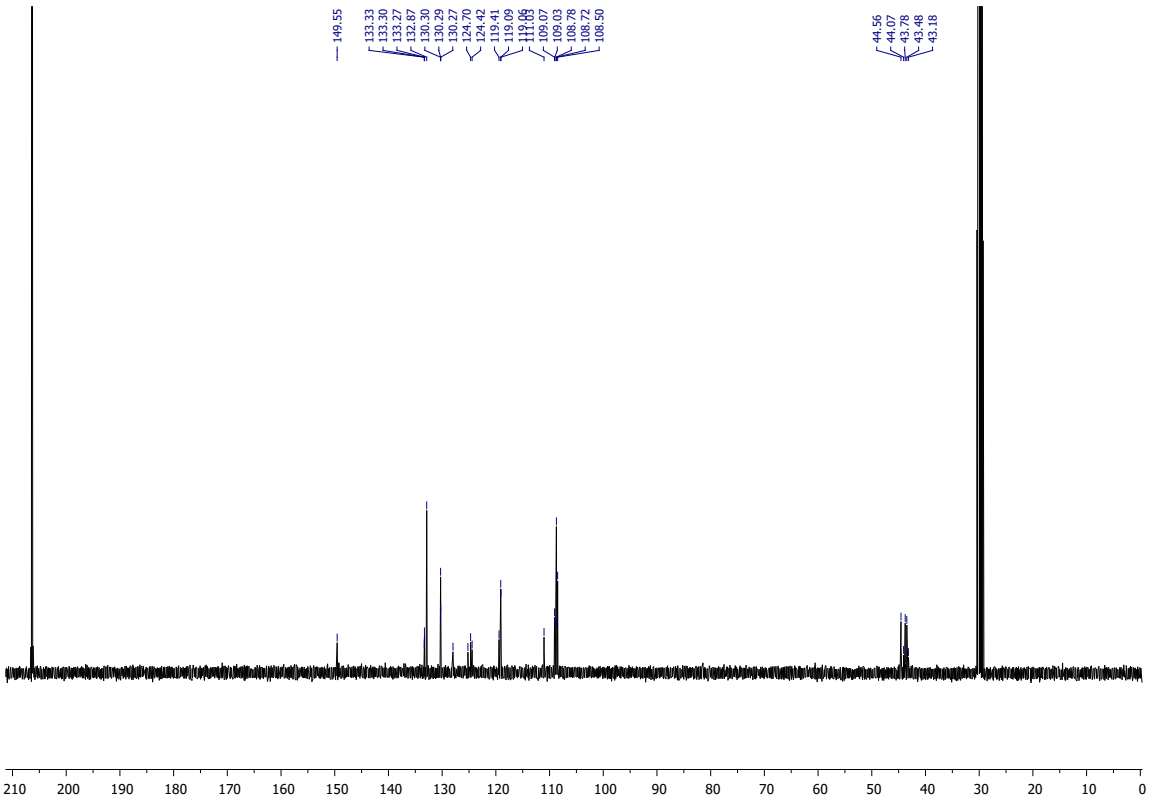

Figure S25: ^{13}C NMR spectrum of bilane **6a** (acetone-d_6, 298 K).

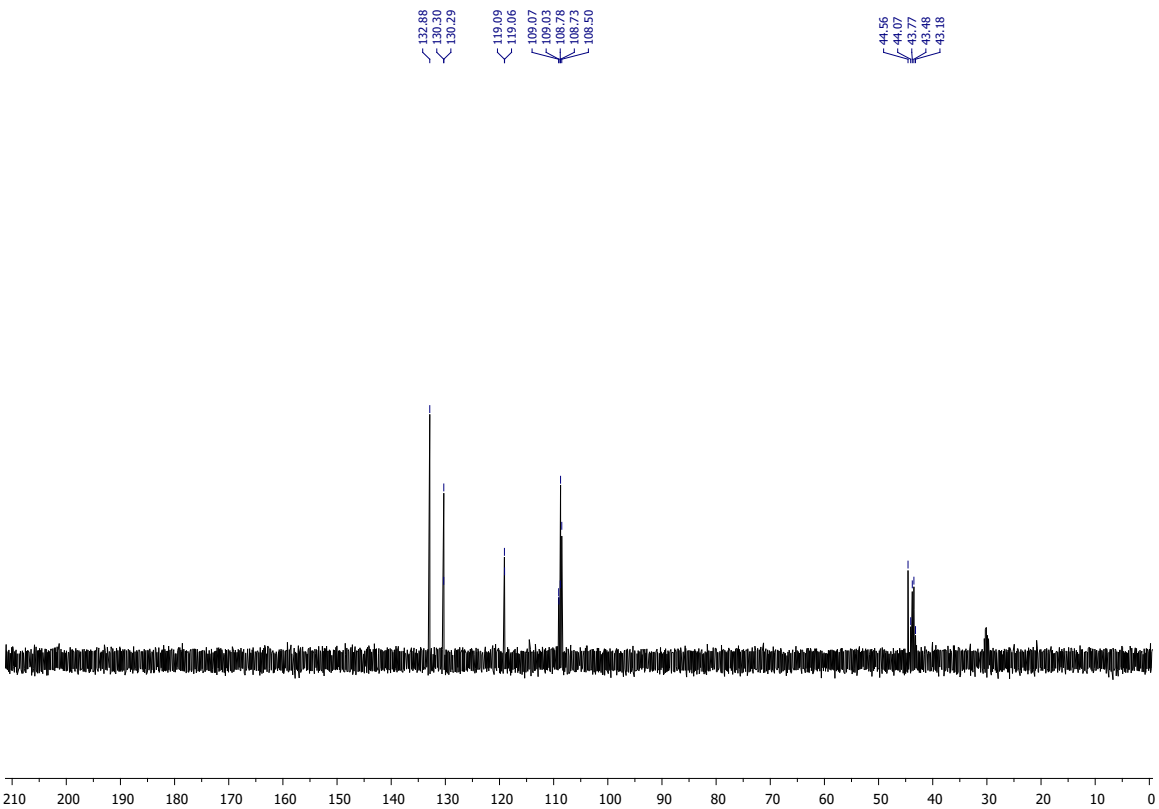

Figure S26: ^{13}C NMR (DEPT 135) spectrum of bilane **6a** (acetone-d_6, 298 K).

5,15-bis-trifluoromethyl-10-(*p*-tolyl)-bilane 6b

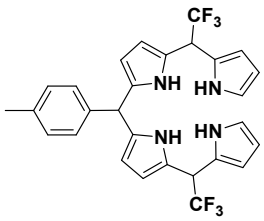

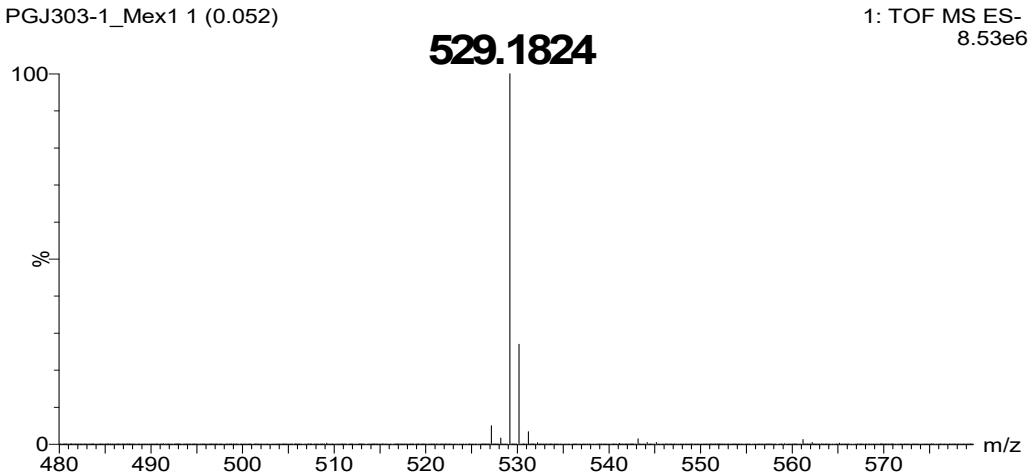

Figure S27: HRMS spectrum of bilane **6b**.

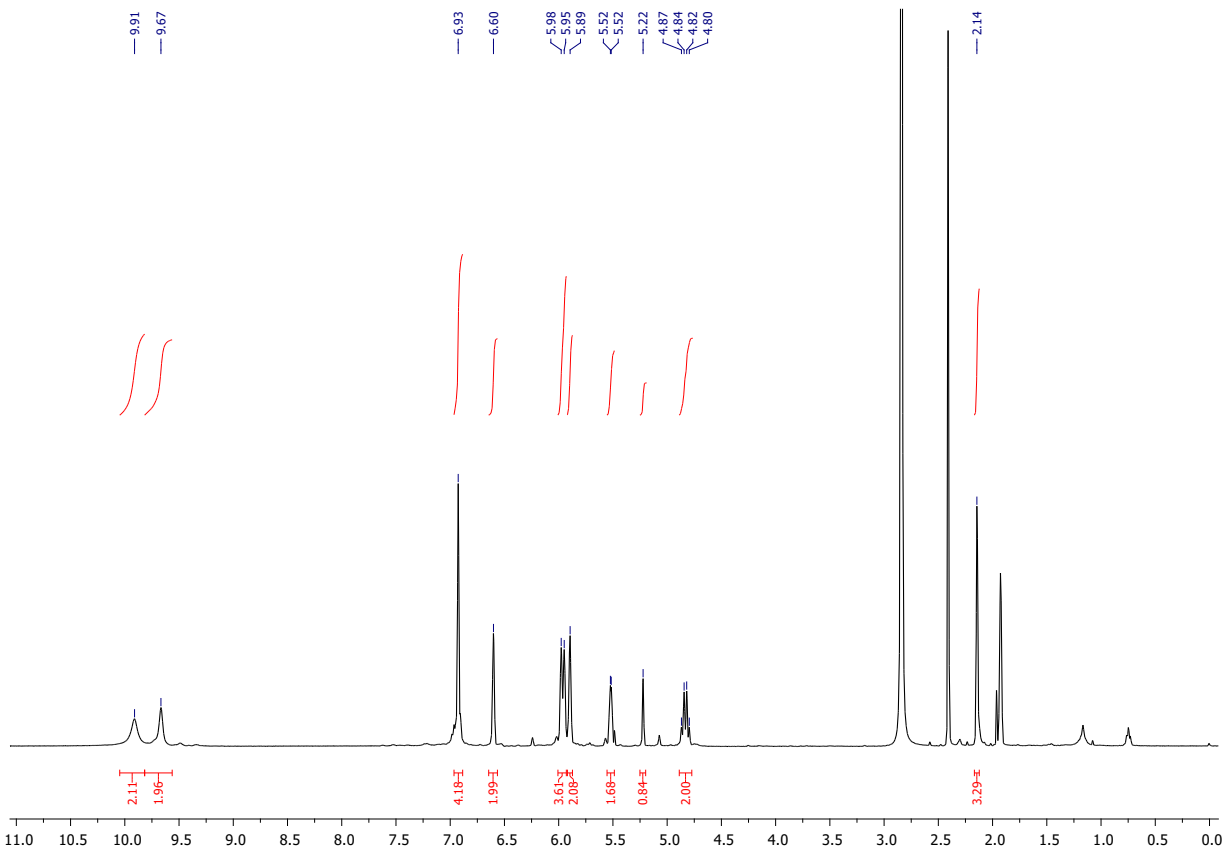

Figure S28: ^{1}H NMR spectrum of bilane **6b** (acetone-d_6, 298 K).

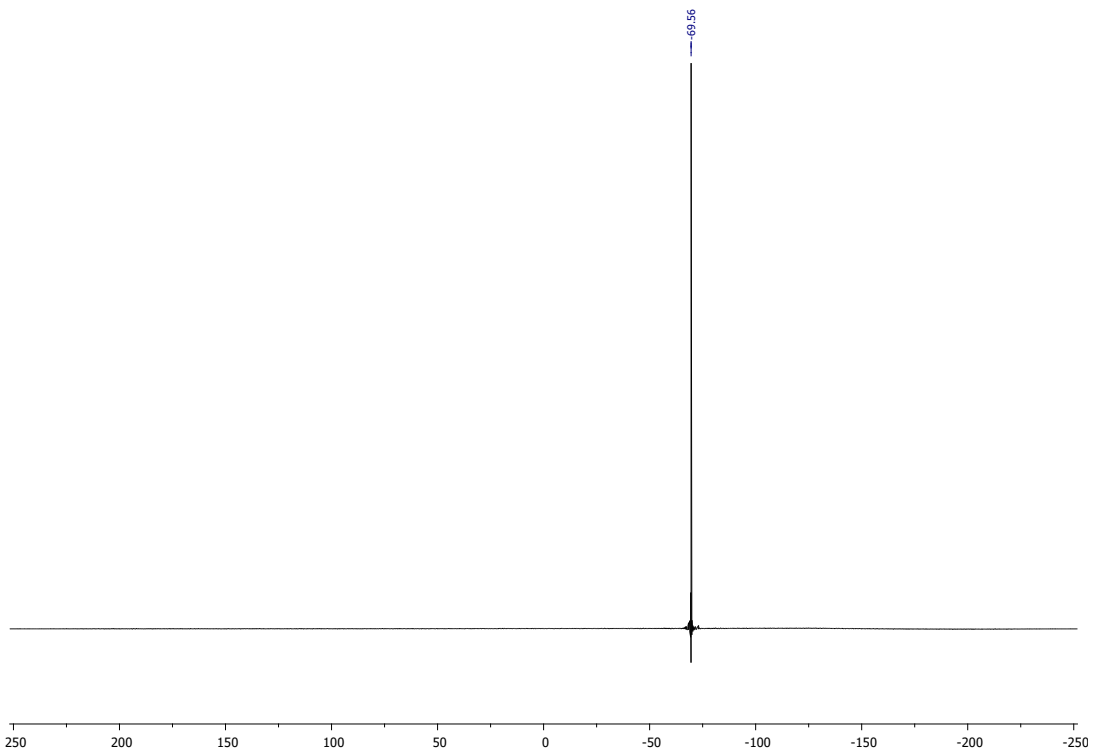

Figure S29: ^{19}F NMR spectrum of bilane **6b** (acetone-d_6, 298 K).

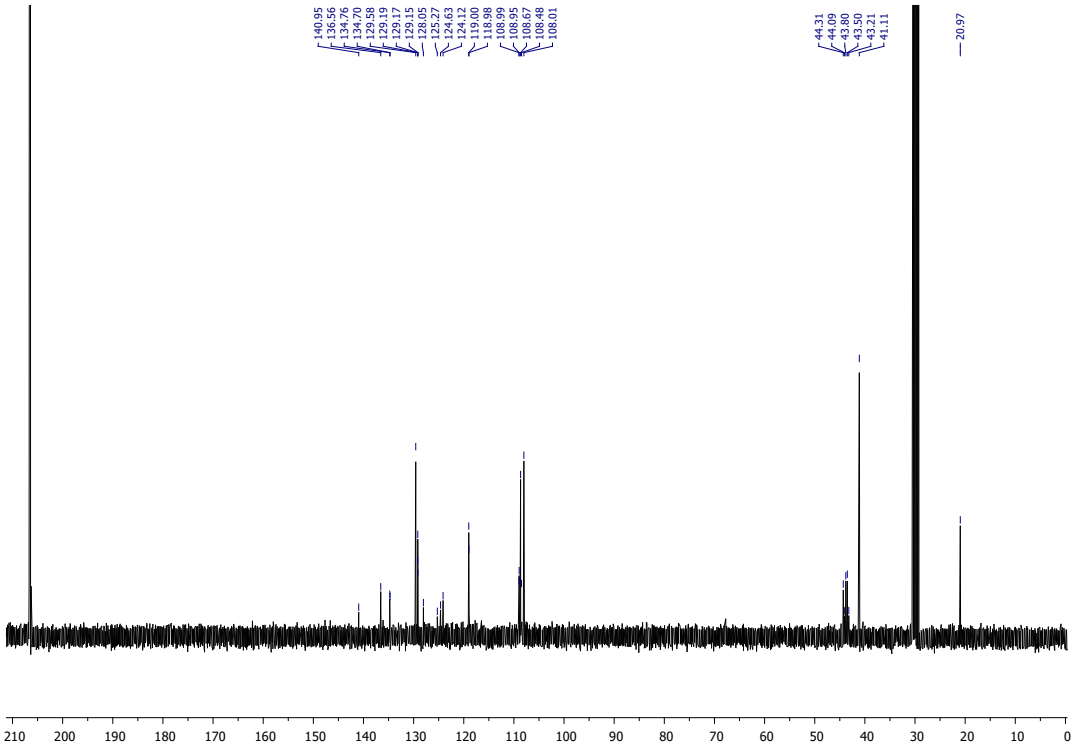

Figure S30: ^{13}C NMR spectrum of bilane **6b** (acetone-d_6, 298 K).

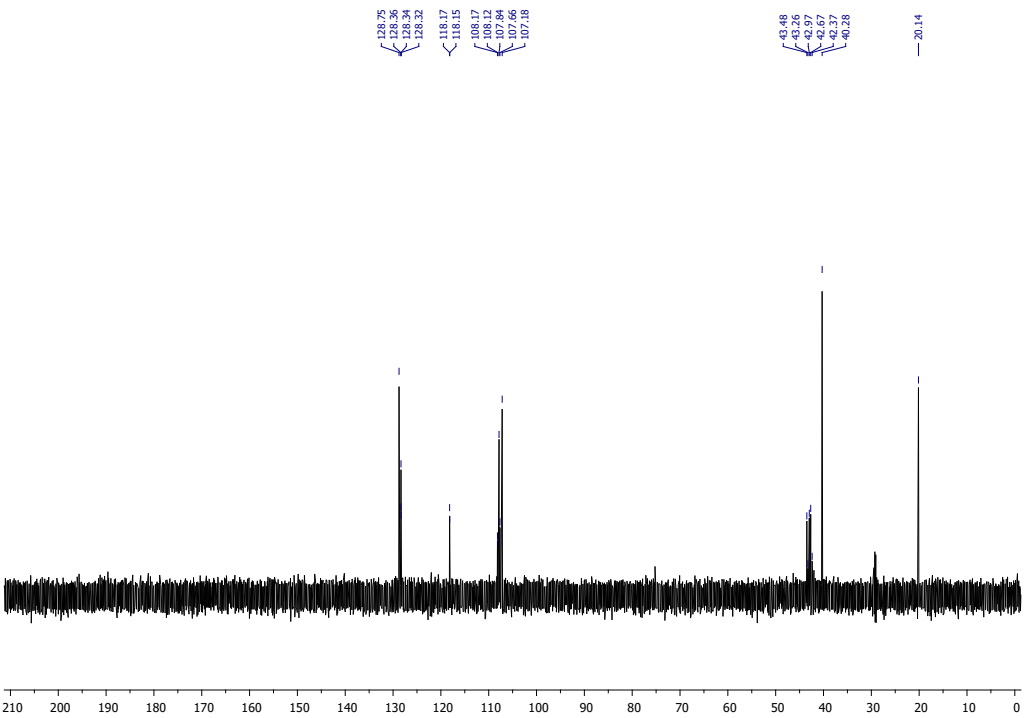

Figure S31: ^{13}C NMR (DEPT 135) spectrum of bilane **6b** (acetone-d_6, 298 K).

5,15-bis-trifluoromethyl-10-(*p*-anisyl)-bilane 6c

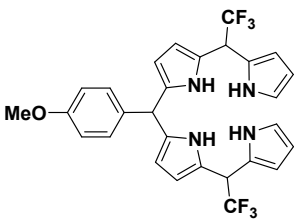

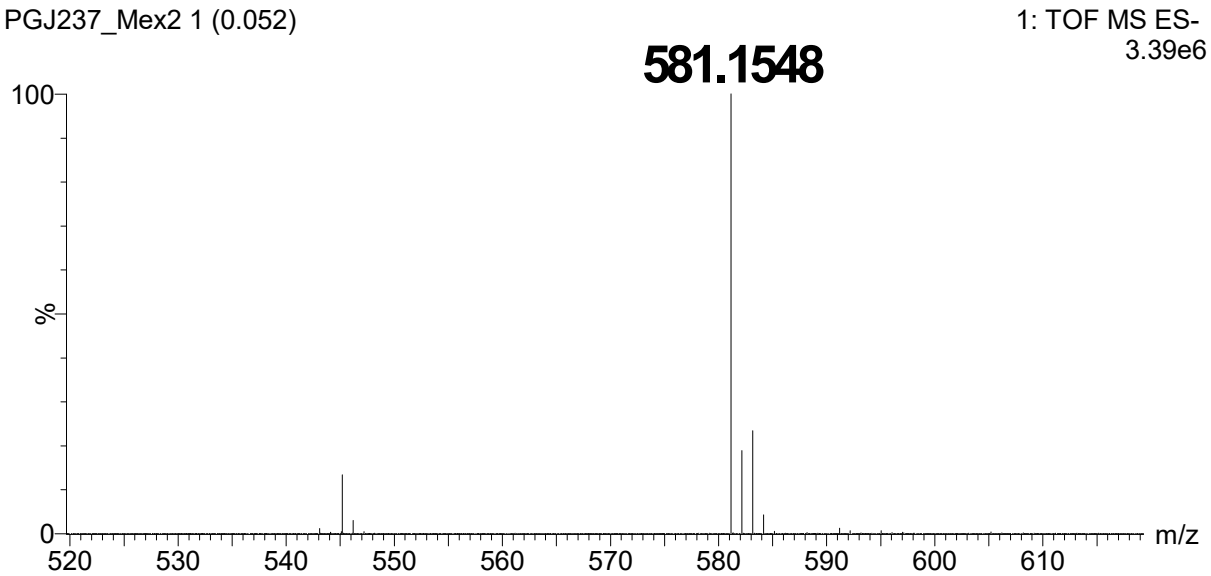

Figure S32: HRMS spectrum of bilane **6c**.

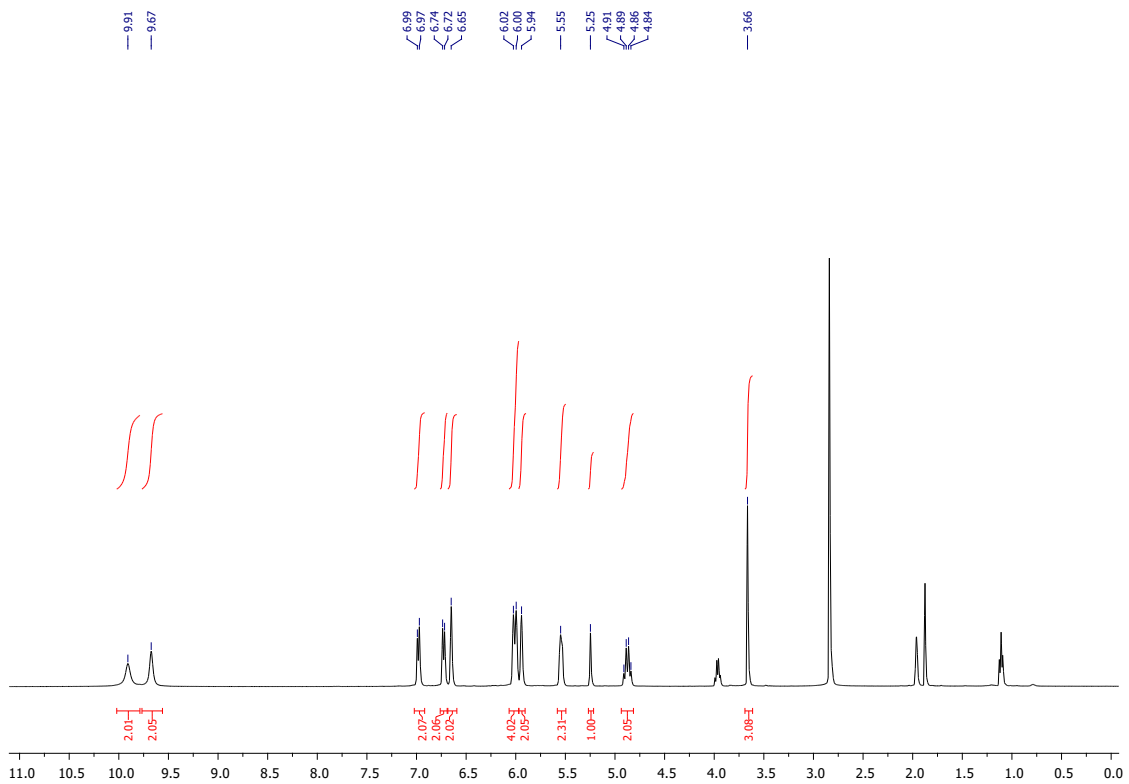

Figure S33: ^{1}H NMR spectrum of bilane **6c** (acetone-d_6, 298 K).

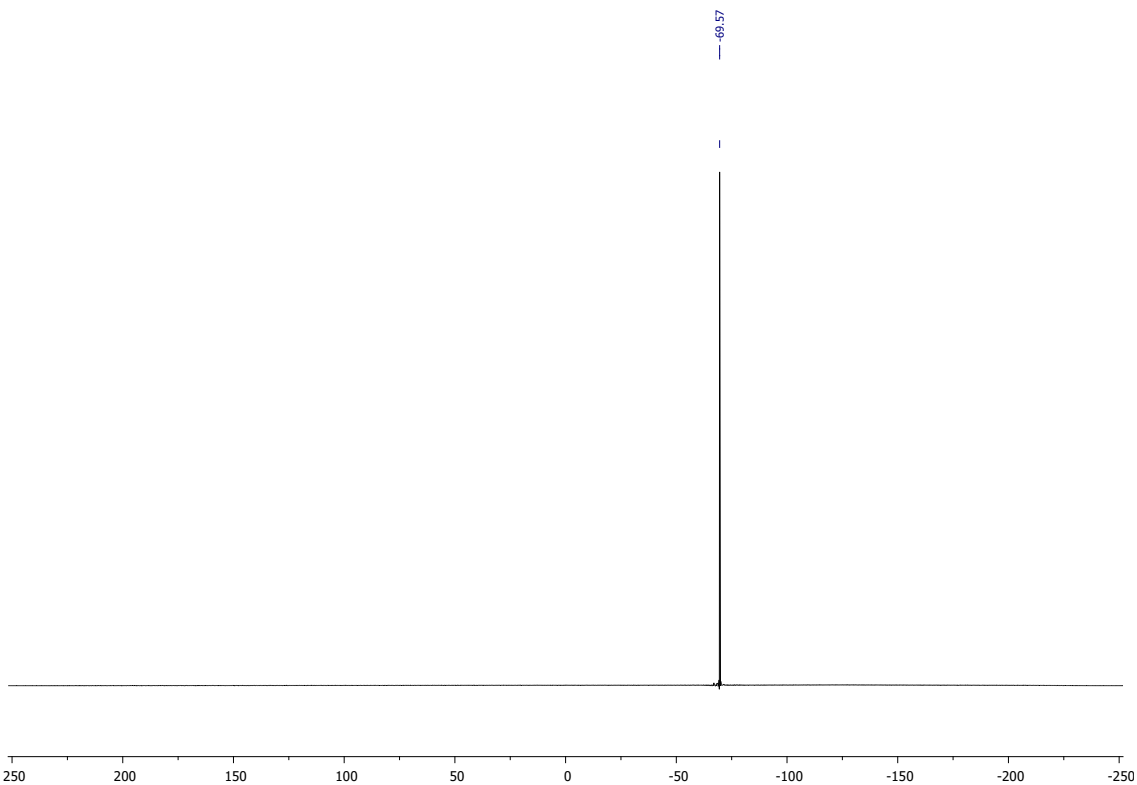

Figure S34: ^{19}F NMR spectrum of bilane **6c** (acetone-d_6, 298 K).

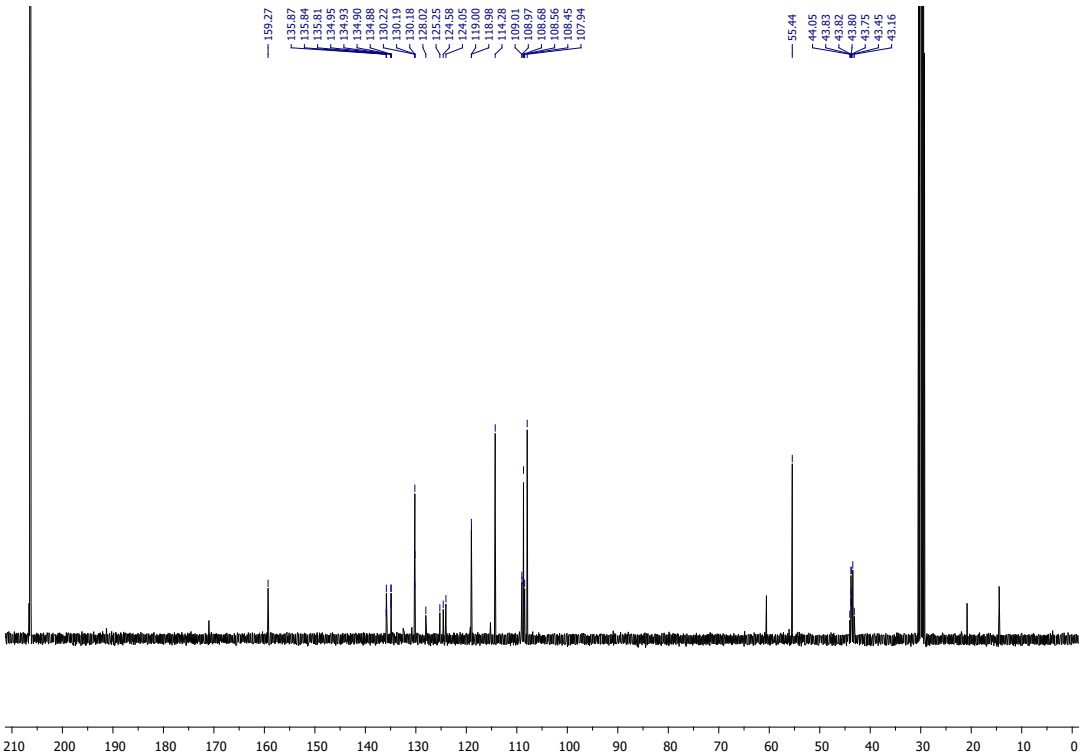

Figure S35: ^{13}C NMR spectrum of bilane **6c** (acetone-d_6, 298 K).

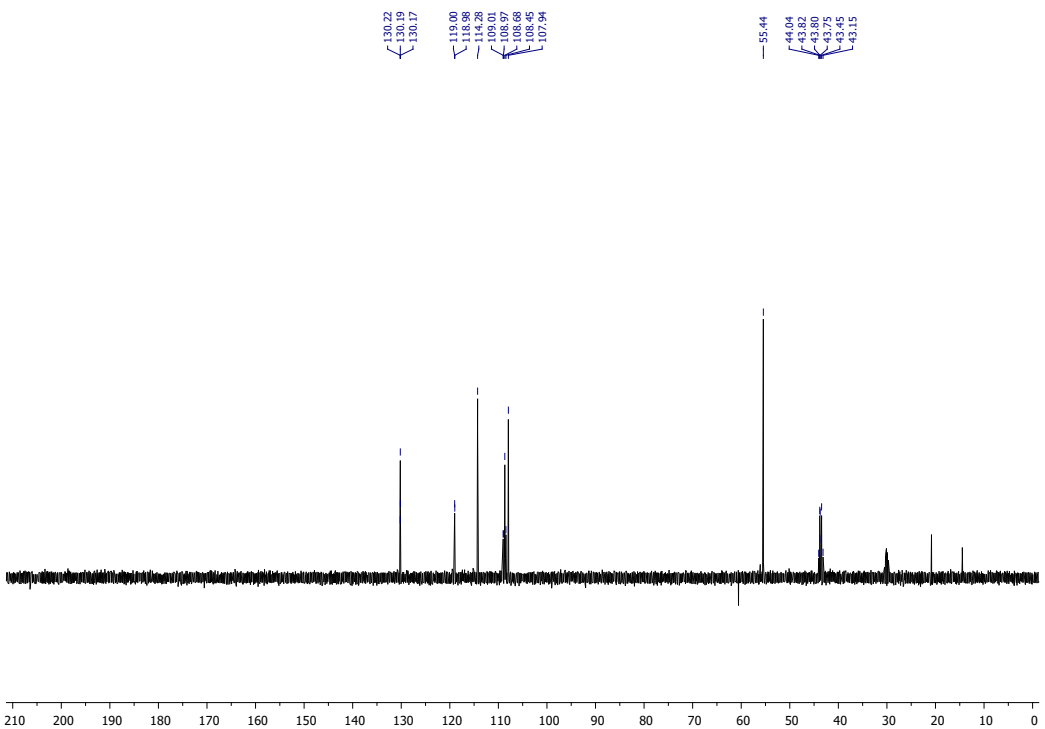

Figure S36: ^{13}C NMR (DEPT 135) spectrum of bilane **6c** (acetone-d_6, 298 K).

5,15-bis-trifluoromethyl-10-(pentafluorophenyl)-bilane 6j

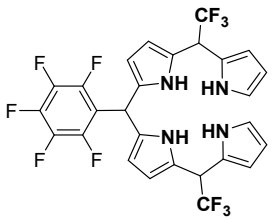

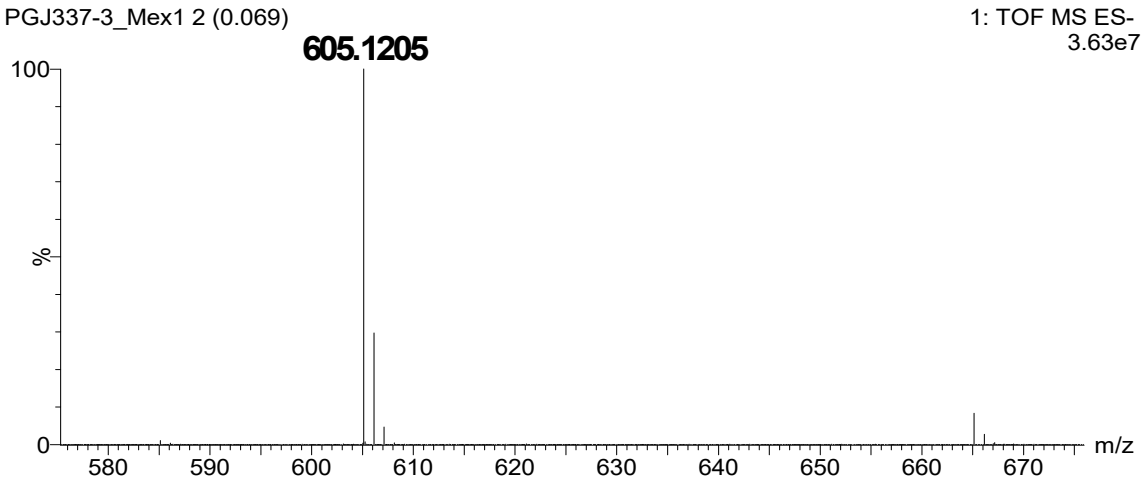

Figure S37: HRMS spectrum of bilane **6j**.

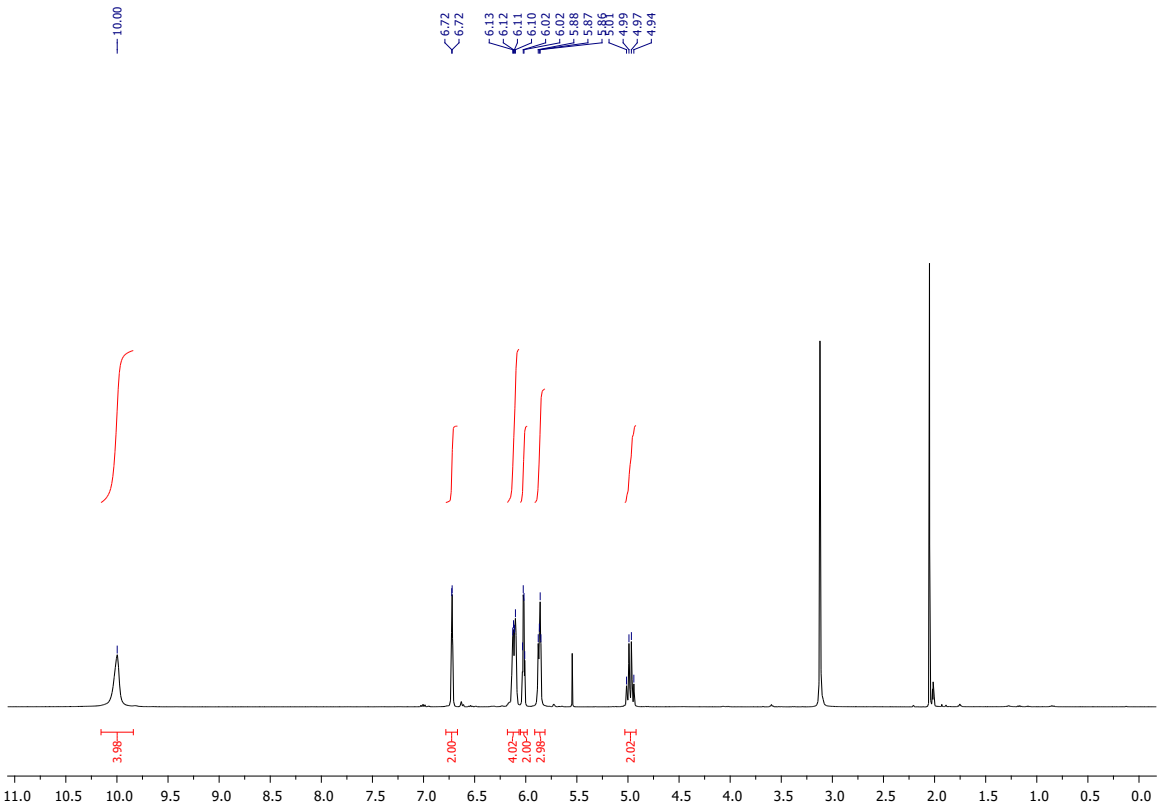

Figure S38: ^{1}H NMR spectrum of bilane **6j** (acetone-d_6, 298 K).

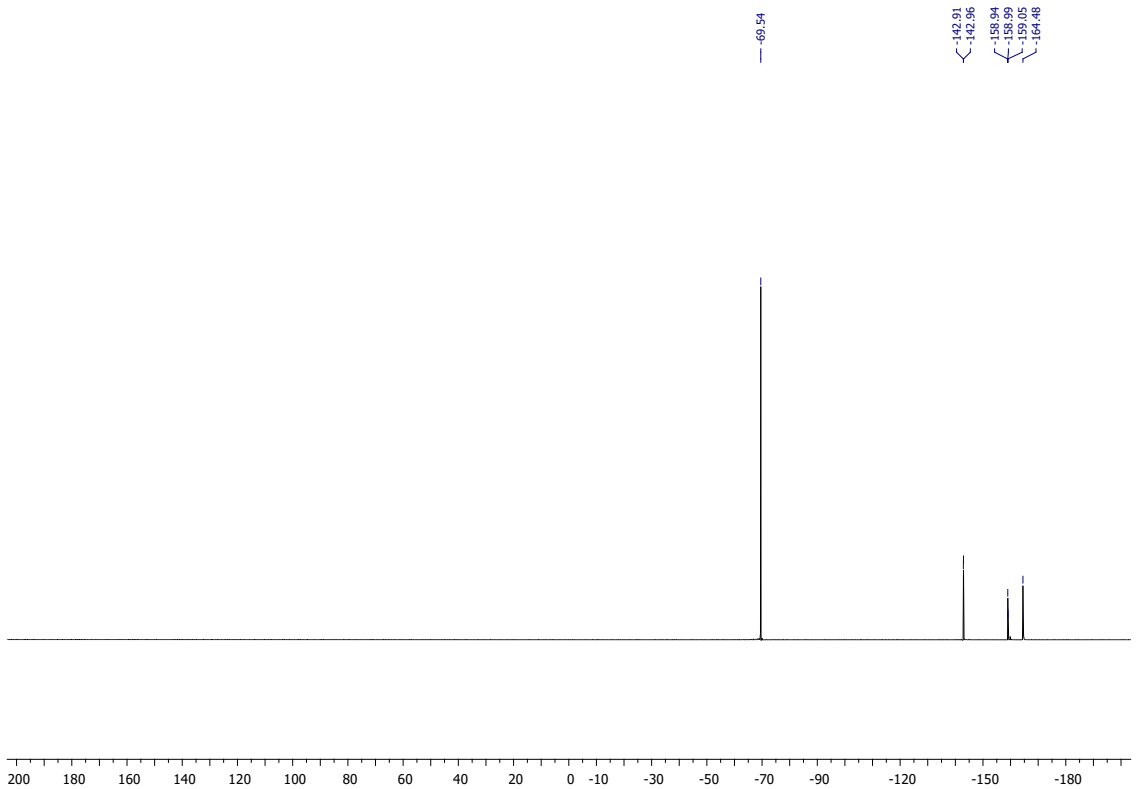

Figure S39: ^{19}F NMR spectrum of bilane **6j** (acetone-d_6, 298 K).

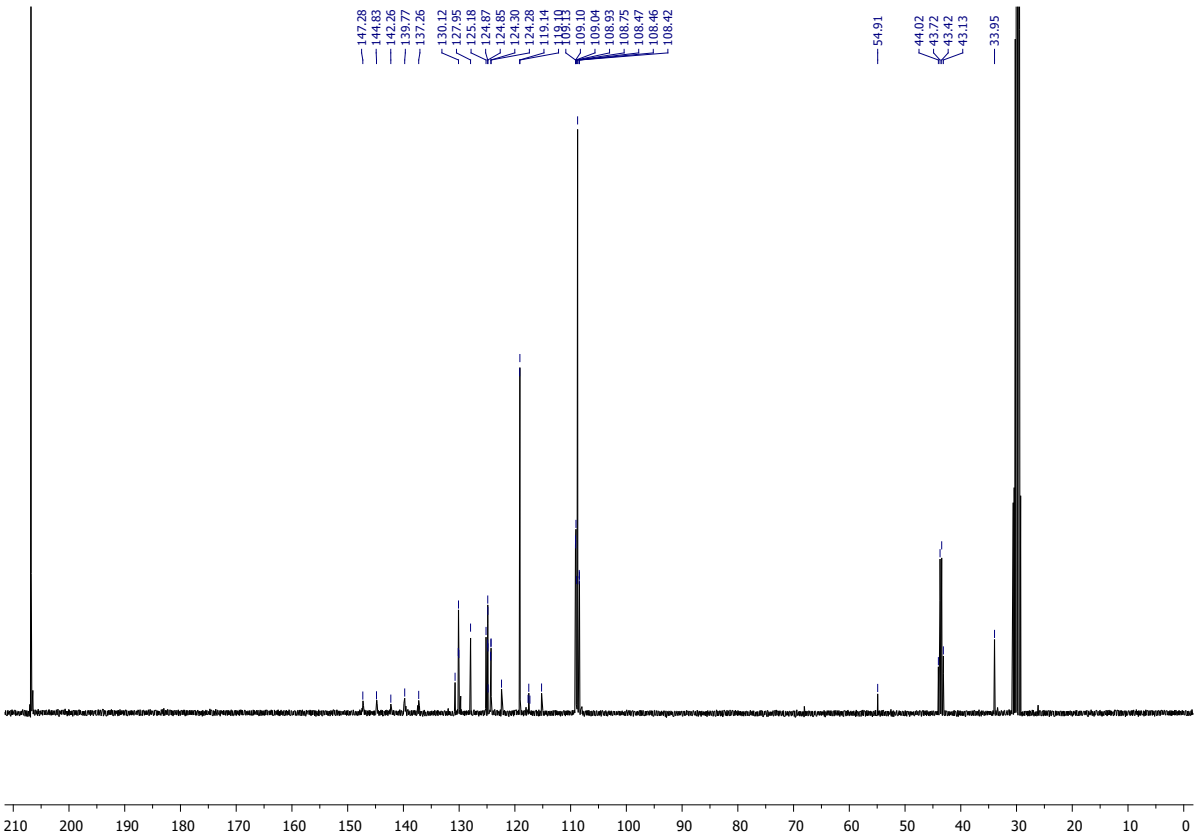

Figure S40: ^{13}C NMR spectrum of bilane **6j** (acetone-d_6, 298 K).

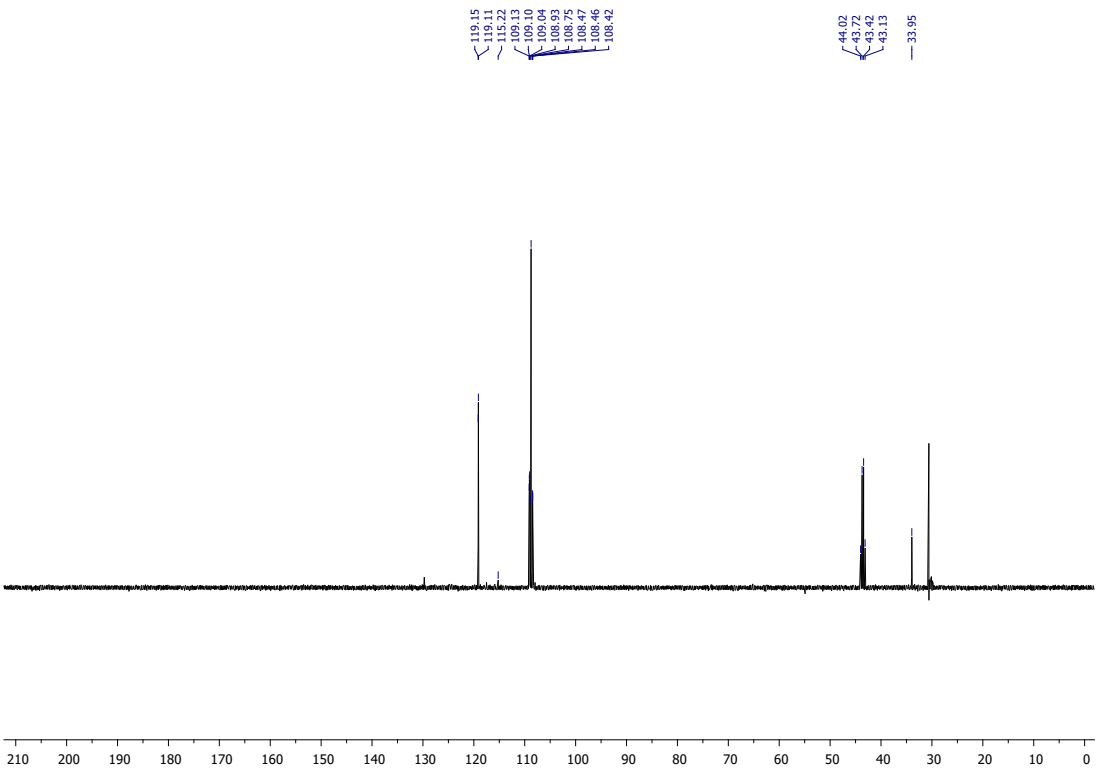

Figure S41: ^{13}C NMR (DEPT 135) spectrum of bilane **6j** (acetone-d_6, 298 K).

5,15-bis-perfluoropropyl-10-(4-cyanophenyl)-bilane 6d

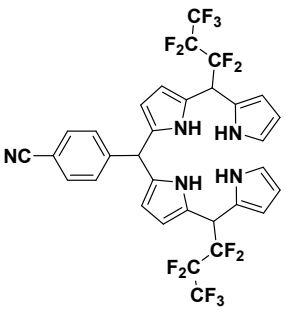

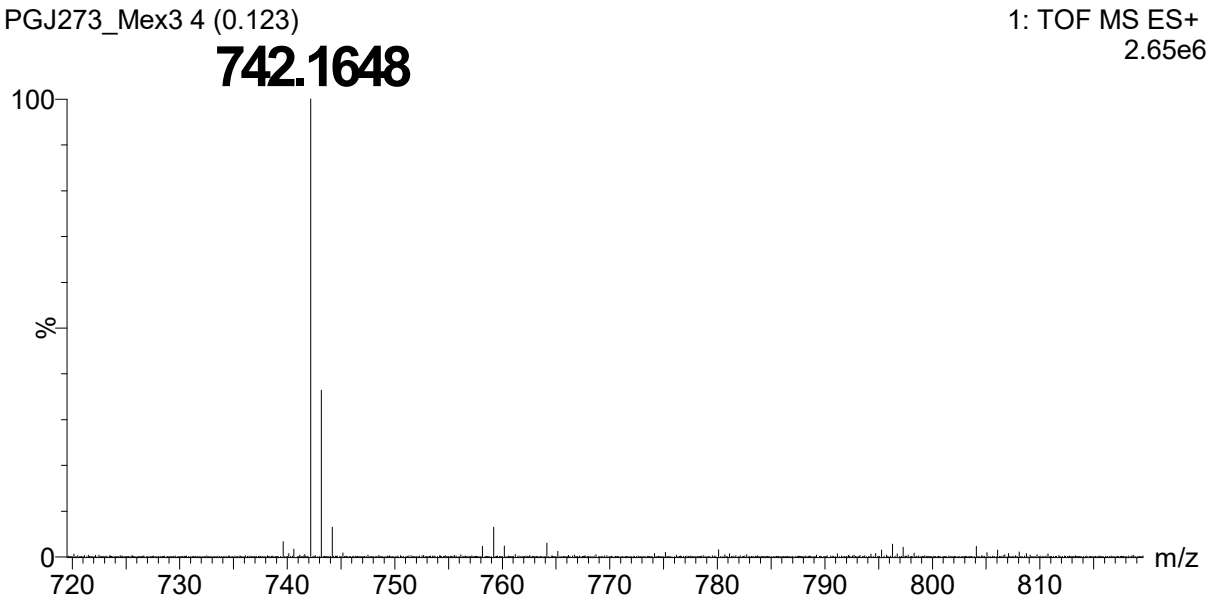

Figure S42: HRMS spectrum of bilane **6d**.

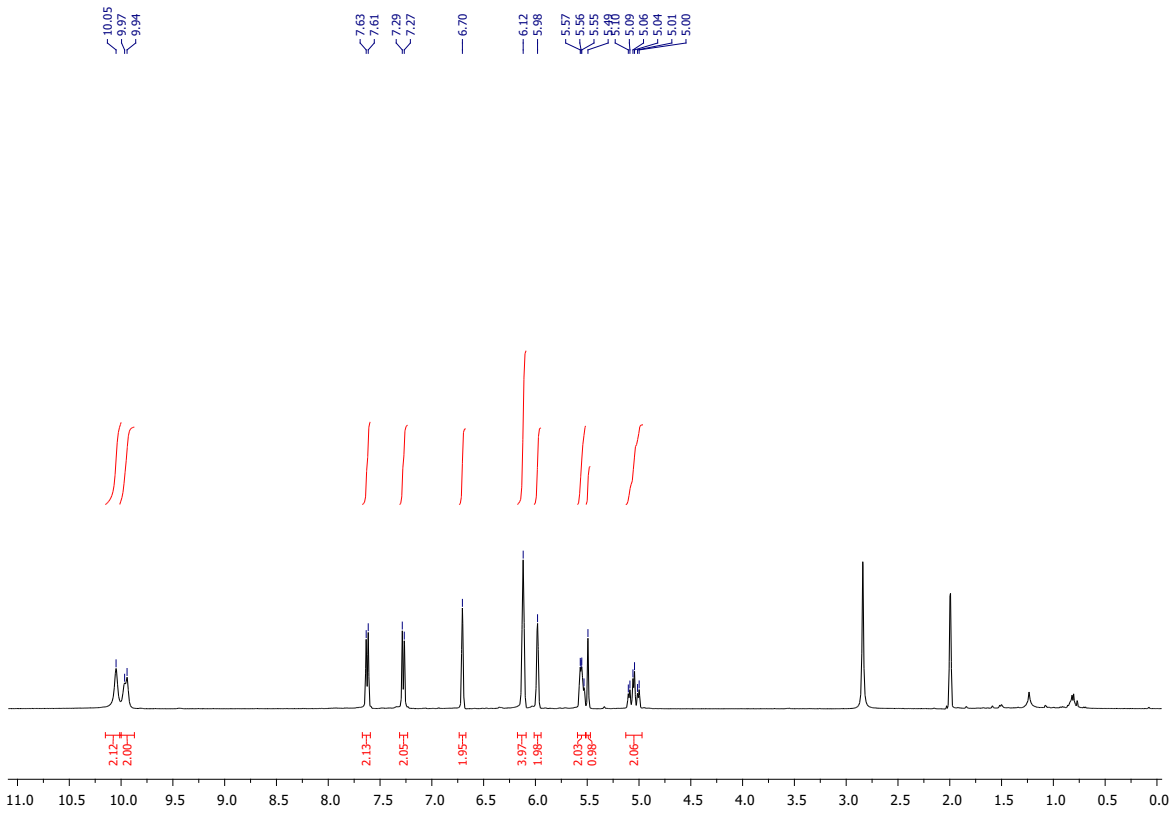

Figure S43: ^{1}H NMR spectrum of bilane **6d** (acetone-d_6, 298 K).

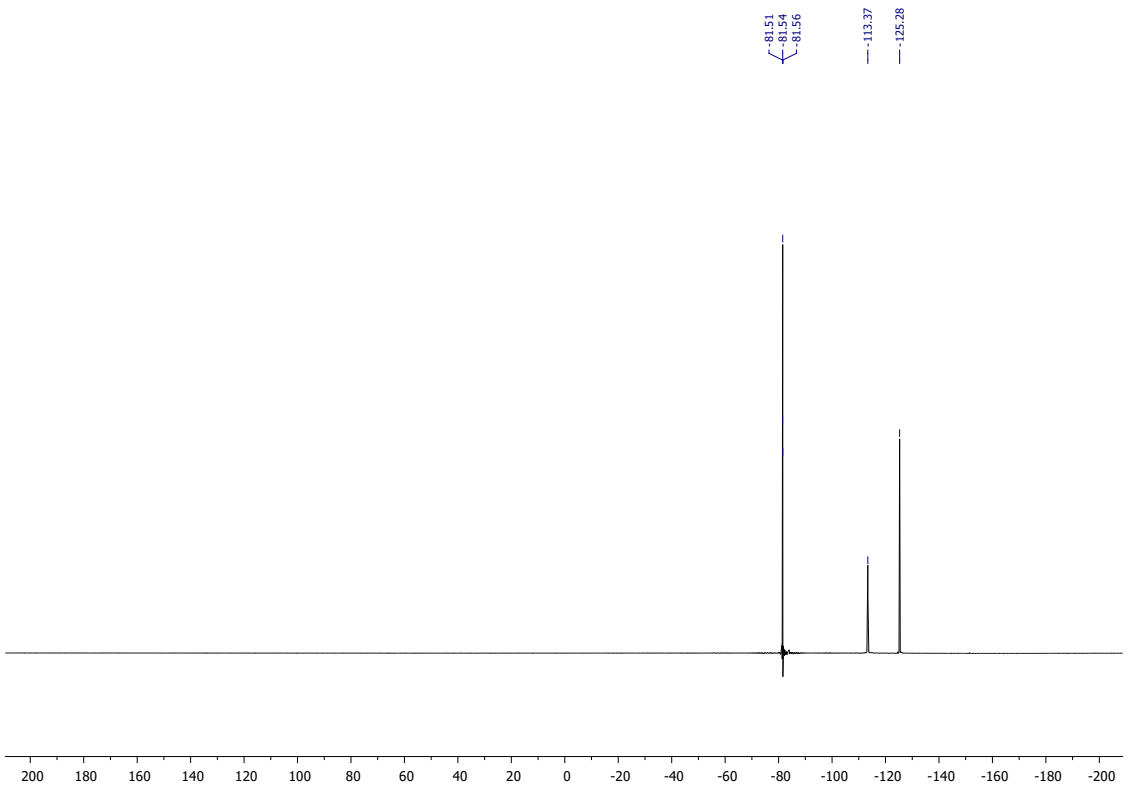

Figure S44: ^{19}F NMR spectrum of bilane **6d** (acetone-d_6, 298 K).

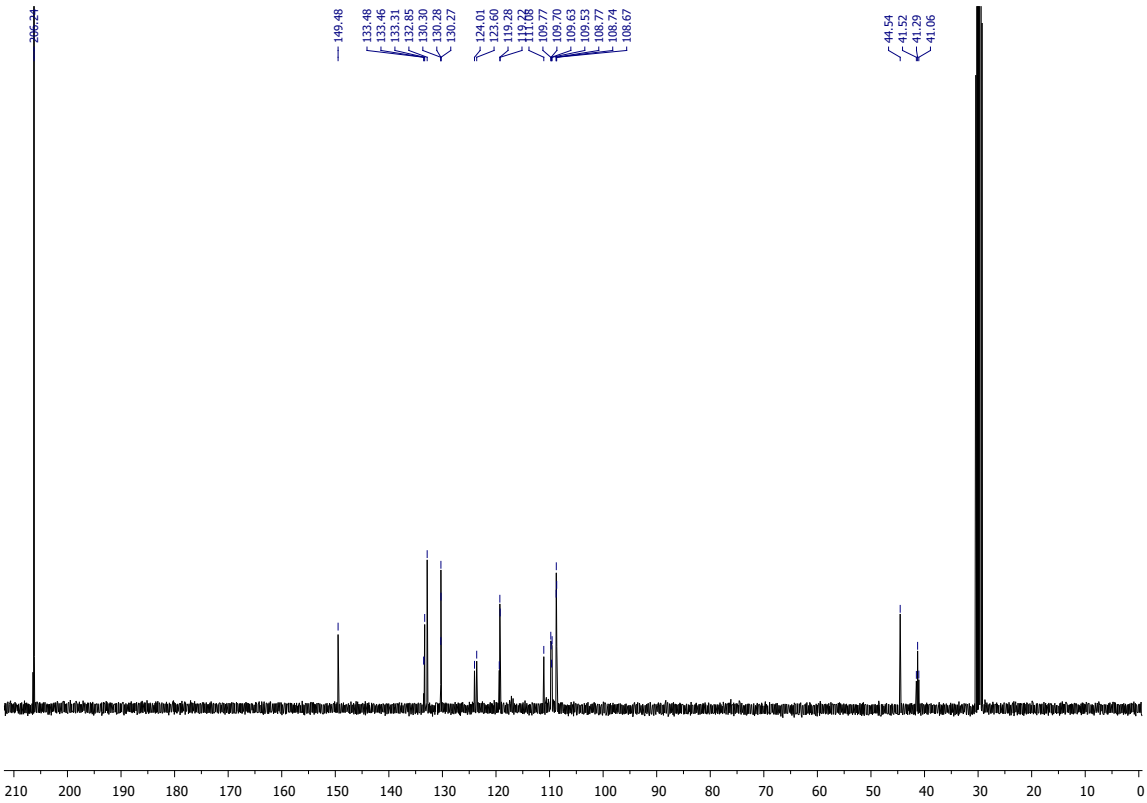

Figure S45: ^{13}C NMR spectrum of bilane **6d** (acetone-d_6, 298 K).

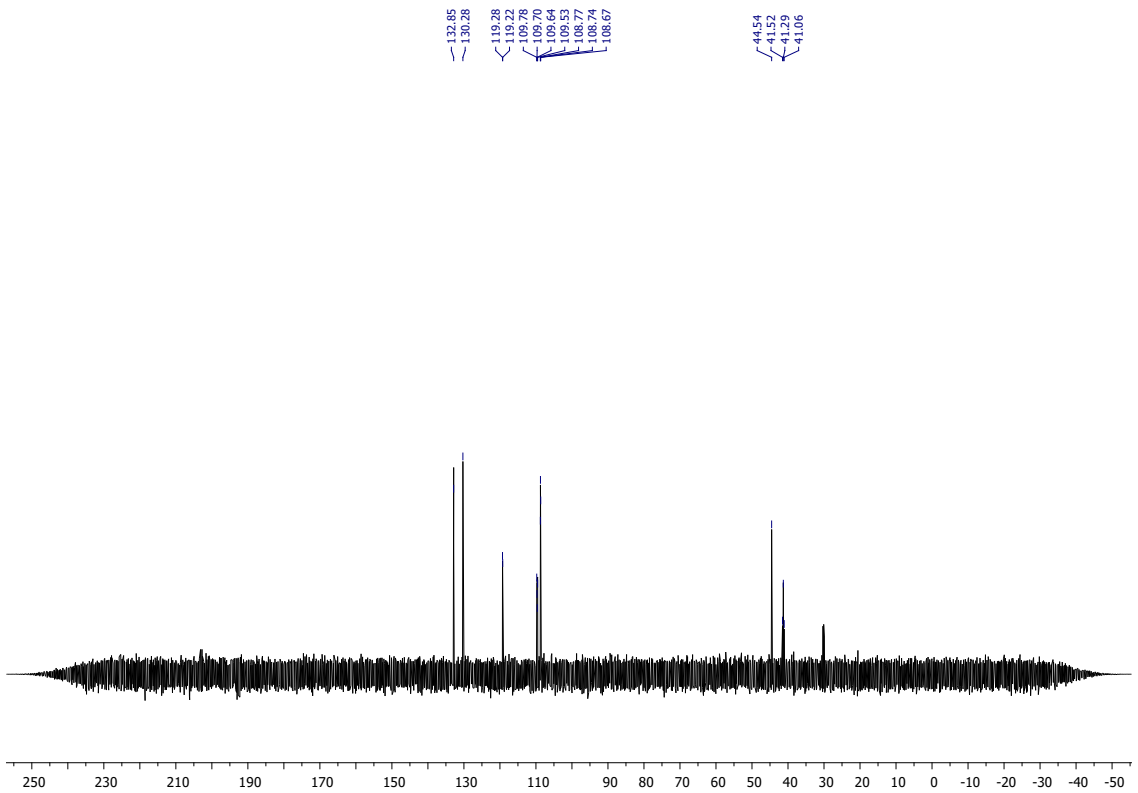

Figure S46: ^{13}C NMR (DEPT 135) spectrum of bilane **6d** (acetone-d_6, 298 K).

5,15-bis-perfluoropropyl-10-(*p*-tolyl)-bilane 6e

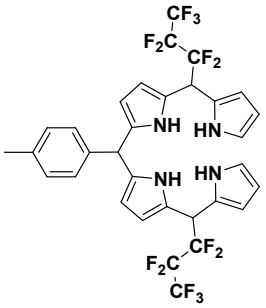

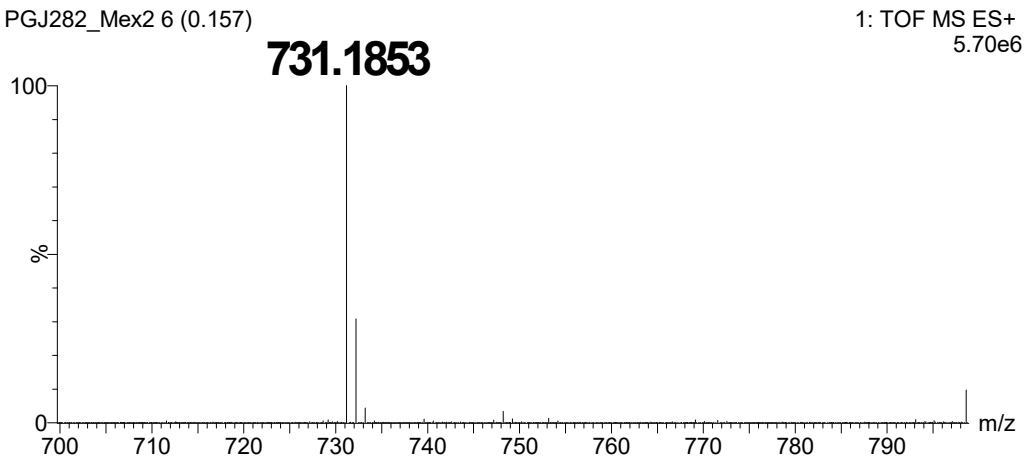

Figure S47: HRMS spectrum of bilane **6e**.

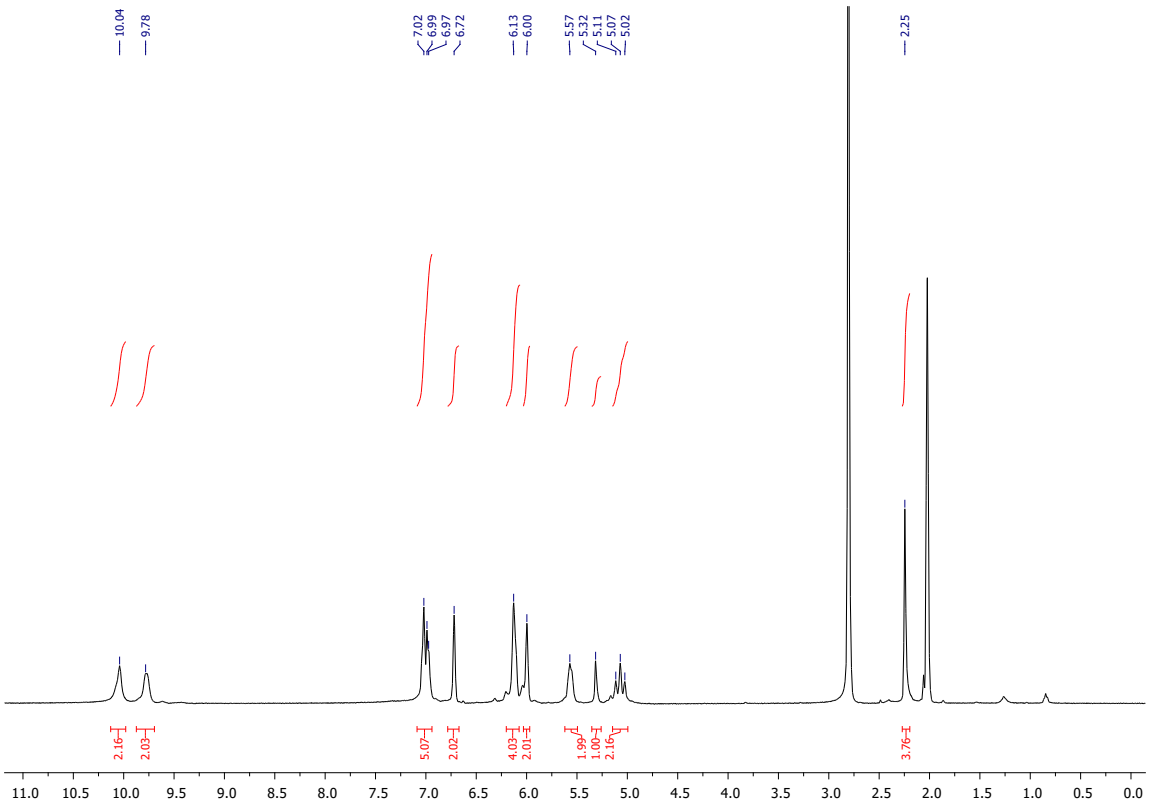

Figure S48: ^{1}H NMR spectrum of bilane **6e** (acetone-d_6, 298 K).

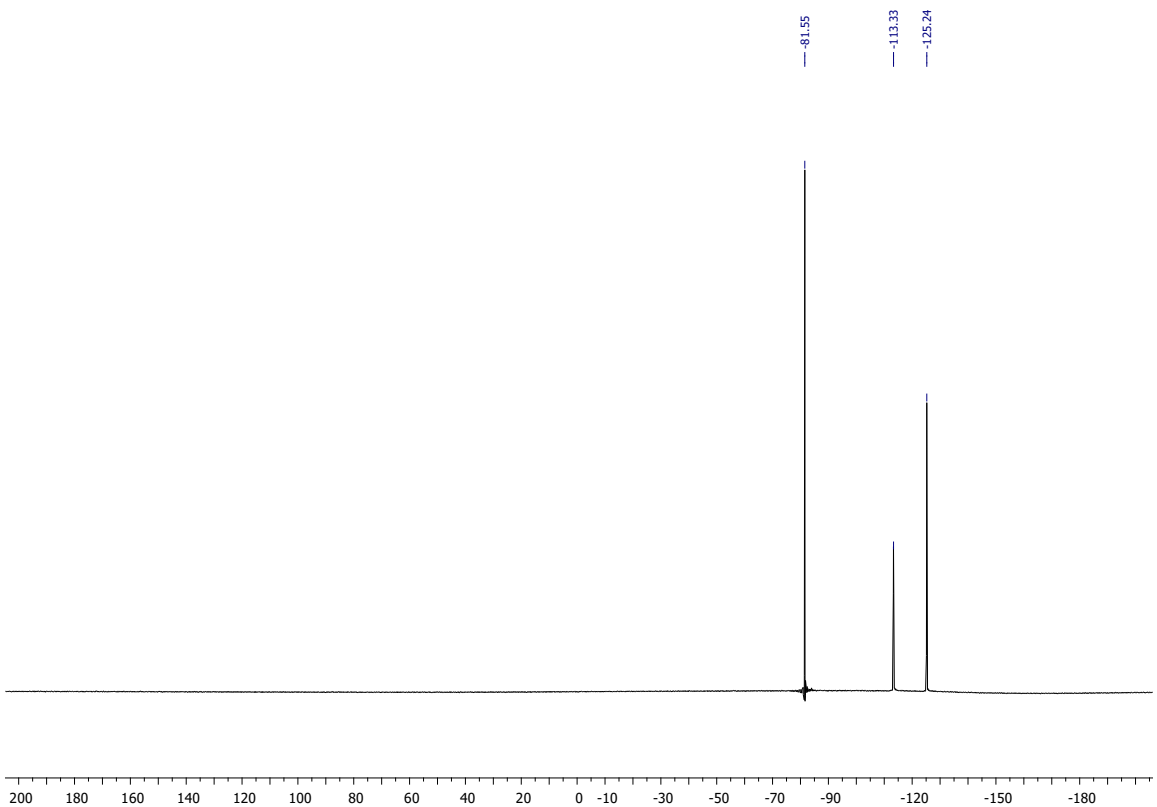

Figure S49: ^{19}F NMR spectrum of bilane **6e** (acetone-d_6, 298 K).

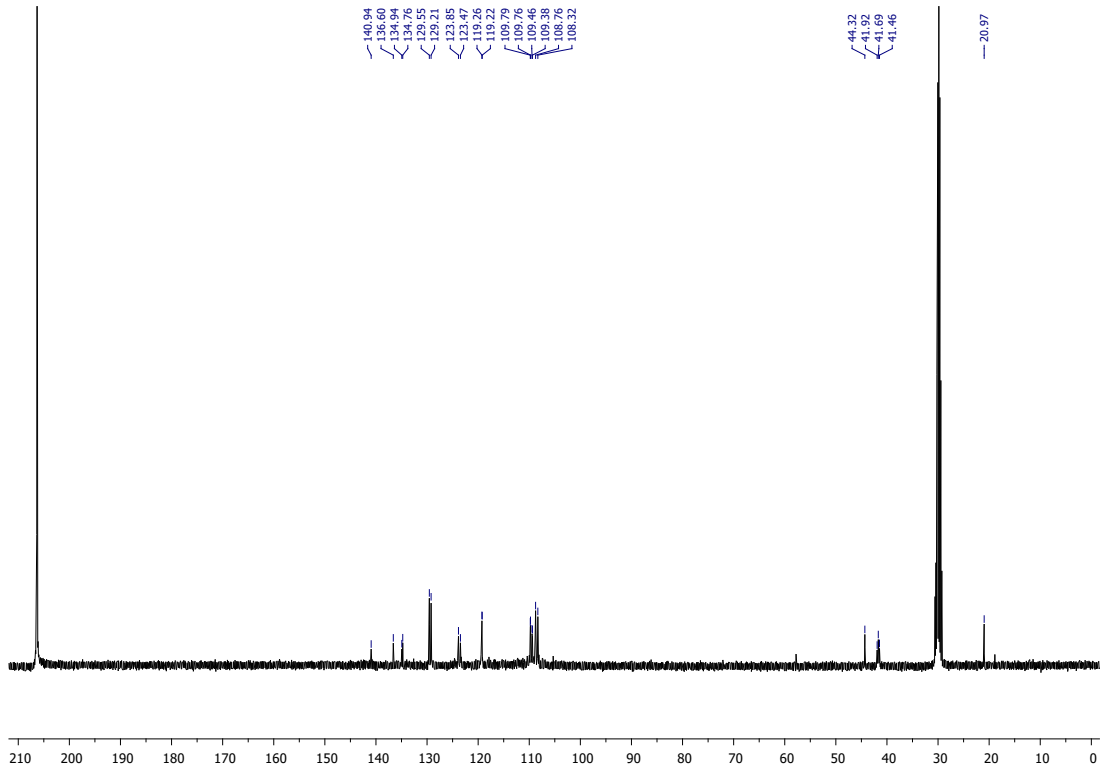

Figure S50: ^{13}C NMR spectrum of bilane **6e** (acetone-d_6, 298 K).

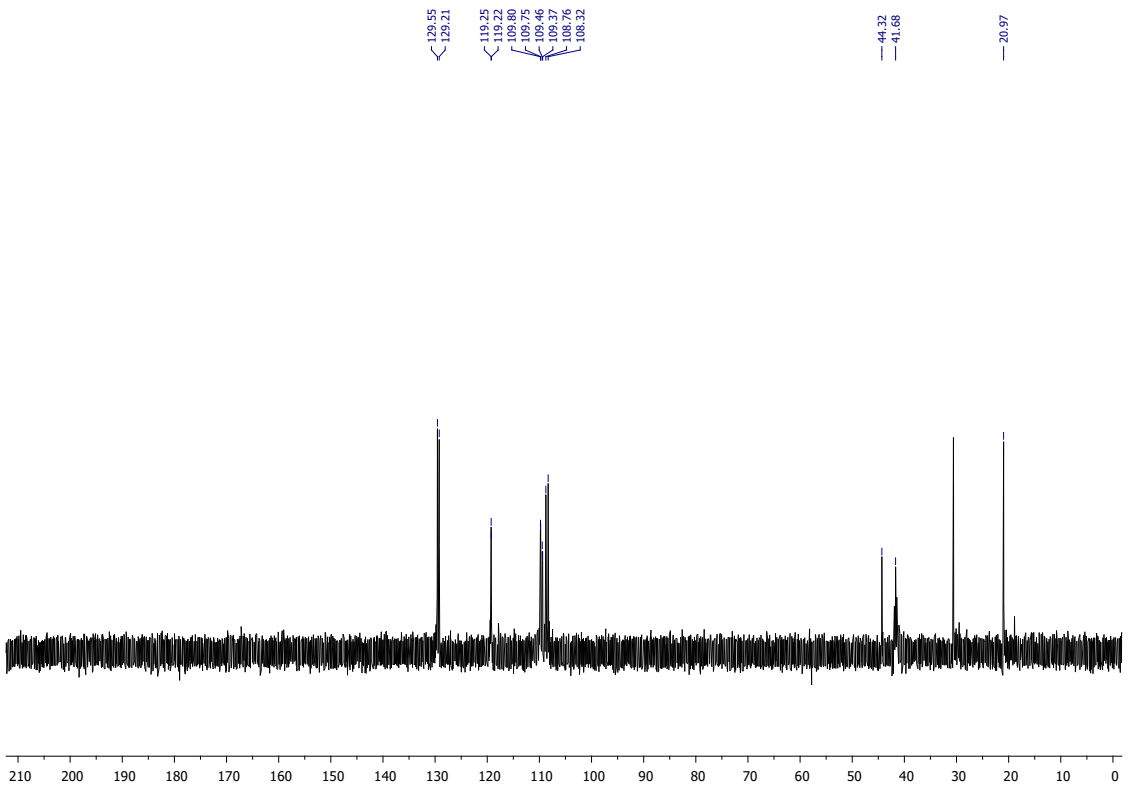

Figure S51: ^{13}C NMR (DEPT 135) spectrum of bilane **6e** (acetone-d_6, 298 K).

5,15-bis-perfluoropropyl-10-(*p*-anisyl)-bilane 6f

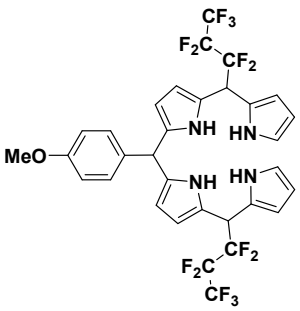

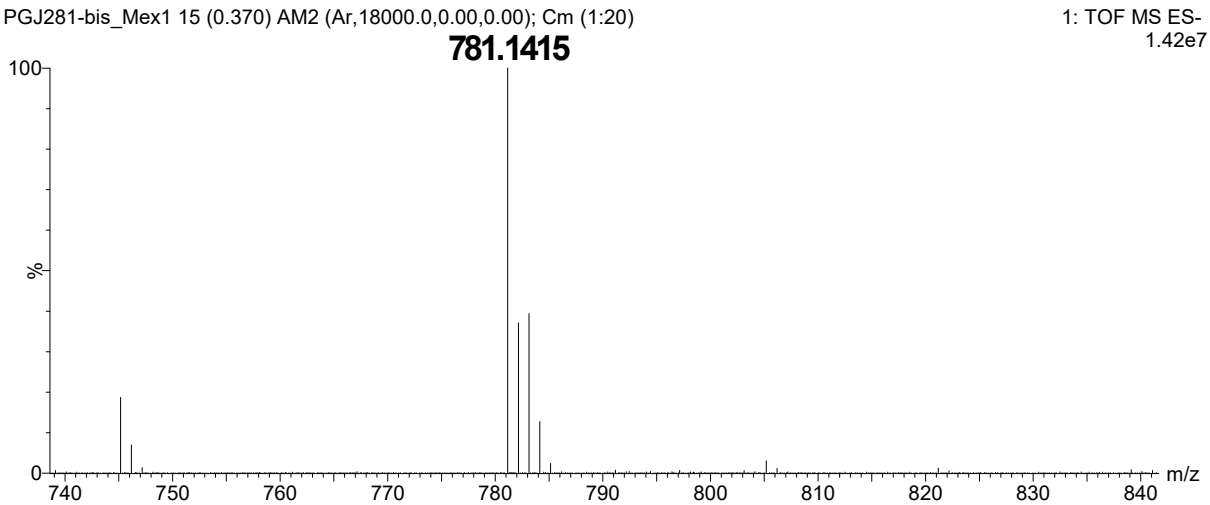

Figure S52: HRMS spectrum of bilane **6f**.

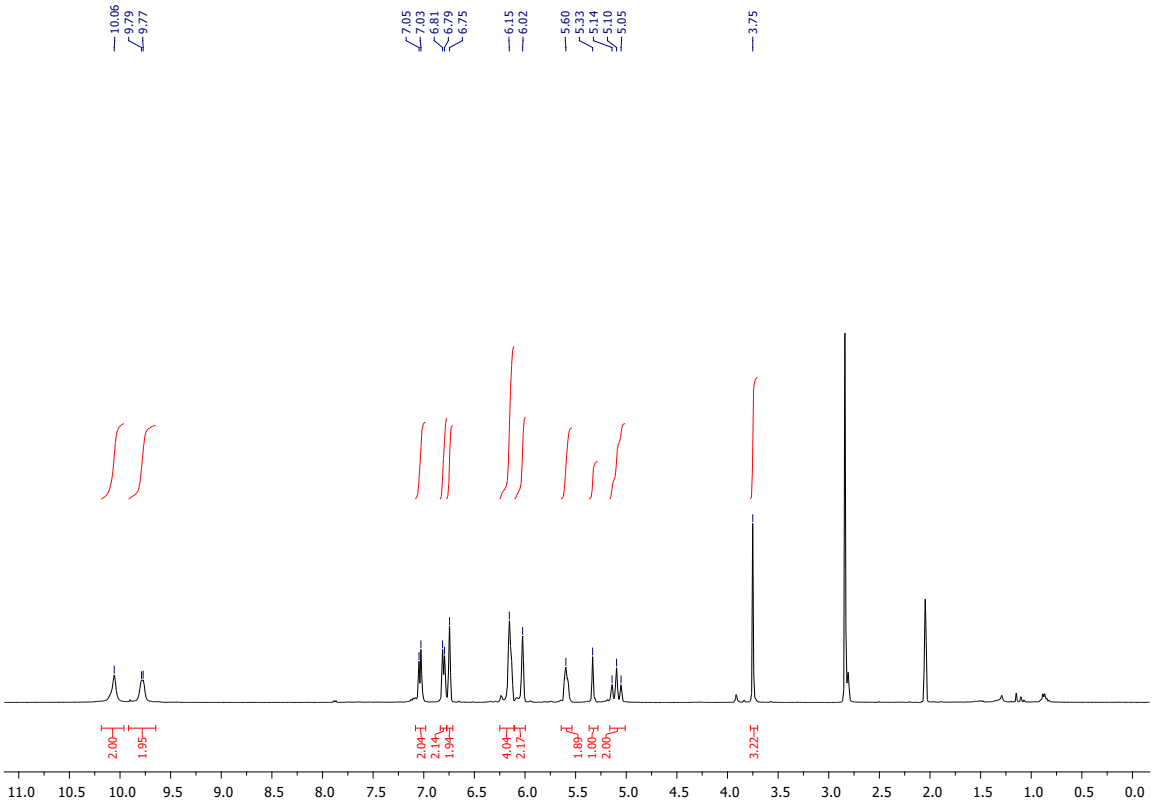

Figure S53: ^{1}H NMR spectrum of bilane **6f** (acetone-d_6, 298 K).

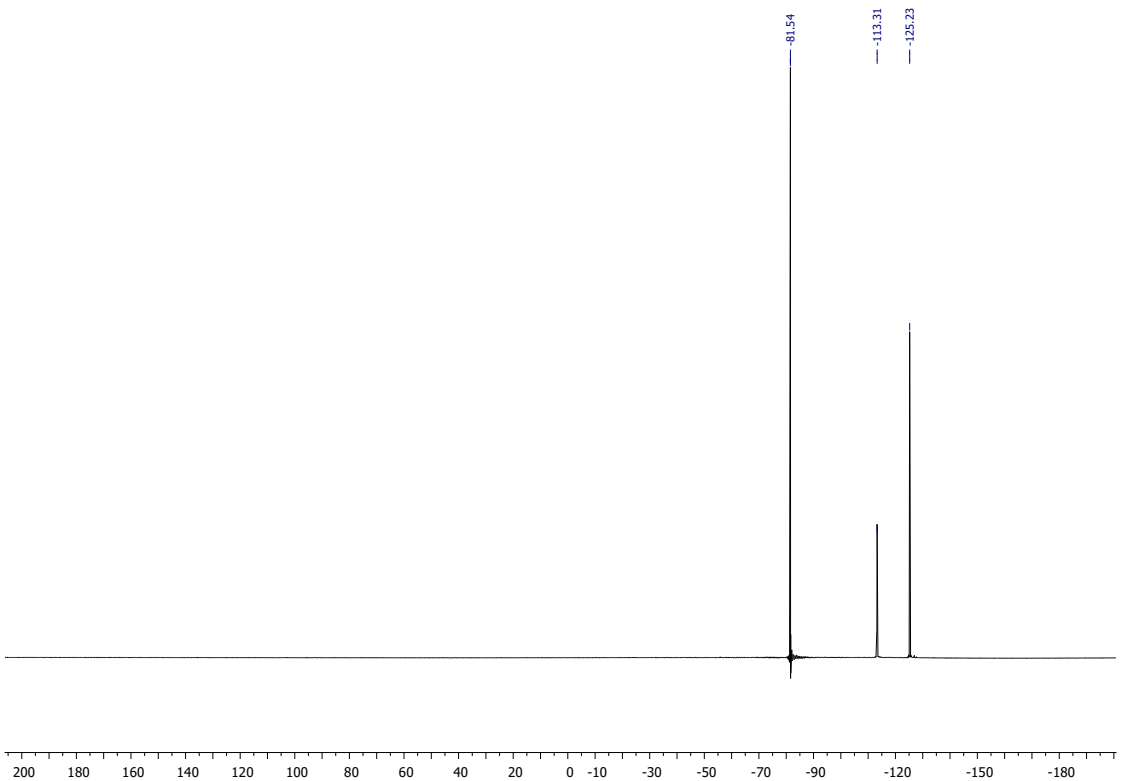

Figure S54: ^{19}F NMR spectrum of bilane **6f** (acetone-d_6, 298 K).

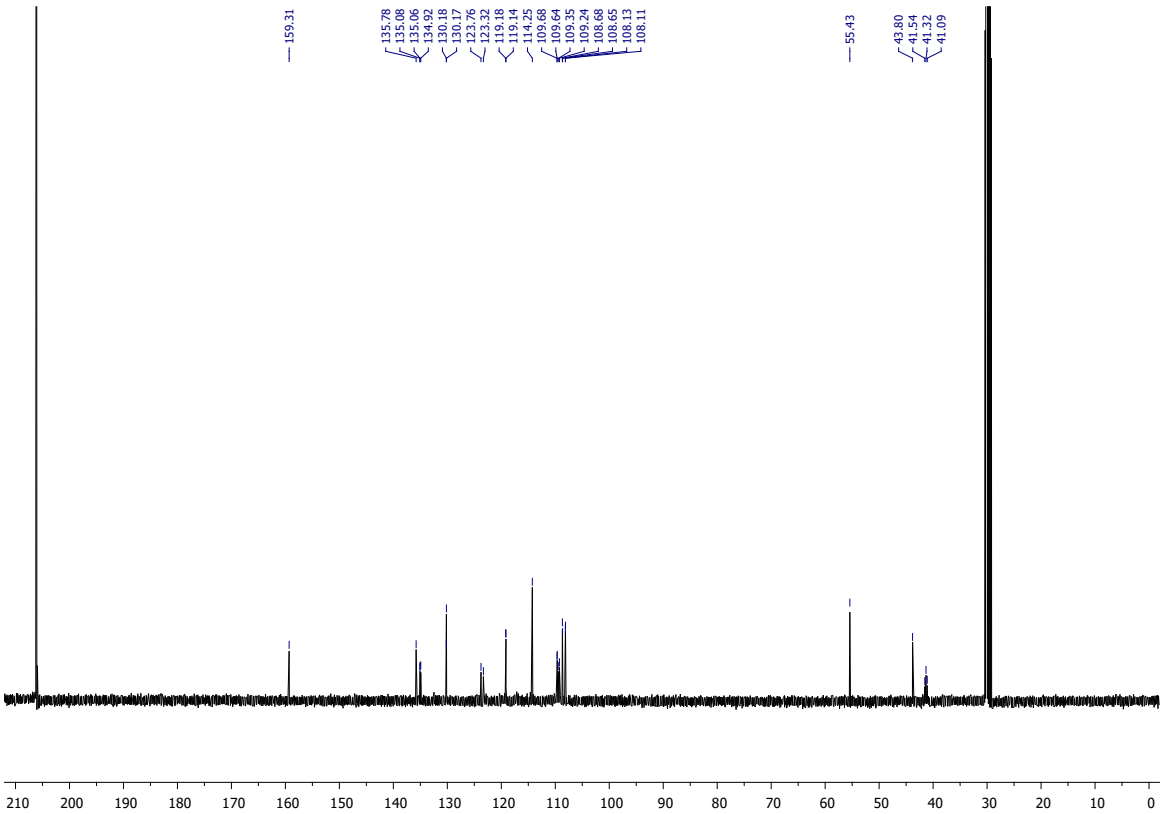

Figure S55: ^{13}C NMR spectrum of bilane **6f** (acetone-d_6, 298 K).

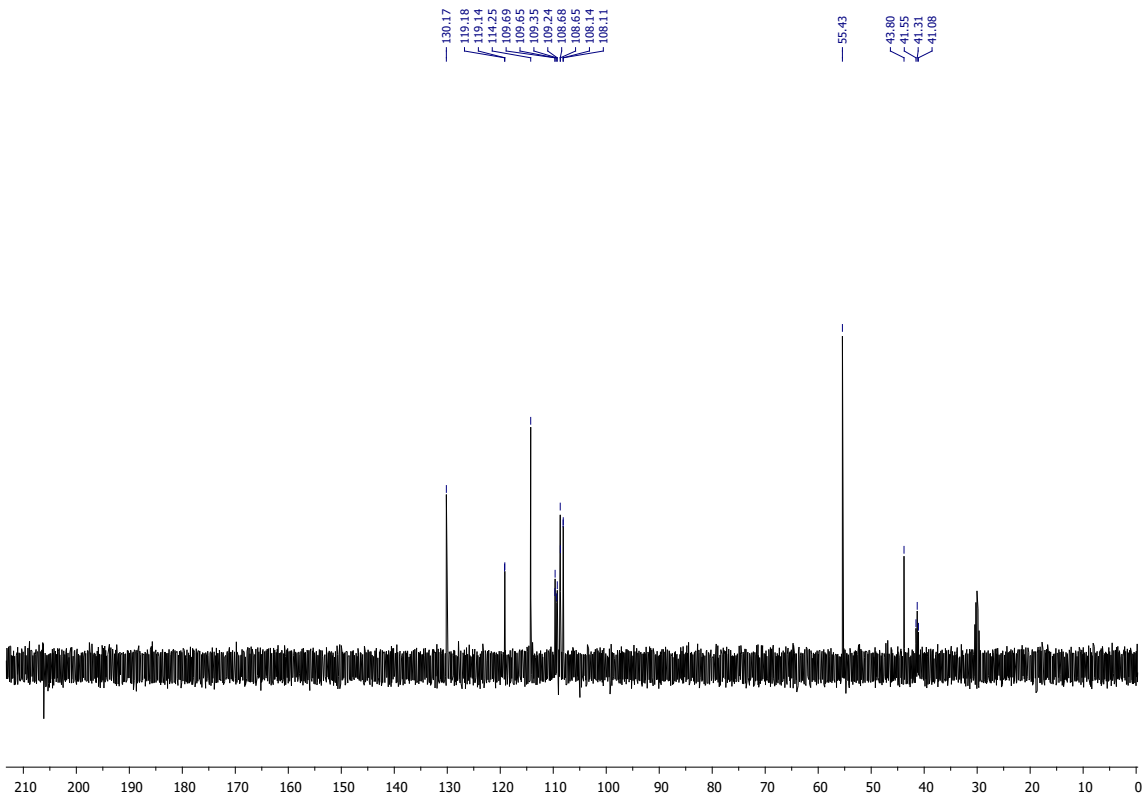

Figure S56: ^{13}C NMR (DEPT 135) spectrum of bilane **6f** (acetone-d_6, 298 K).

5,15-bis-perfluoroheptyl-10-(4-cyanophenyl)-bilane 6g

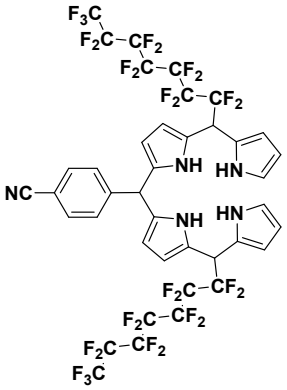

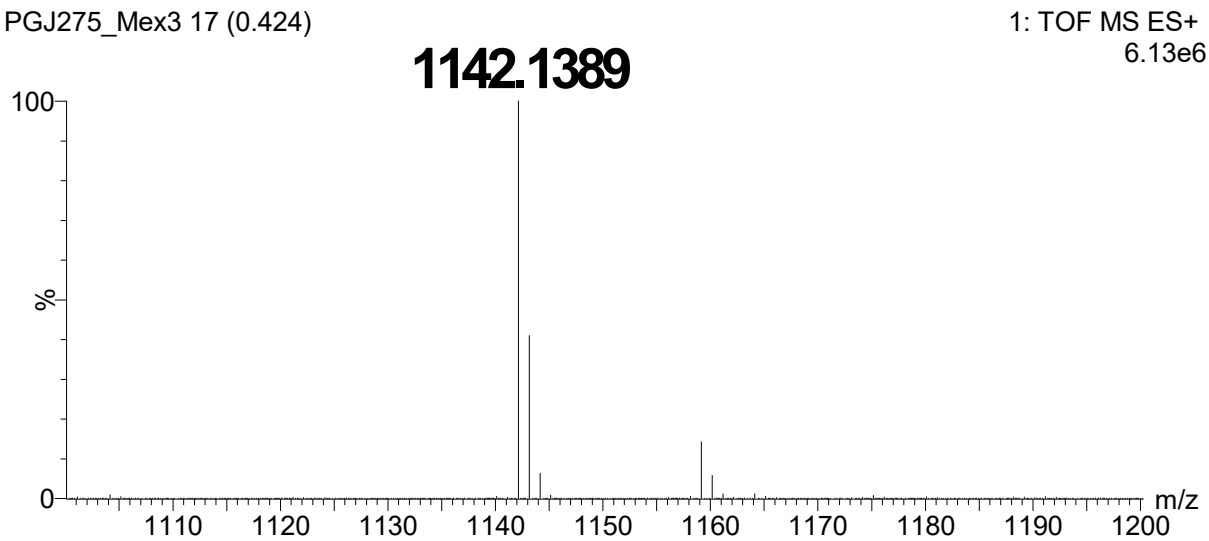

Figure S57: HRMS spectrum of bilane **6g**.

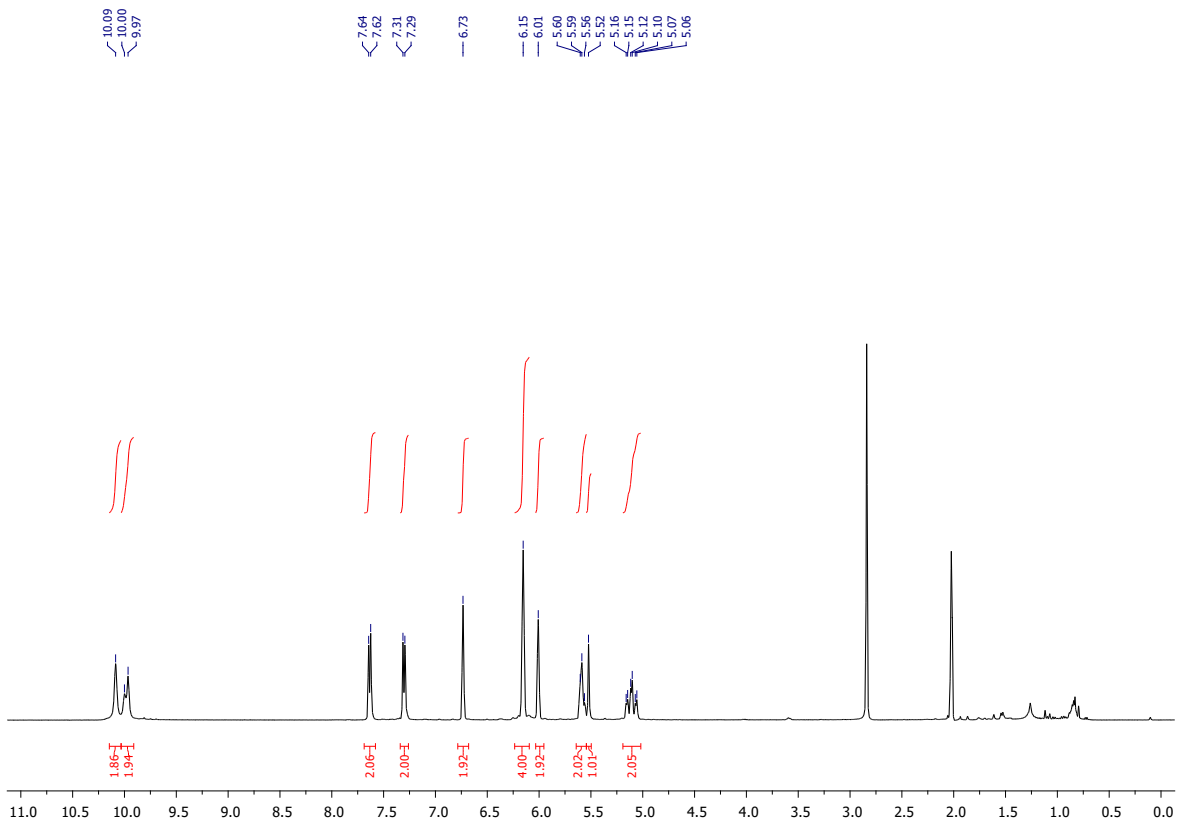

Figure S58: ^{1}H NMR spectrum of bilane **6g** (acetone-d_6, 298 K).

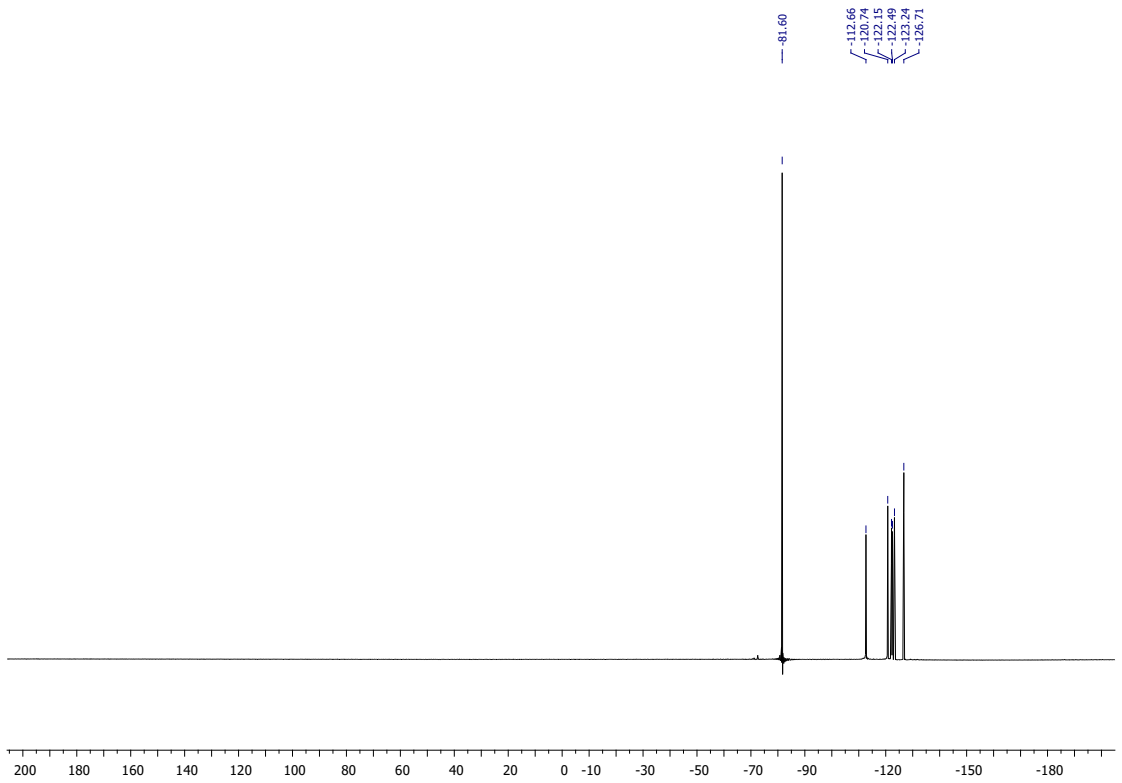

Figure S59: ^{19}F NMR spectrum of bilane **6g** (acetone-d_6, 298 K).

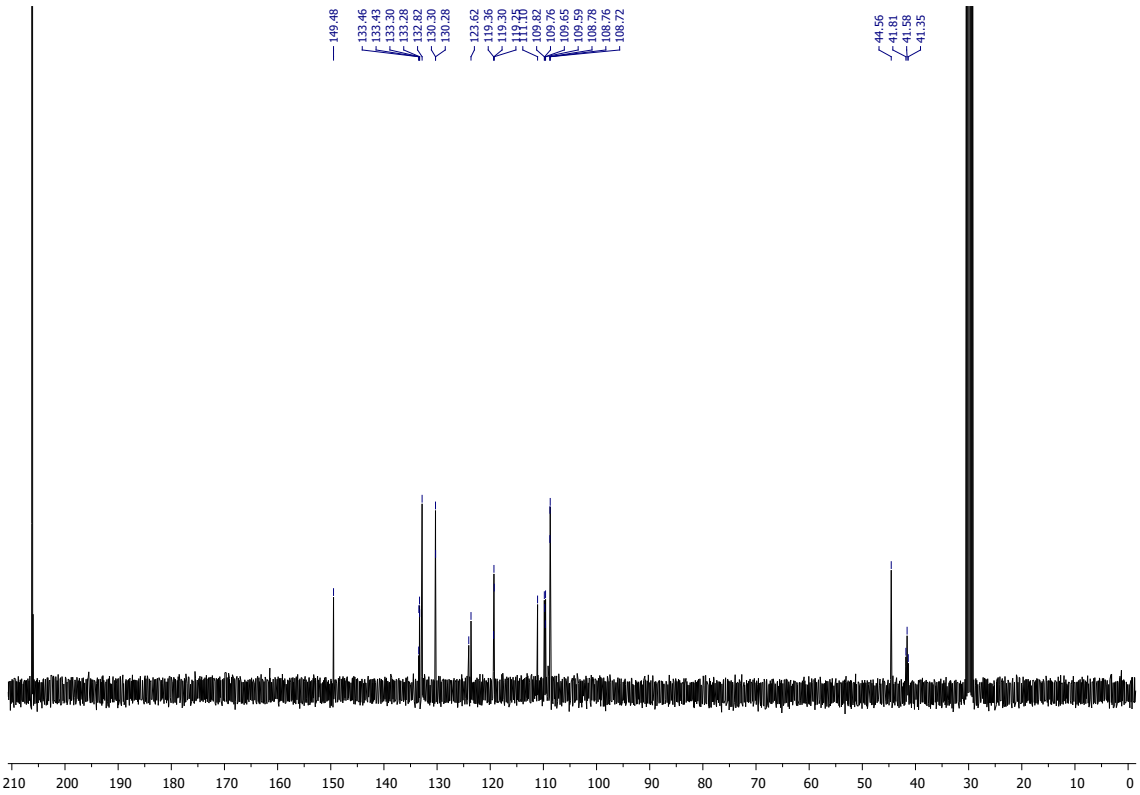

Figure S60: ^{13}C NMR spectrum of bilane **6g** (acetone-d_6, 298 K).

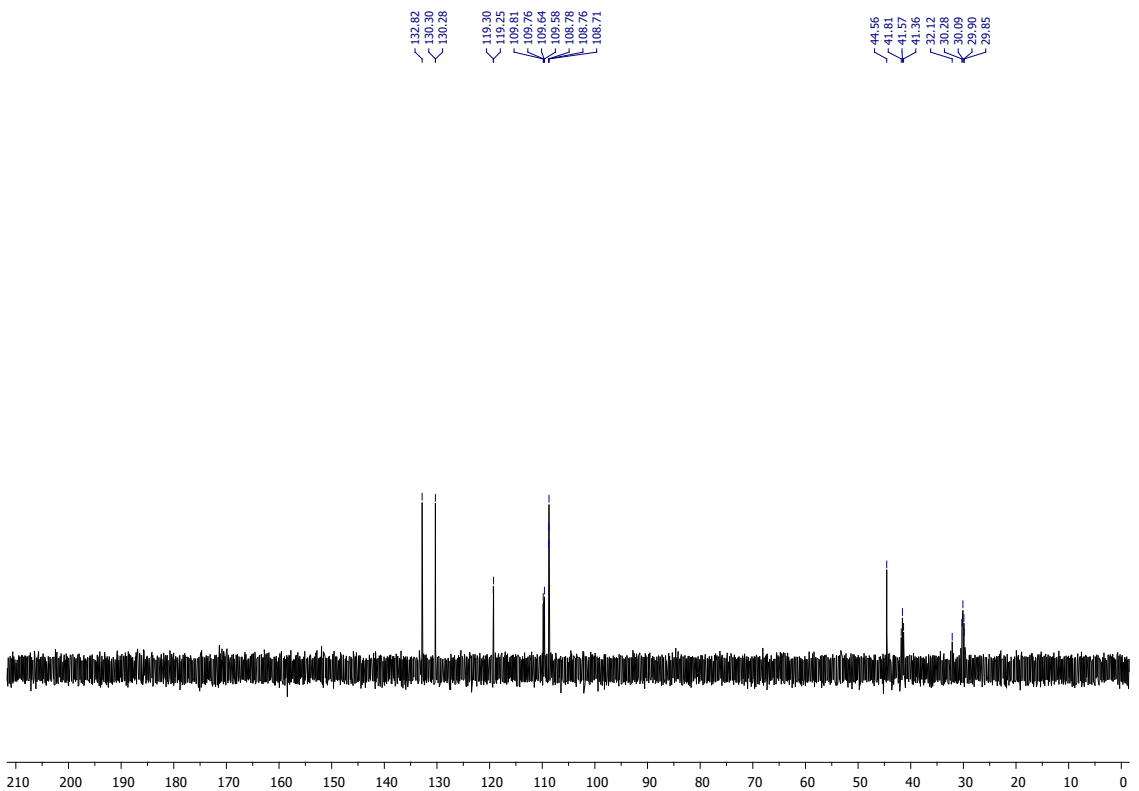

Figure S61: ^{13}C NMR (DEPT 135) spectrum of bilane **6g** (acetone-d_6, 298 K).

5,15-bis-perfluoroheptyl-10-(*p*-tolyl)-bilane 6h

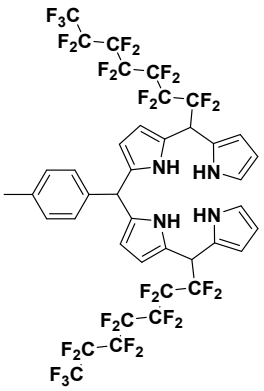

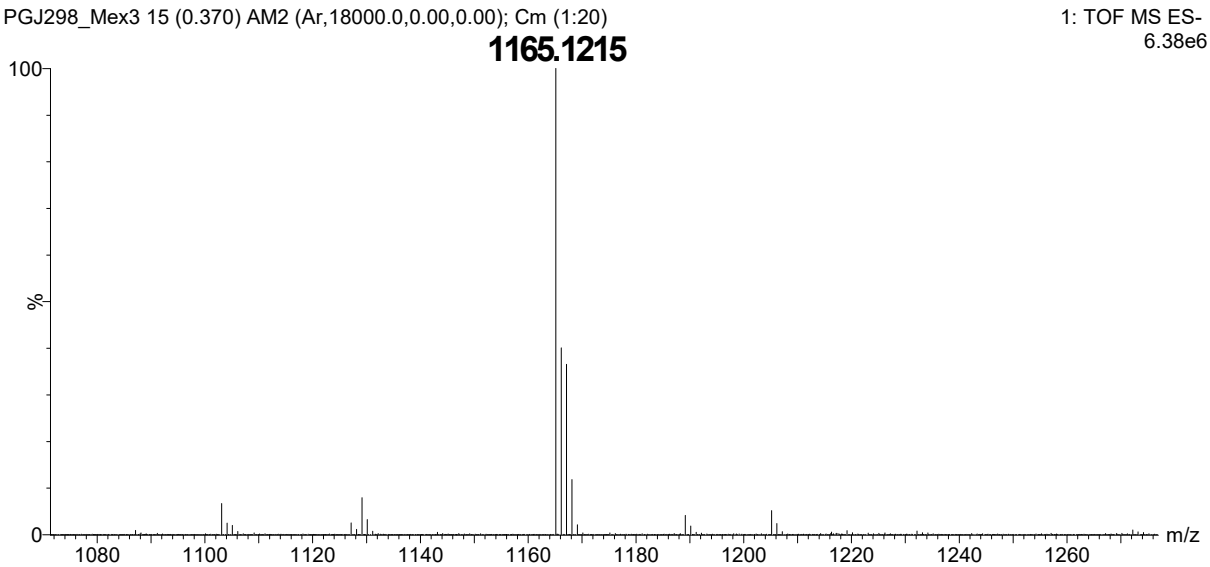

Figure S62: HRMS spectrum of bilane **6h**.

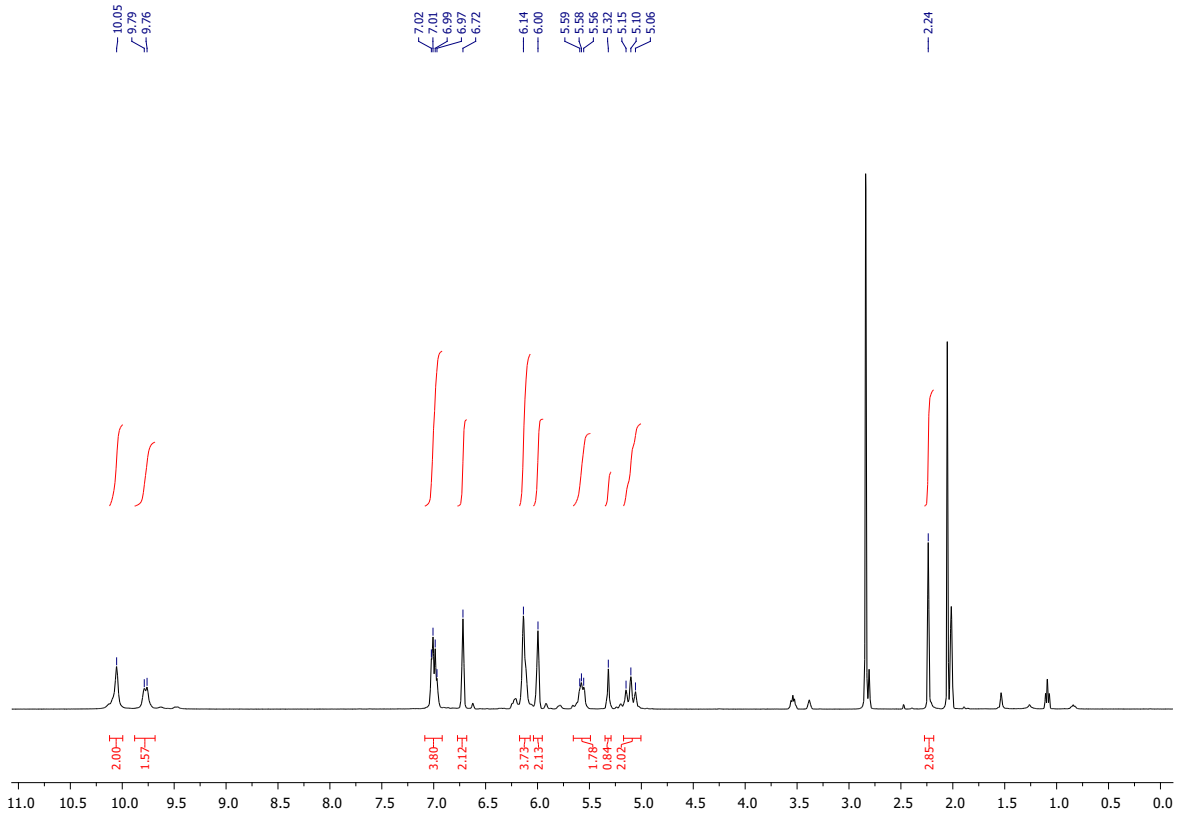

Figure S63: ^{1}H NMR spectrum of bilane **6h** (acetone-d_6, 298 K).

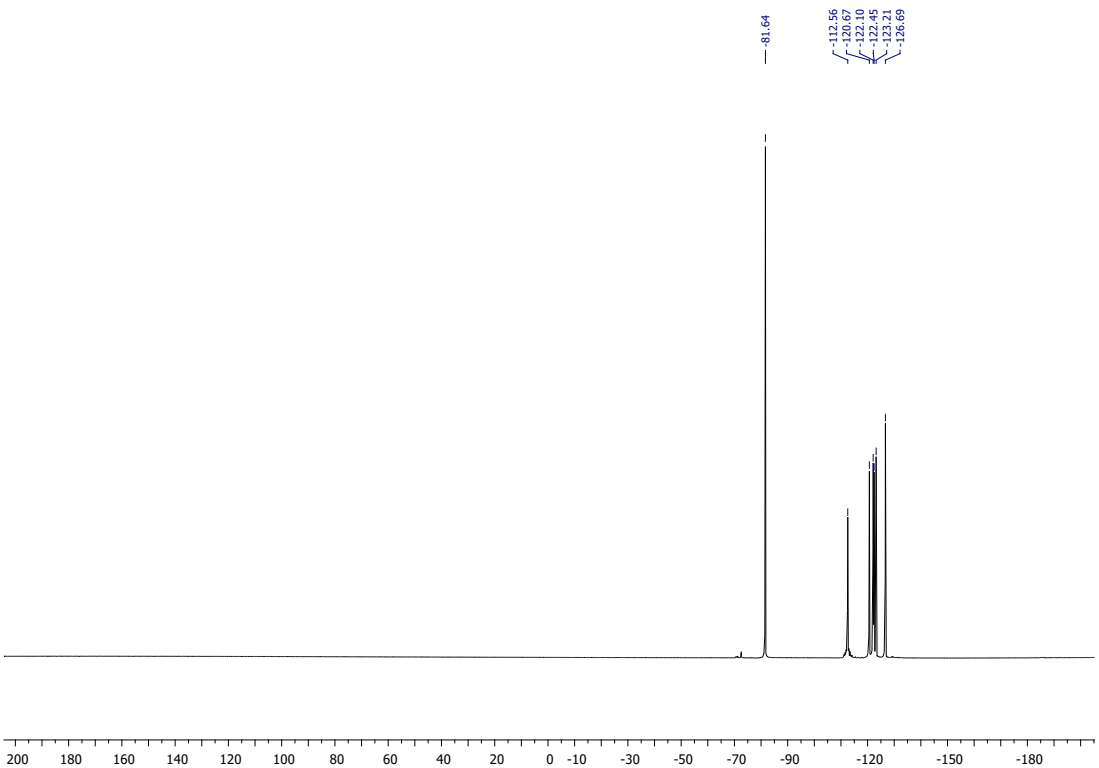

Figure S64: ^{19}F NMR spectrum of bilane **6h** (acetone-d_6, 298 K).

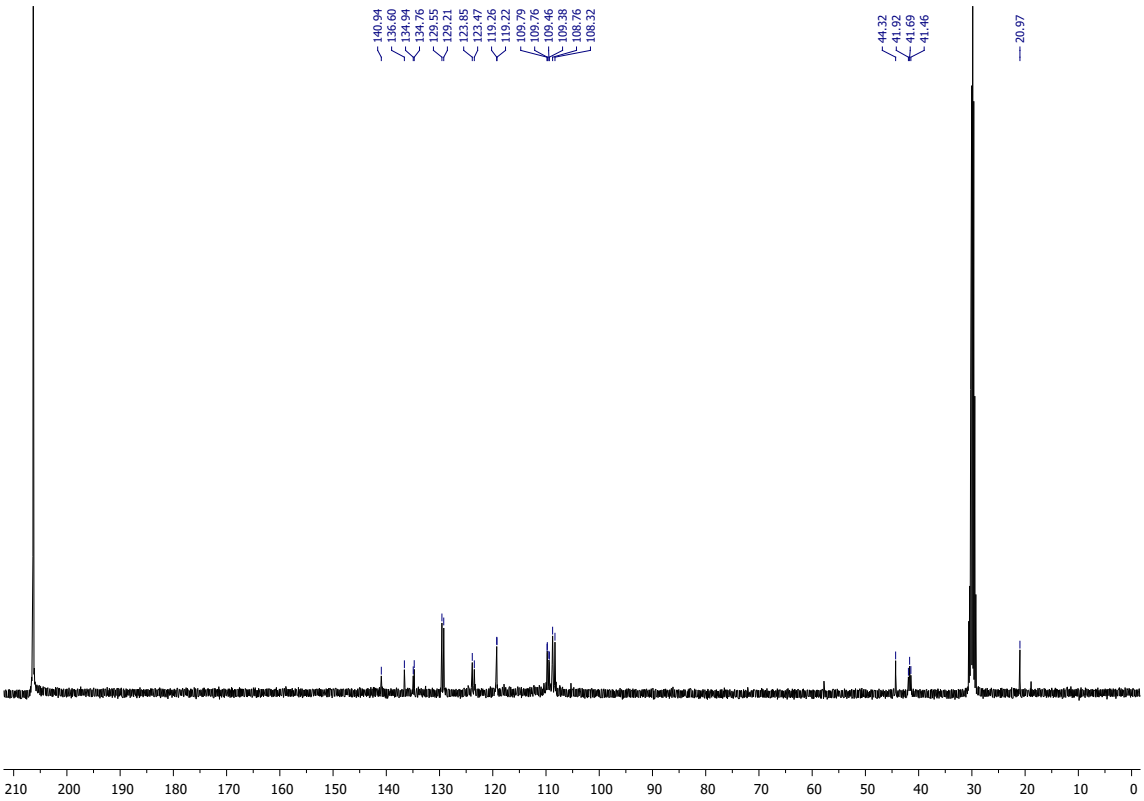

Figure S65: ^{13}C NMR spectrum of bilane **6h** (acetone-d_6, 298 K).

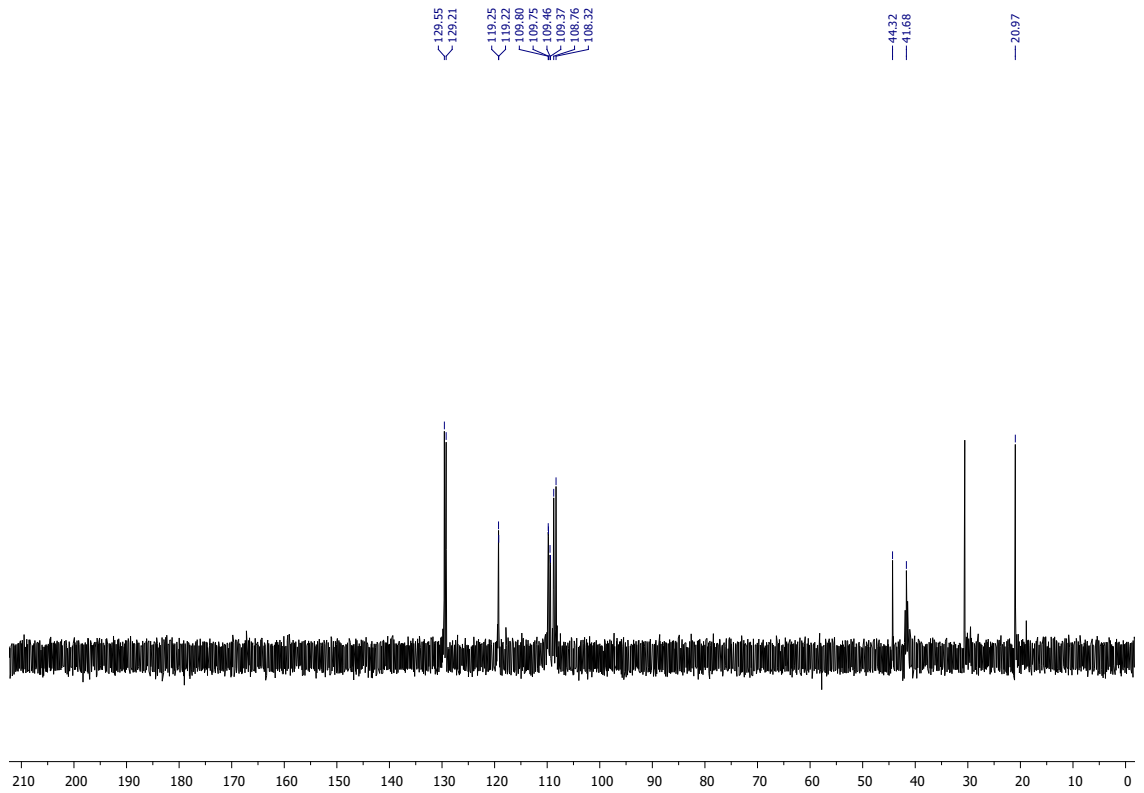

Figure S66: ^{13}C NMR (DEPT 135) spectrum of bilane **6h** (acetone-d_6, 298 K).

5,15-bis-perfluoroheptyl-10-(*p*-anisyl)-bilane 6i

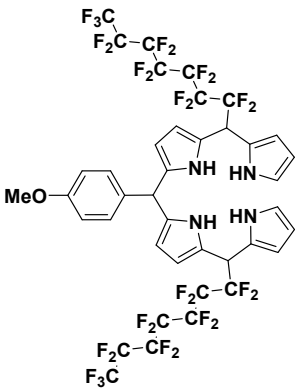

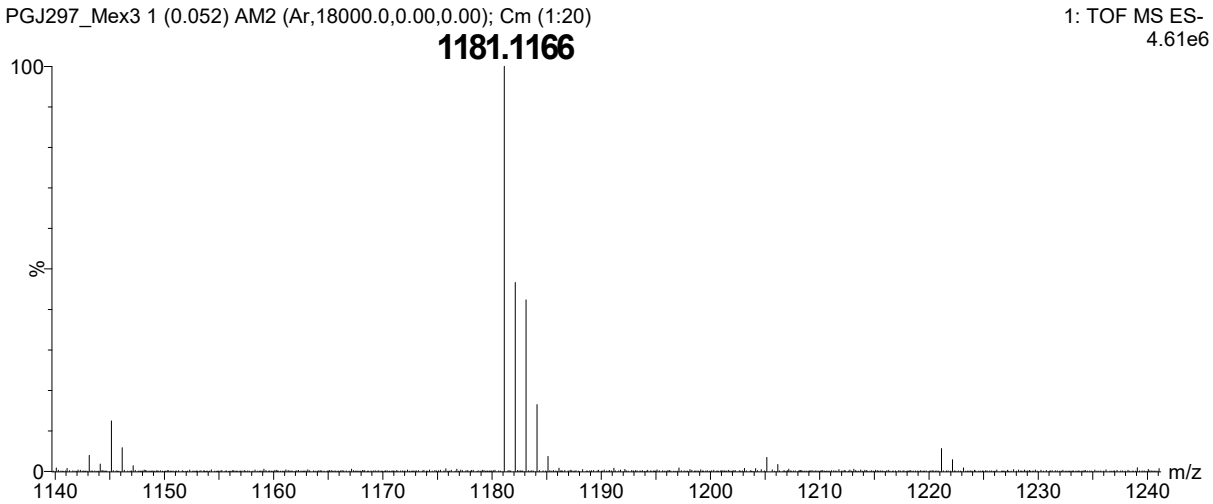

Figure S67: HRMS spectrum of bilane **6i**.

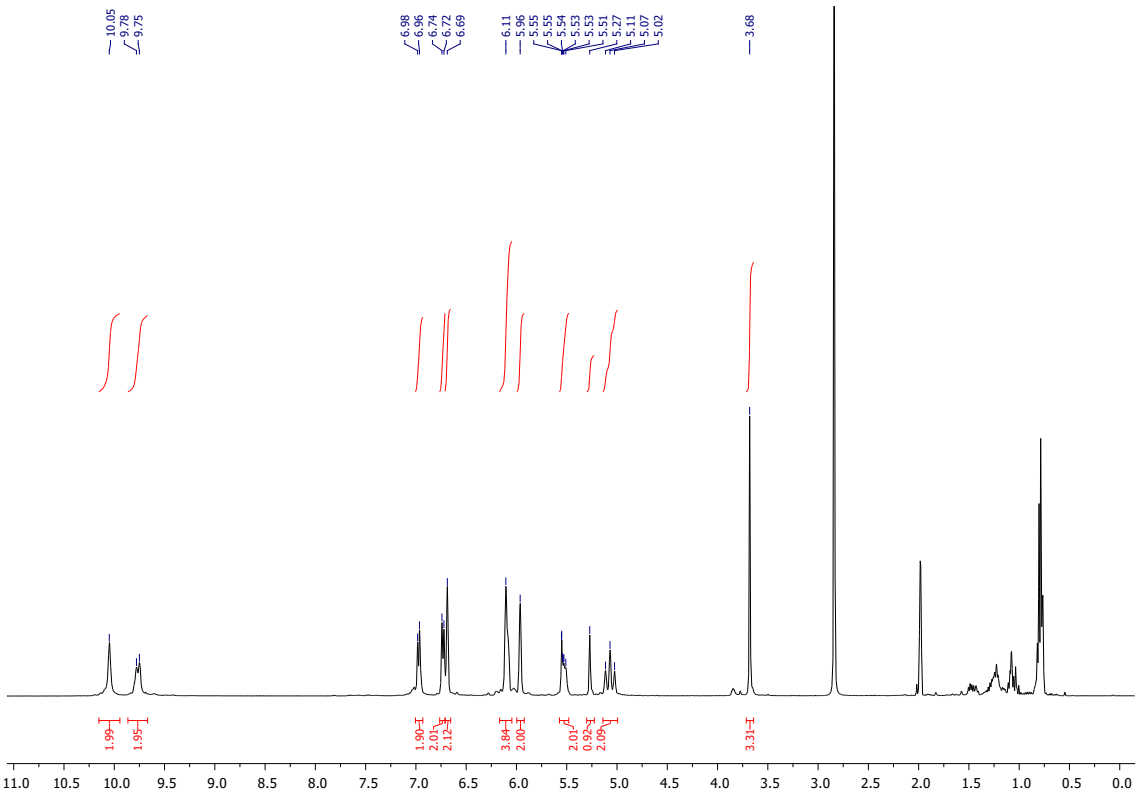

Figure S68: ^{1}H NMR spectrum of bilane **6i** (acetone-d_6, 298 K).

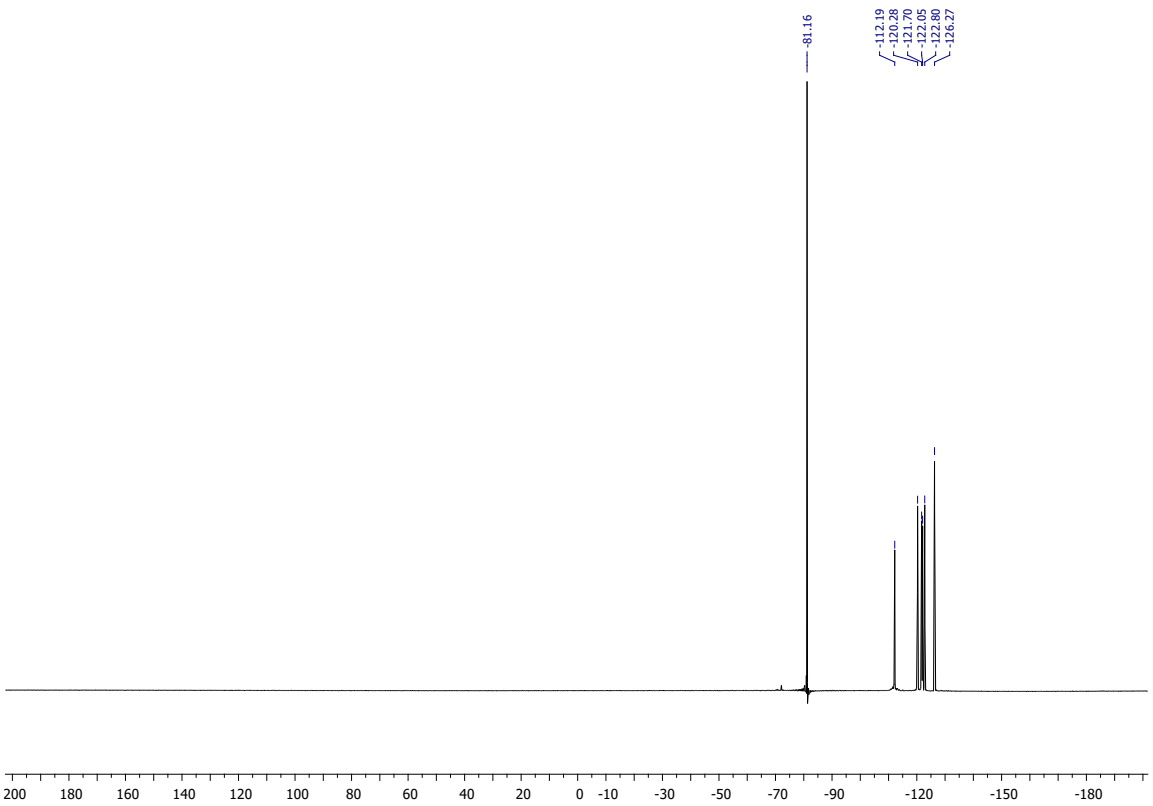

Figure S69: ^{19}F NMR spectrum of bilane **6i** (acetone-d_6, 298 K).

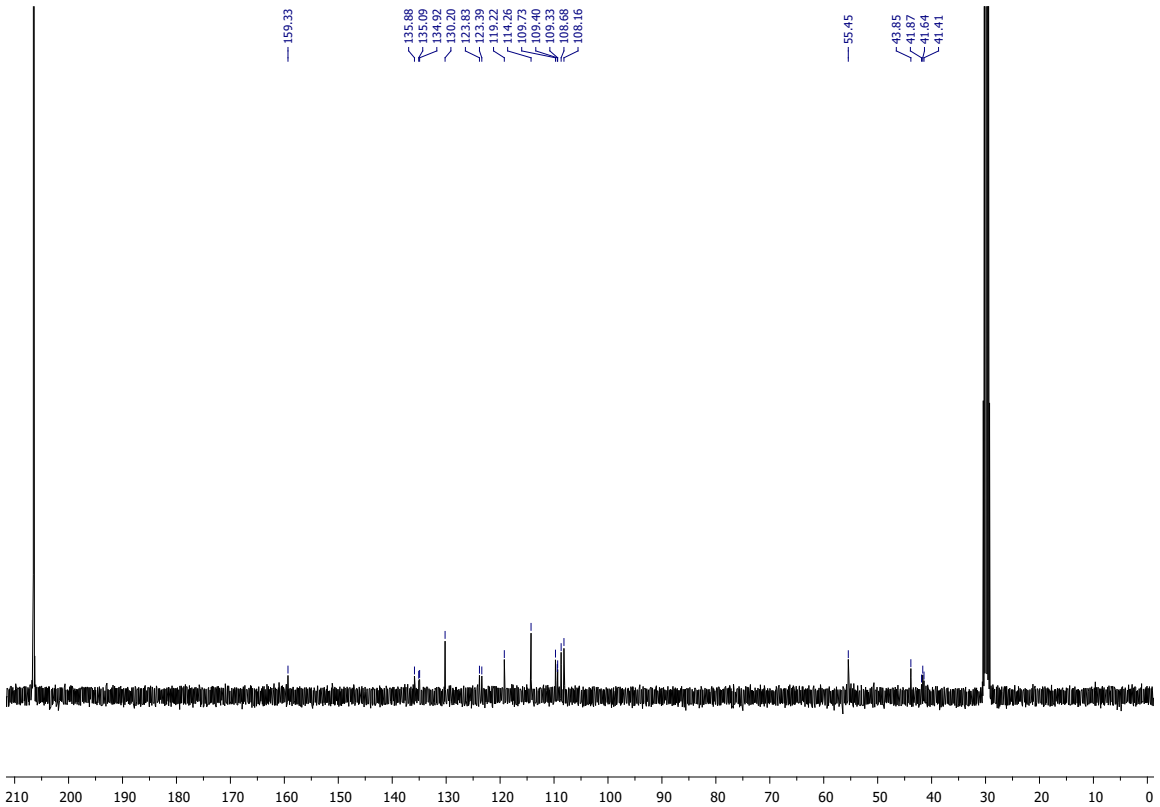

Figure S70: ^{13}C NMR spectrum of bilane **6i** (acetone-d_6, 298 K).

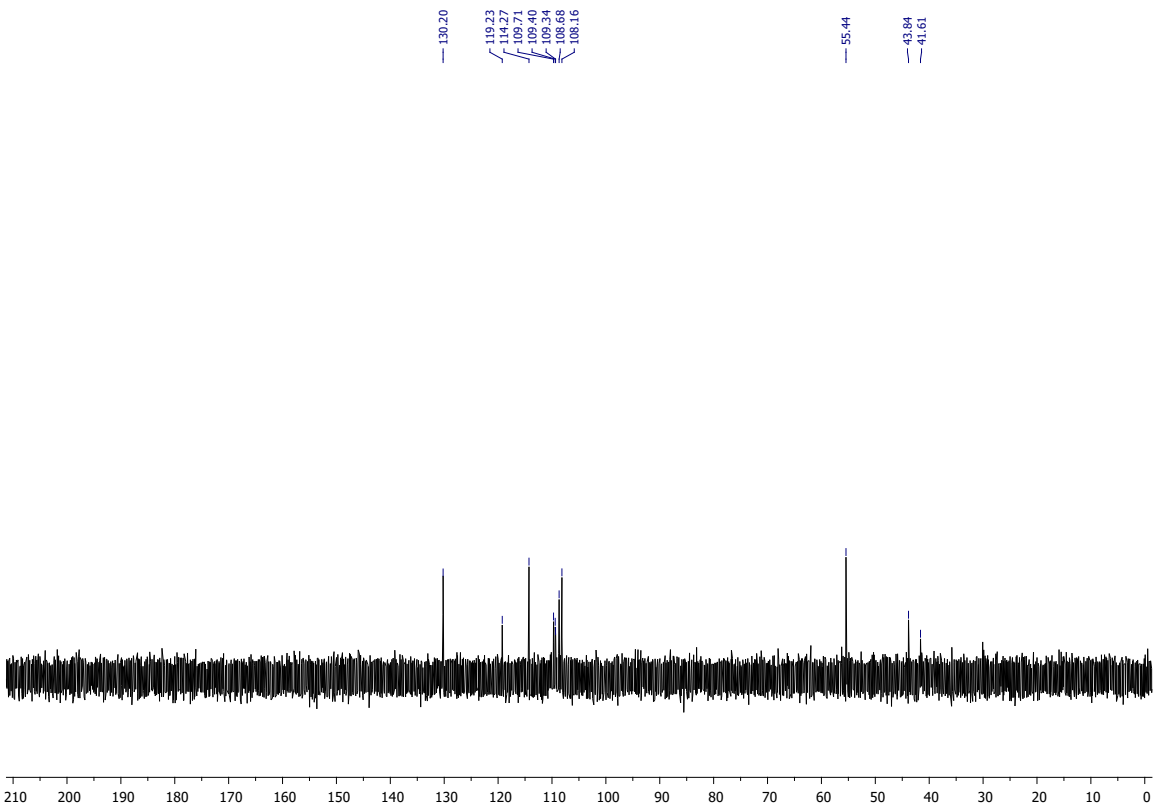

Figure S71: ^{13}C NMR (DEPT 135) spectrum of bilane **6i** (acetone-d_6, 298 K).

Corroles

5,15-bistrifluoromethyl-10-(4-cyanophenyl)-corrole 7a

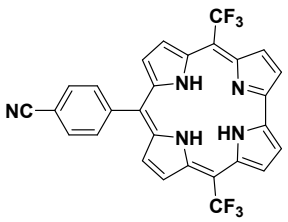

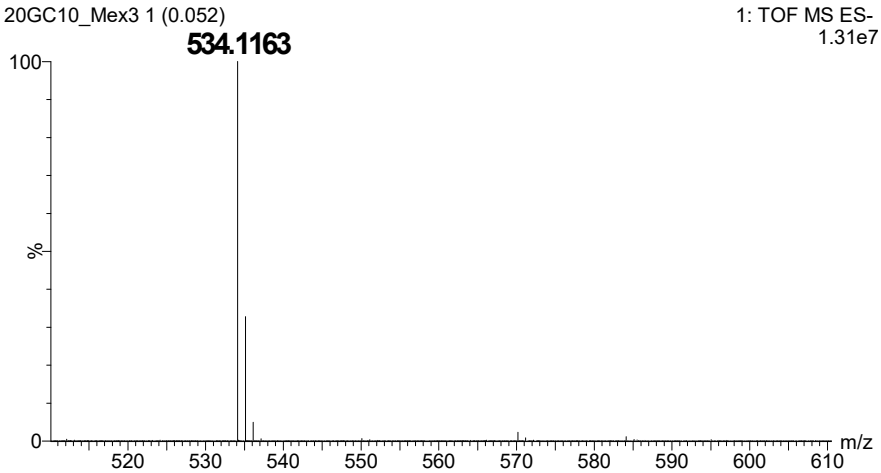

Figure S72: HRMS spectrum of corrole **7a**.

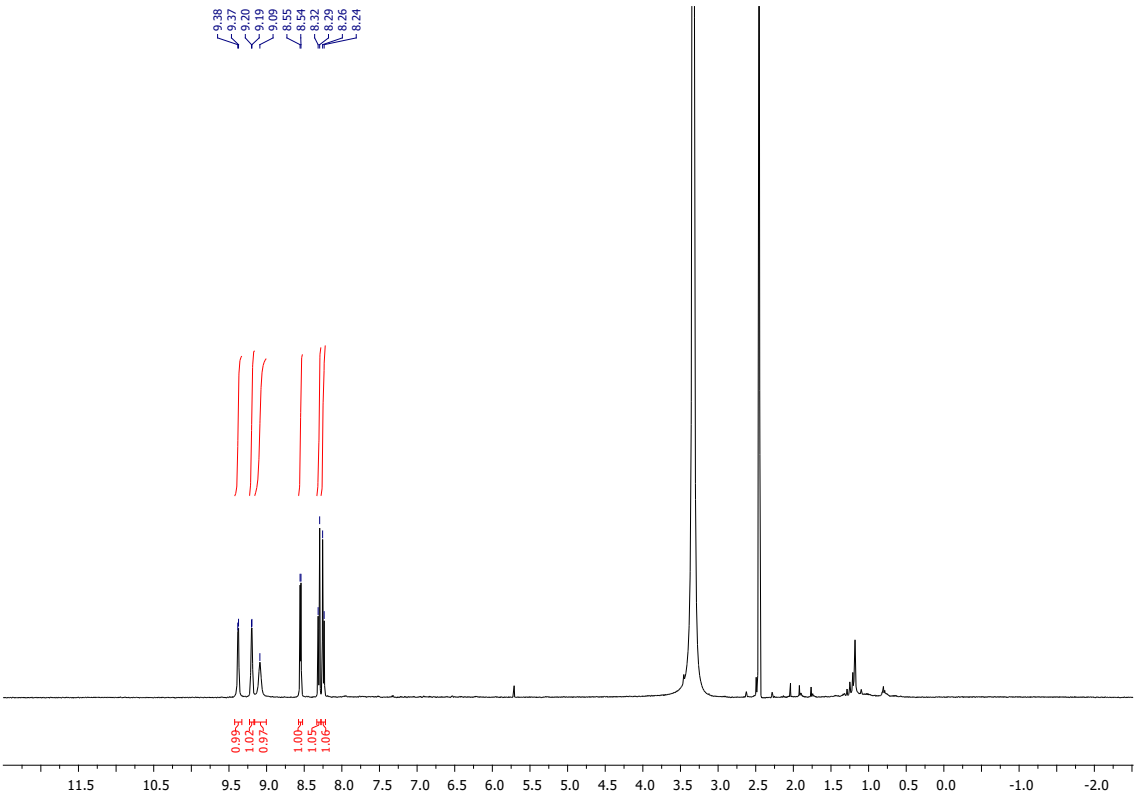

Figure S73: ^{1}H NMR spectrum of corrole **7a** (DMSO-d_6, 298 K).

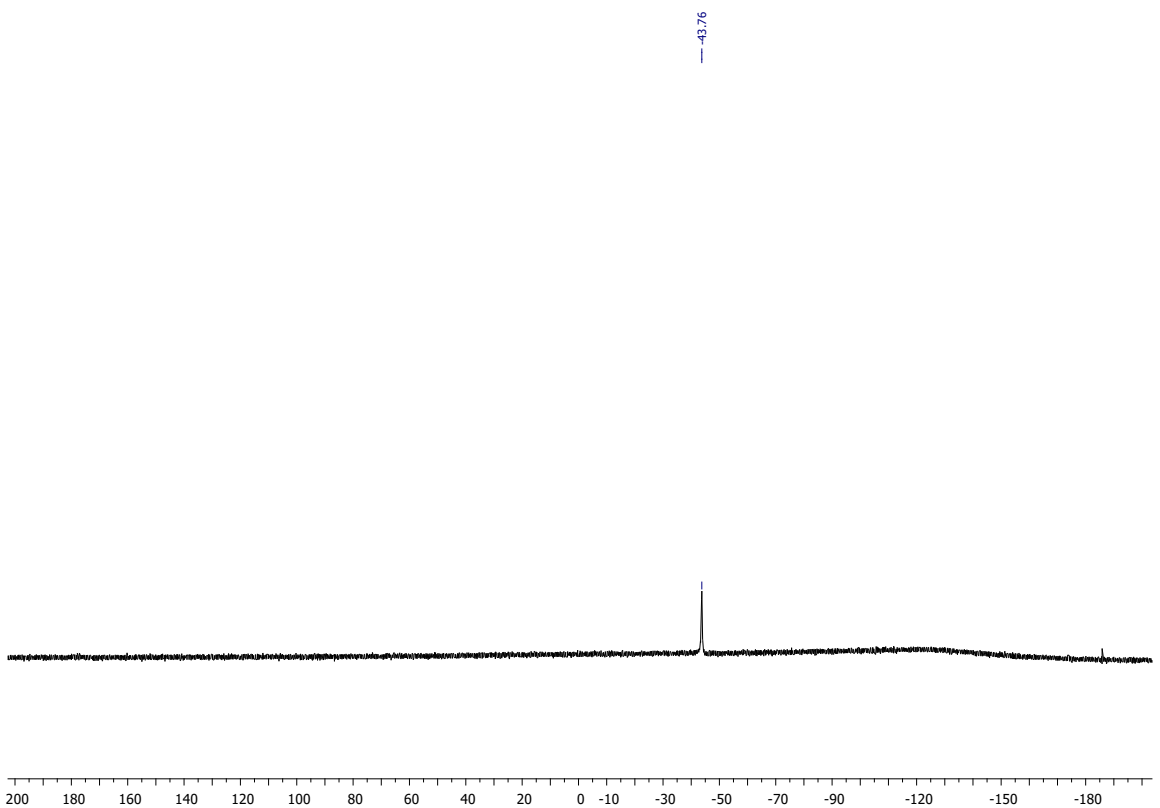

Figure S74: ^{19}F NMR spectrum of corrole **7a** (DMSO-d_6, 298 K).

5,15-bis-trifluoromethyl-10-(*p*-tolyl)-corrole 7b

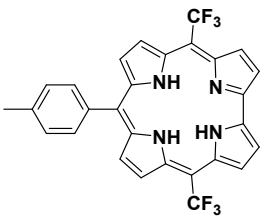

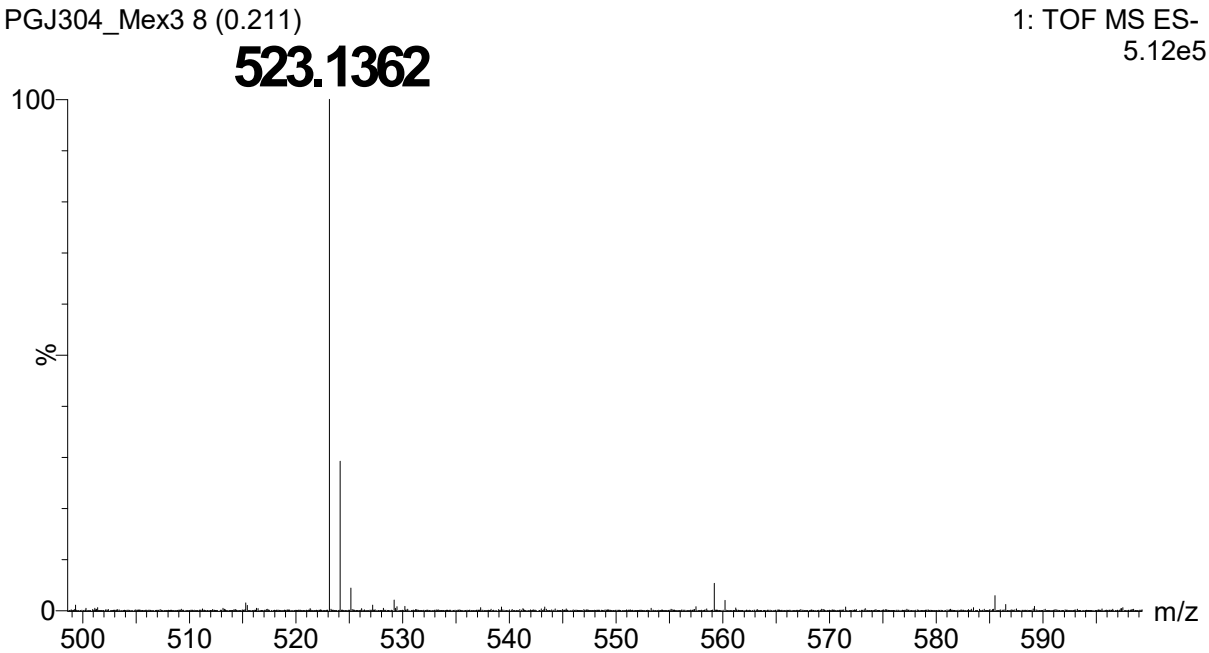

Figure S75: HRMS spectrum of corrole **7b**.

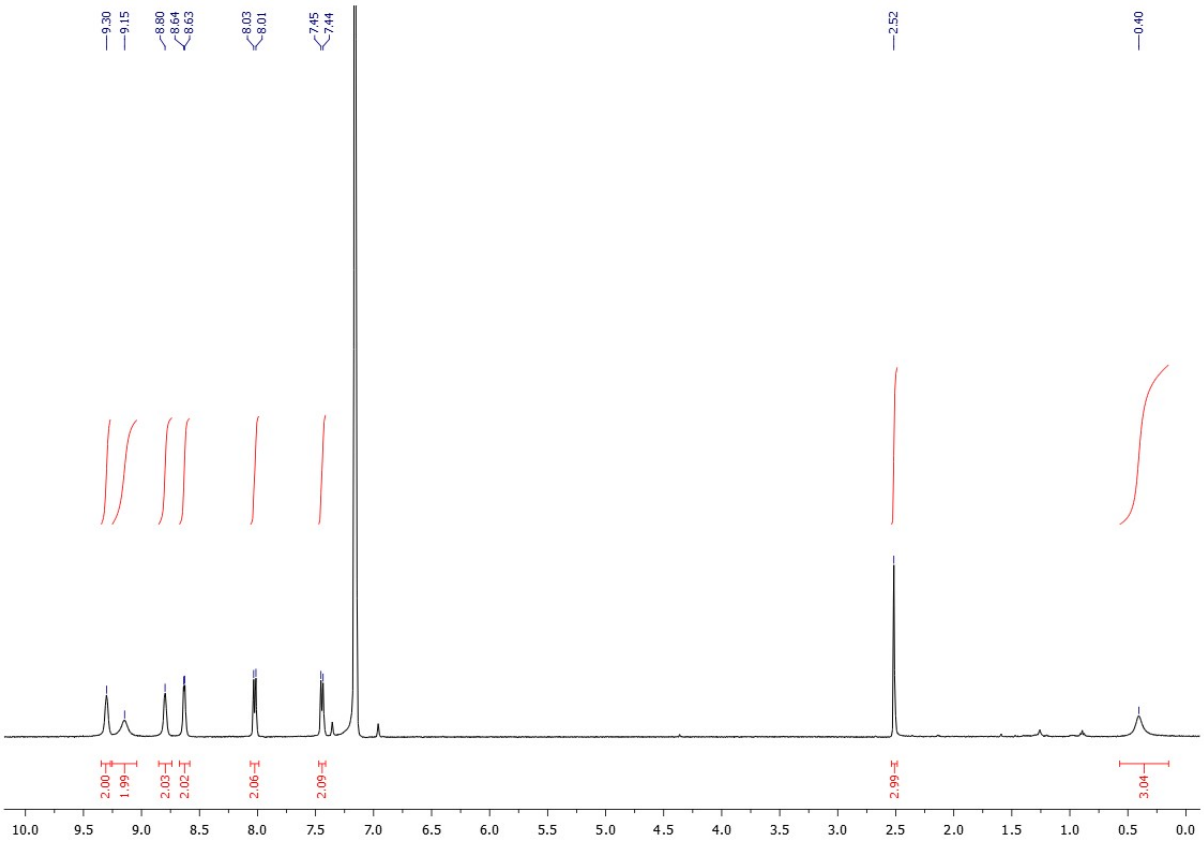

Figure S76: ^{1}H NMR spectrum of corrole **7b** (benzene-d_6, 333 K).

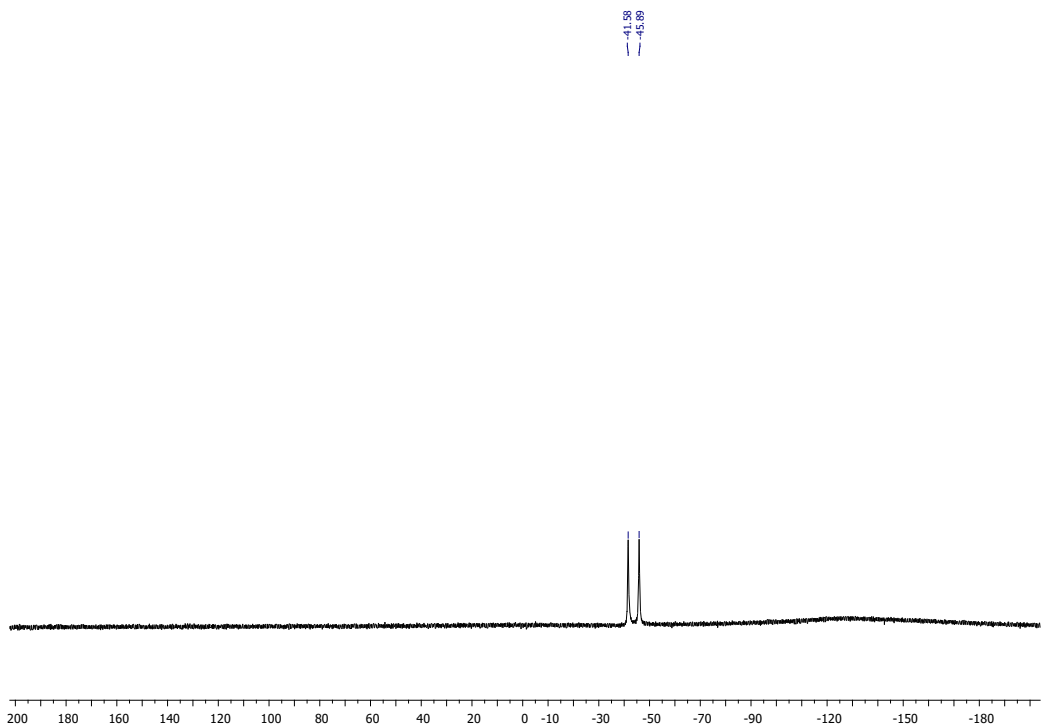

Figure S77: ^{19}F NMR spectrum of corrole **7b** (benzene-d_6, 298 K).

5,15-bis-trifluoromethyl-10-(*p*-anisyl)-corrole 7c

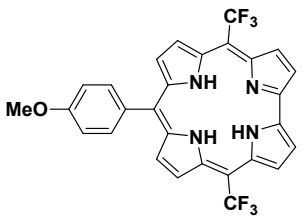

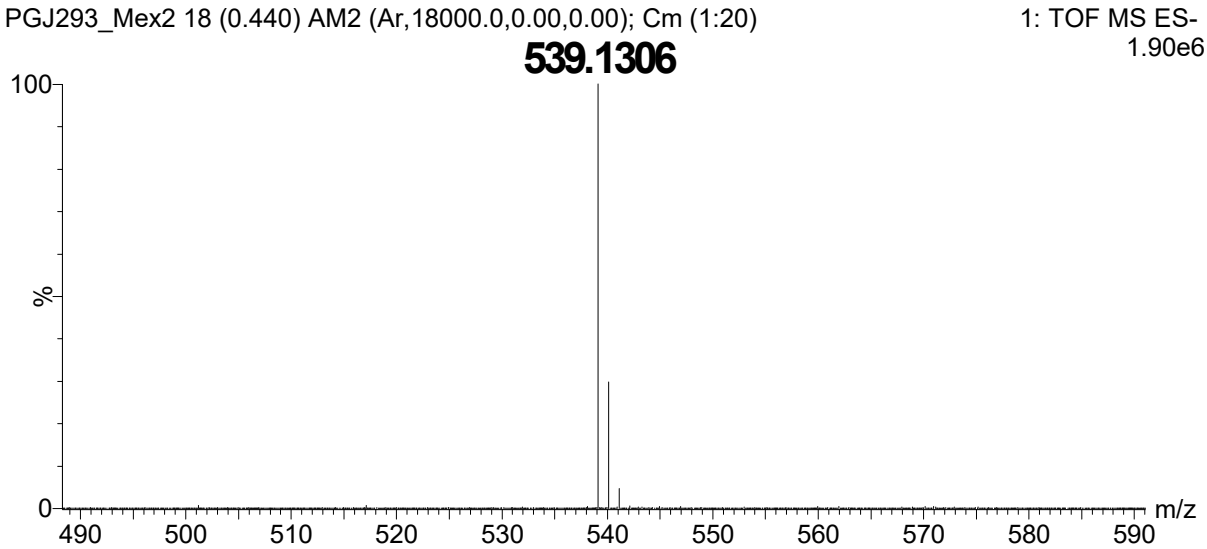

Figure S78: HRMS spectrum of corrole **7c**.

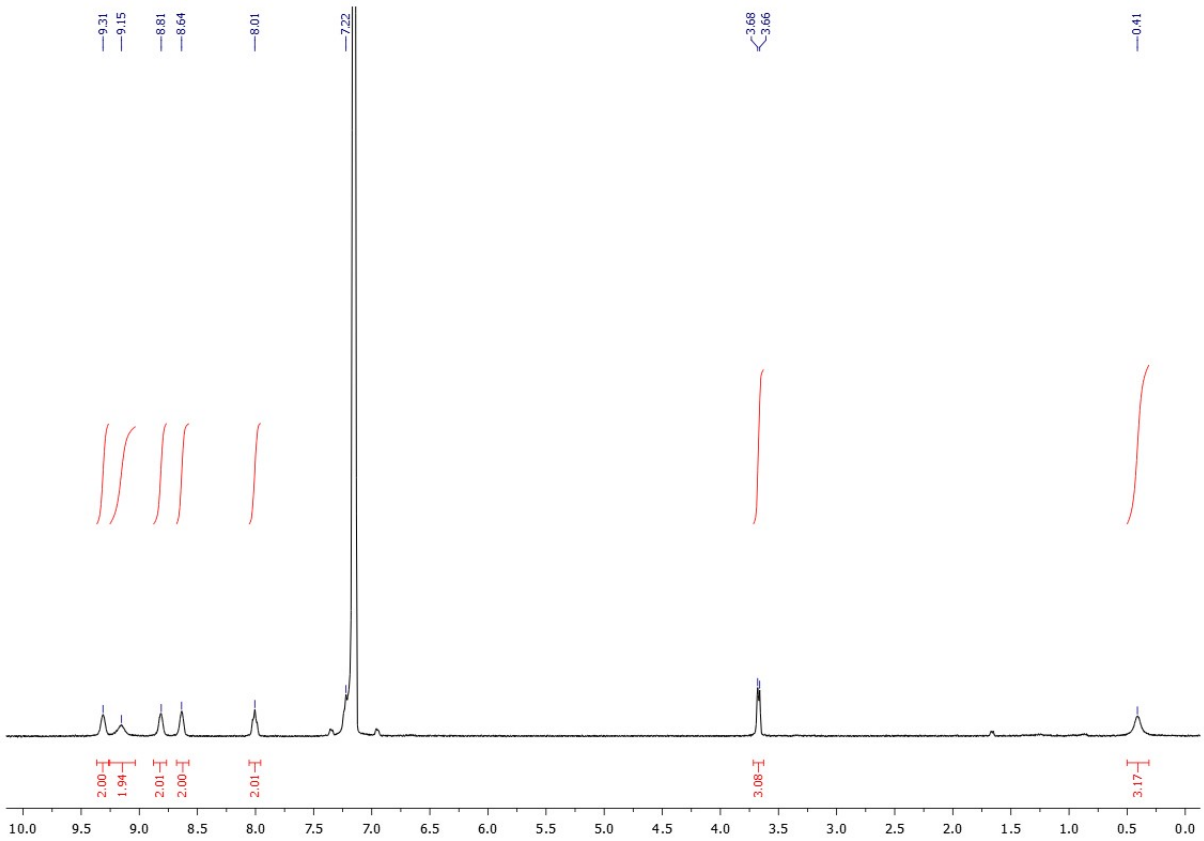

Figure S79: ^{1}H NMR spectrum of corrole **7c** (benzene-d_6, 333 K).

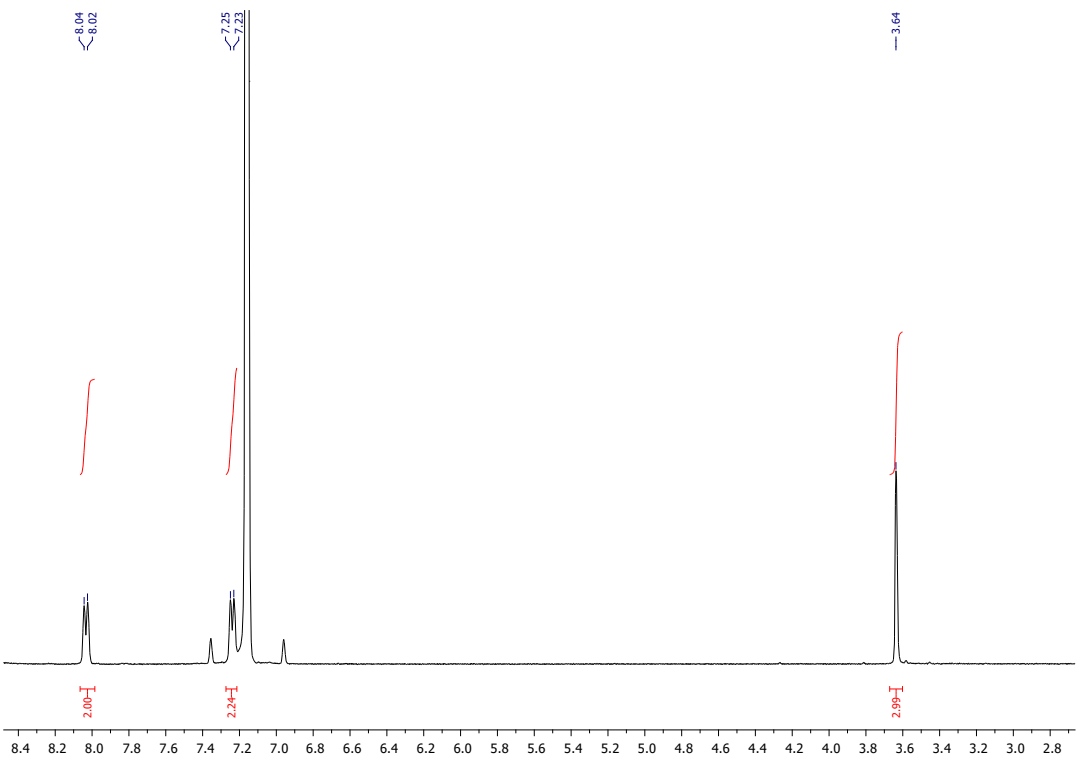

Figure S80: ^{1}H NMR spectrum of corrole **7c** (benzene-d_6, 298 K).

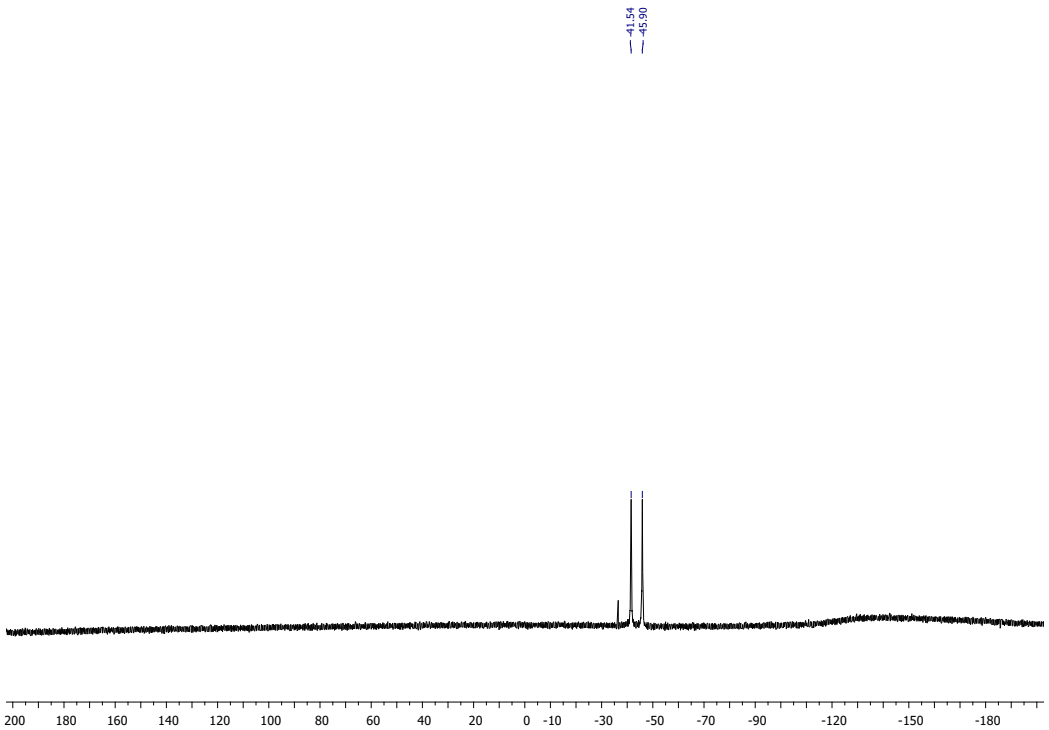

Figure S81: ^{19}F NMR spectrum of corrole **7c** (benzene-d_6, 298 K).

5,15-bis-trifluoromethyl-10-pentafluorophenyl-corrole 3

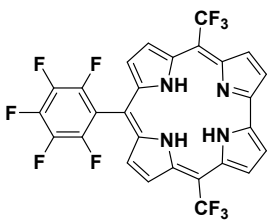

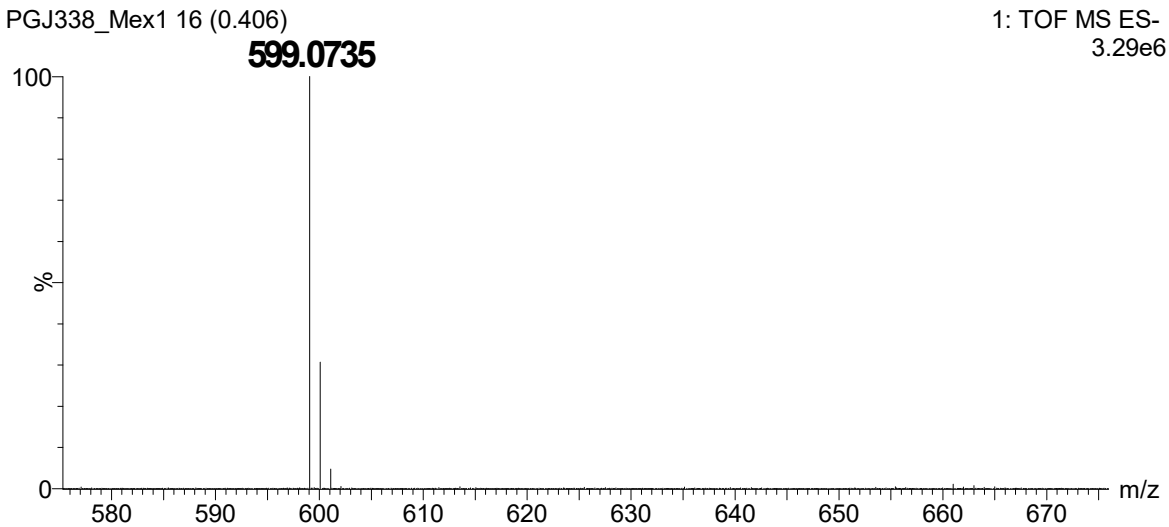

Figure S82: HRMS spectrum of corrole **3**.

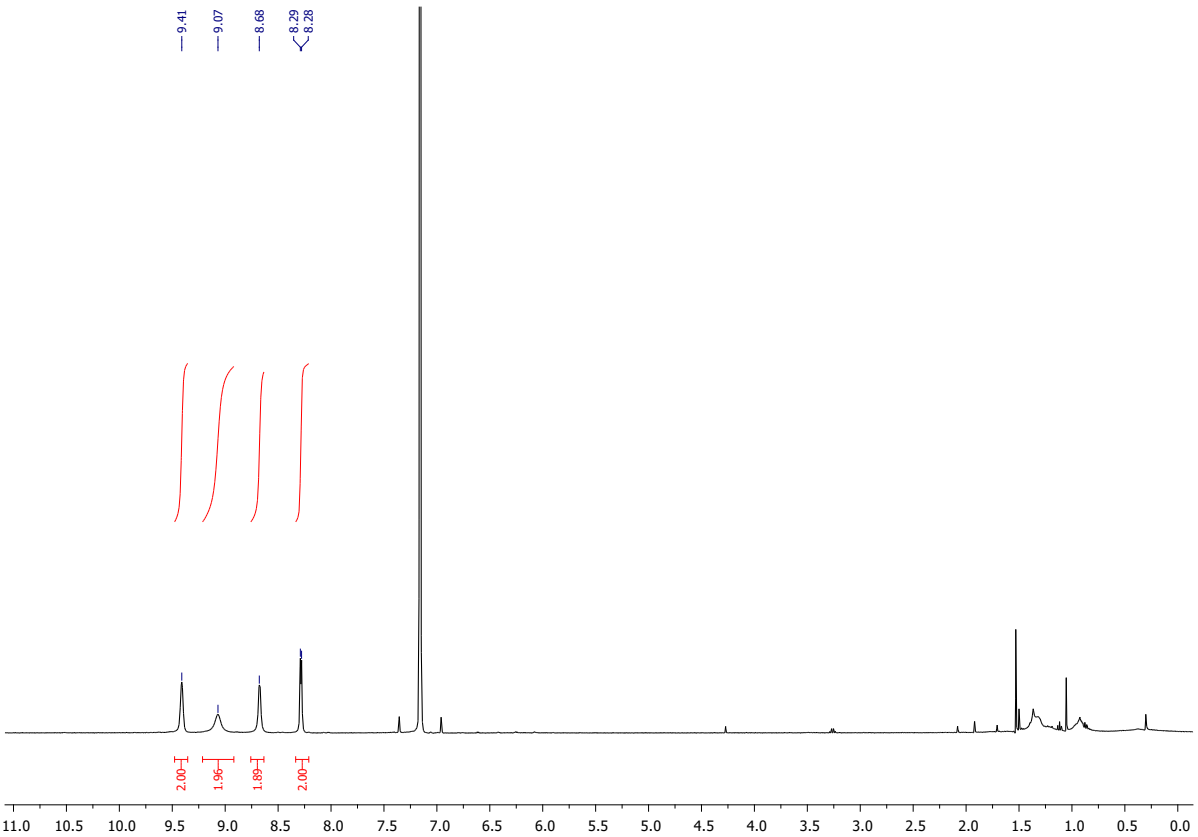

Figure S83: ^{1}H NMR spectrum of corrole **3** (benzene-d_6, 298 K).

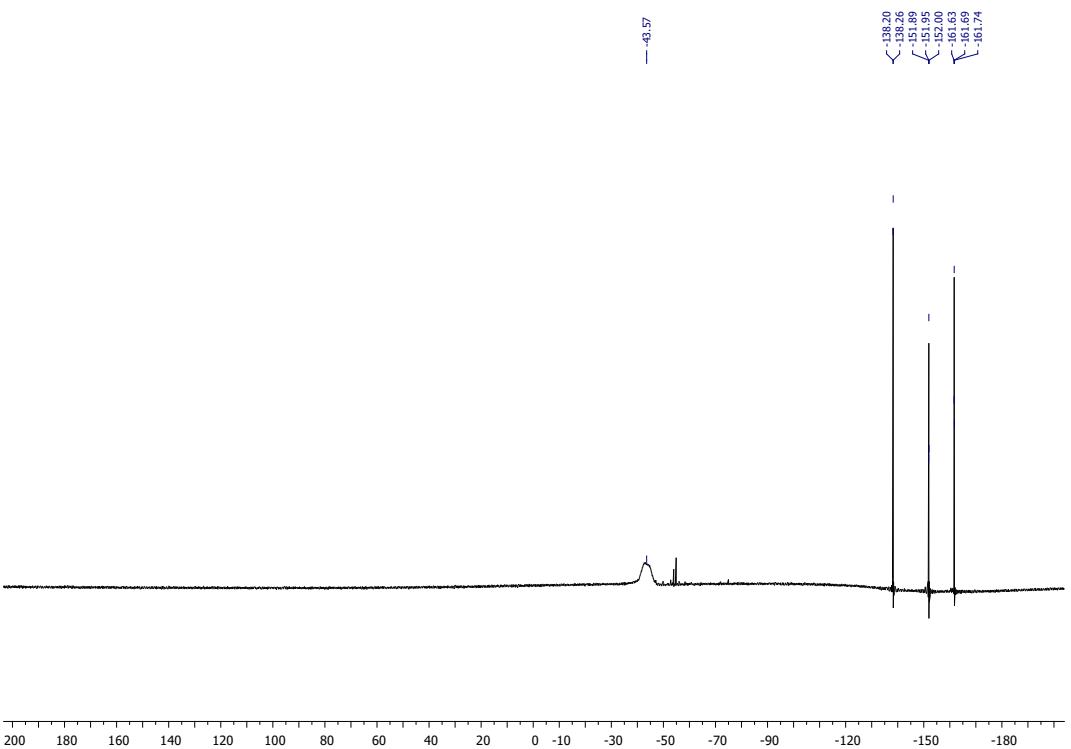

Figure S84: ^{19}F NMR spectrum of corrole **3** (benzene-d_6, 298 K).

5,15-perfluoropropyl-10-(4-cyanophenyl)-corrole 7d

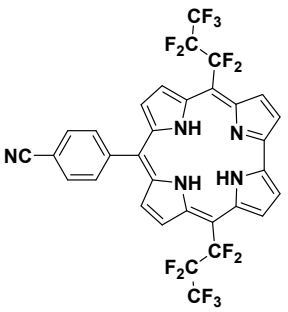

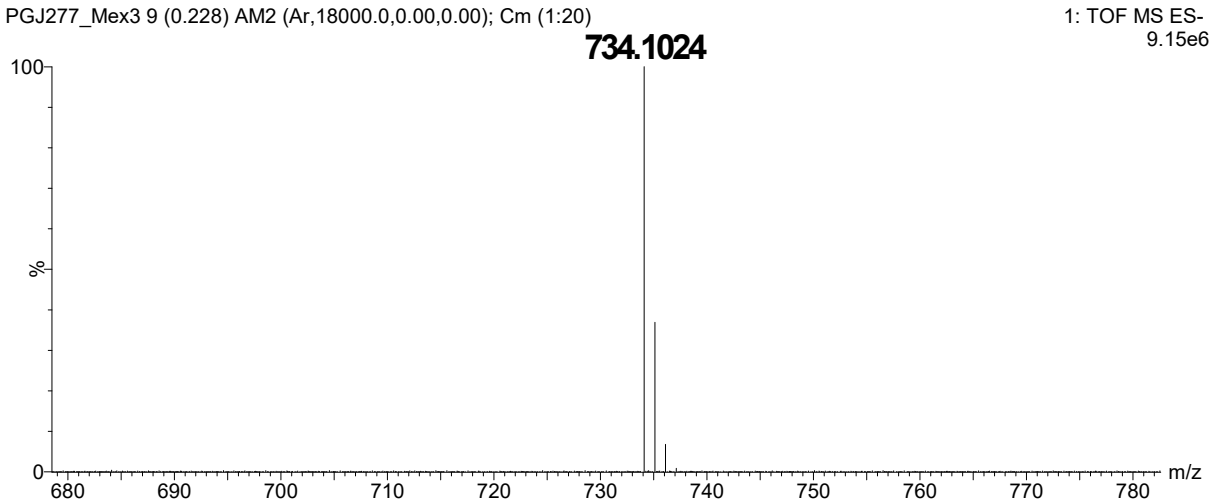

Figure S85: HRMS spectrum of corrole **7d**.

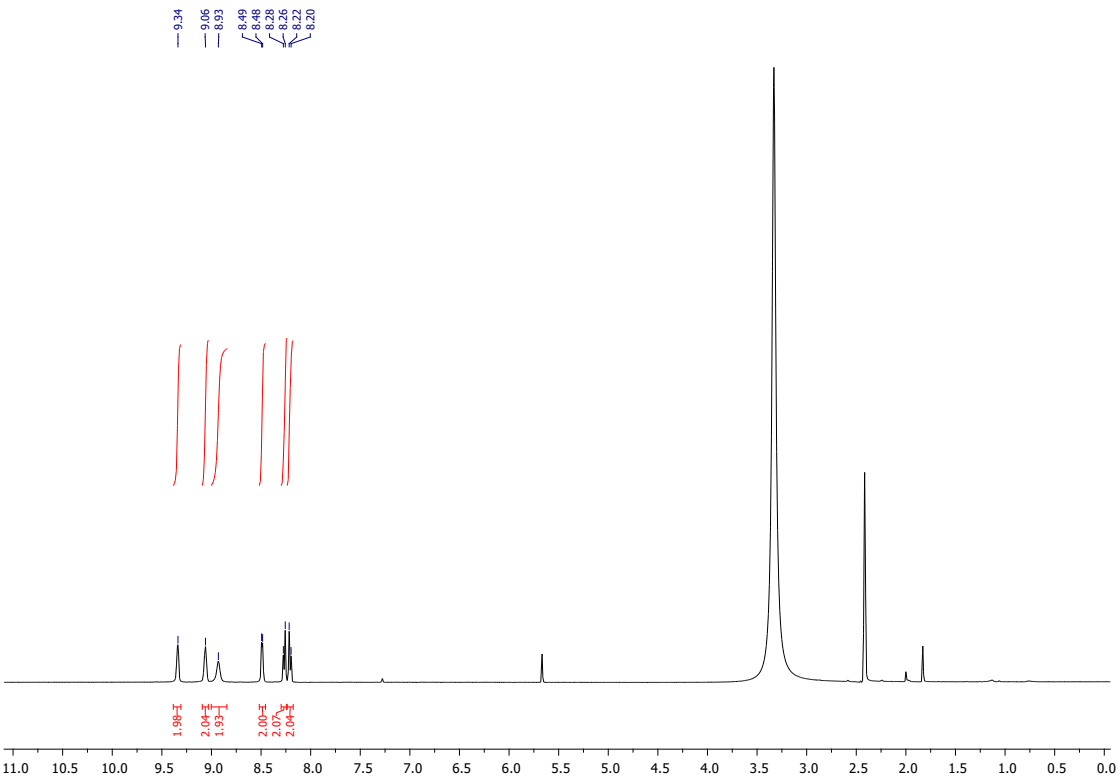

Figure S86: ^{1}H NMR spectrum of corrole **7d** (DMSO-d_6, 298 K).

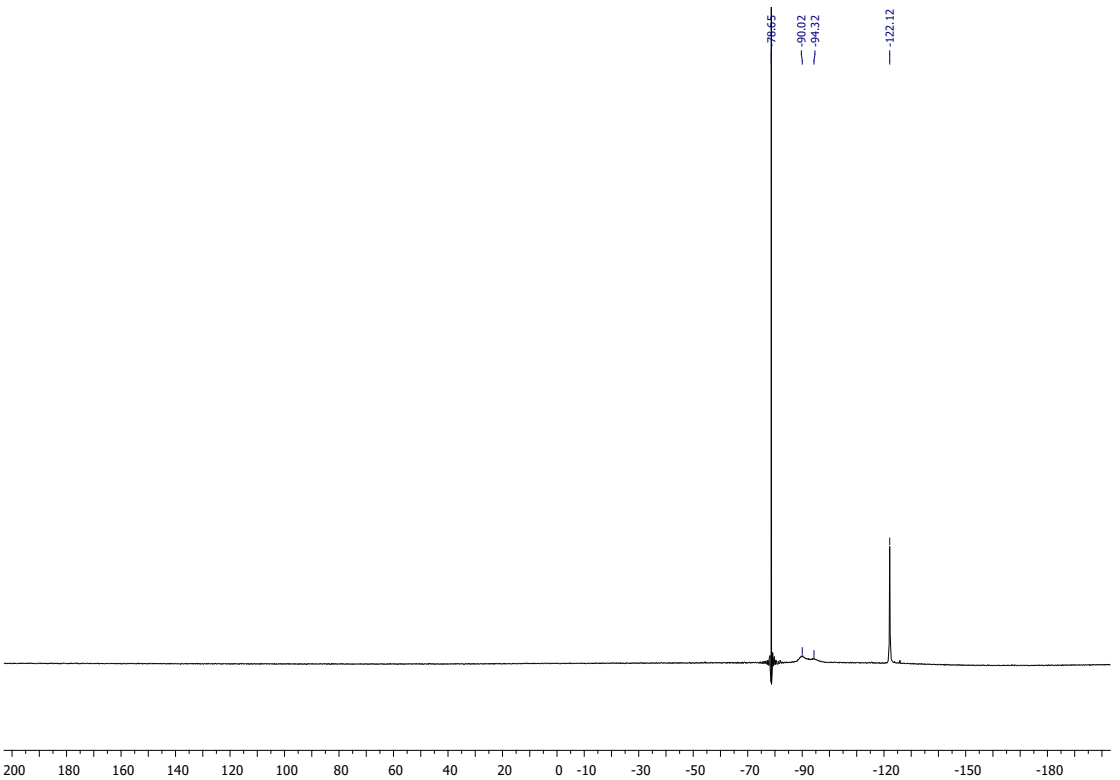

Figure S87: ^{19}F NMR spectrum of corrole **7d** (DMSO-d_6, 298 K).

5,15-perfluoropropyl-10-(*p*-tolyl)-corrole 7e

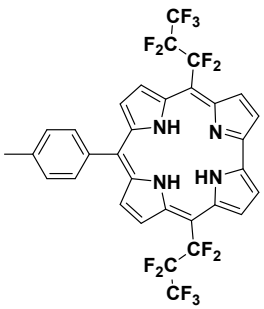

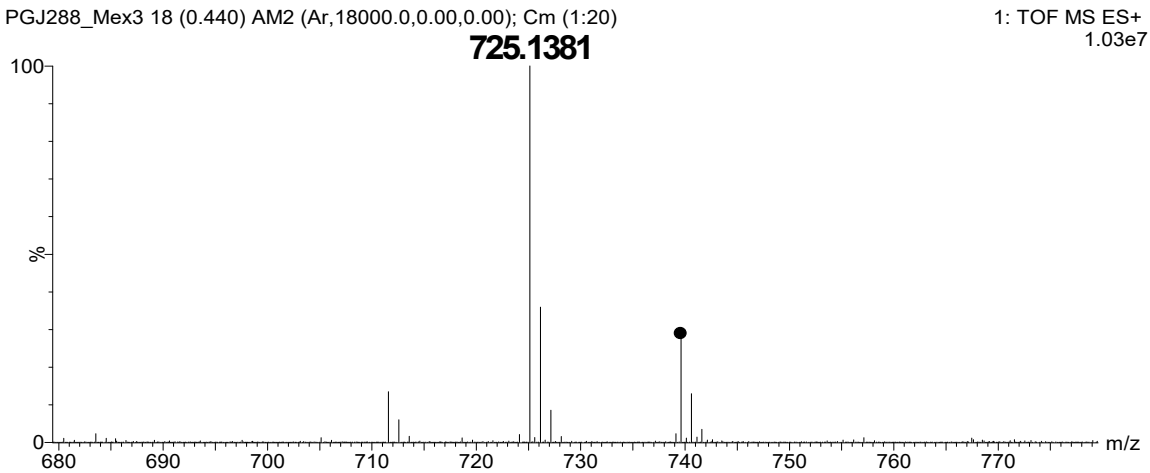

Figure S88: HRMS spectrum of corrole **7e**.

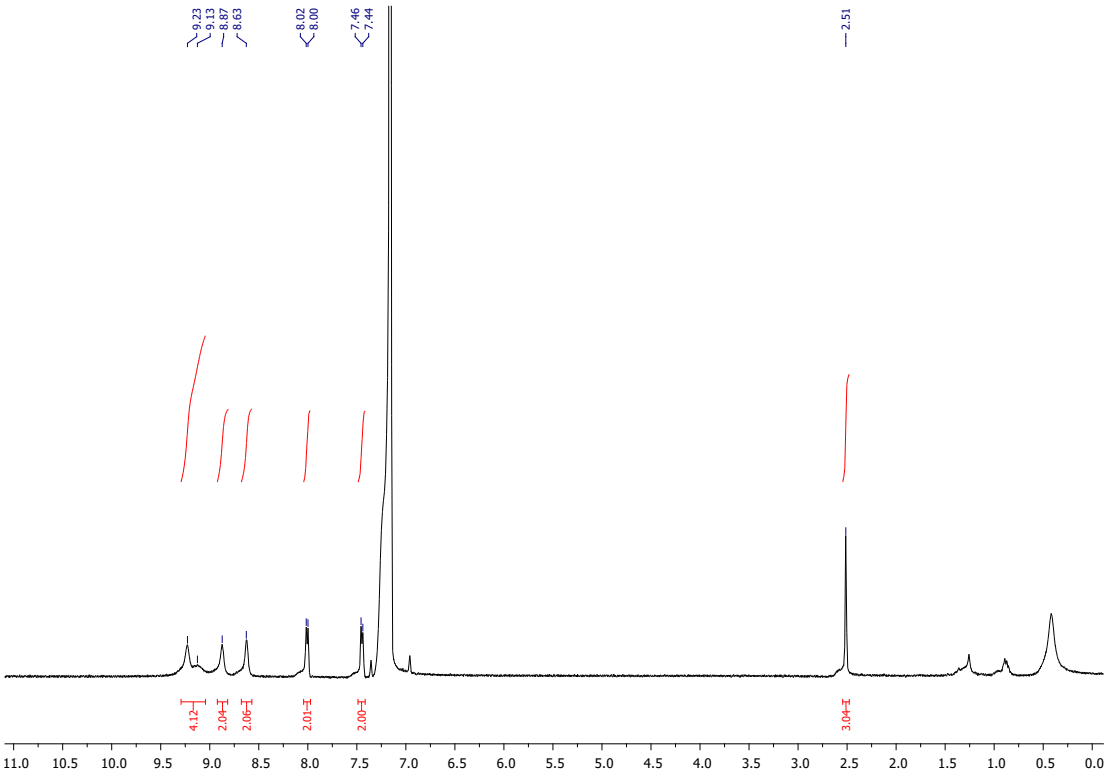

Figure S89: ^{1}H NMR spectrum of corrole **7e** (benzene-d_6, 333 K).

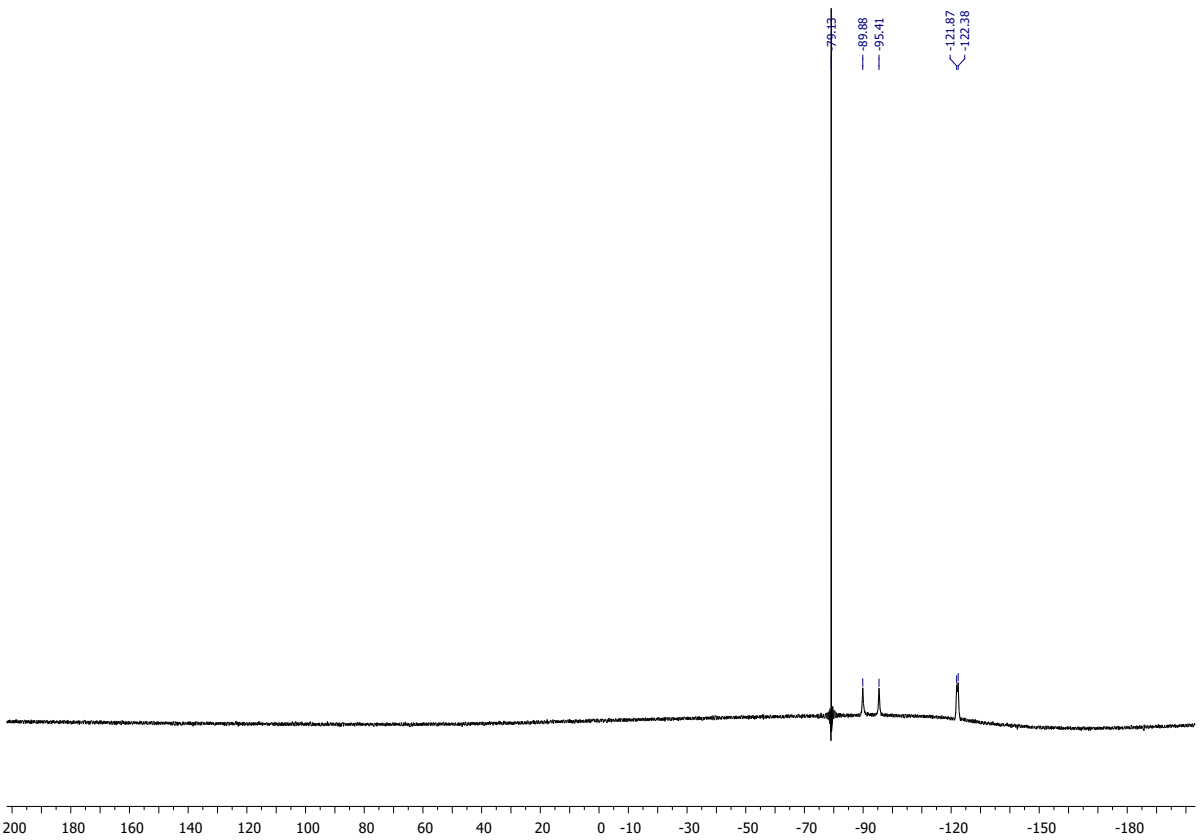

Figure S90: ^{19}F NMR spectrum of corrole **7e** (benzene-d_6, 298 K).

5,15-perfluoropropyl-10-(*p*-anisyl)-corrole 7f

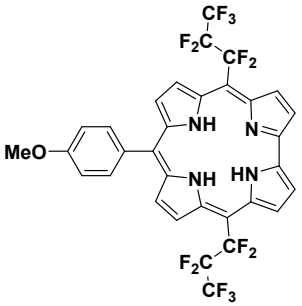

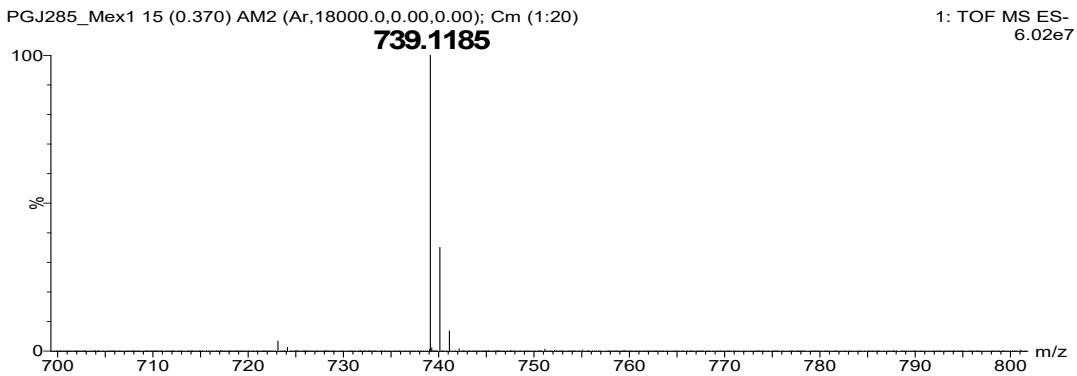

Figure S91: HRMS spectrum of corrole **7f**.

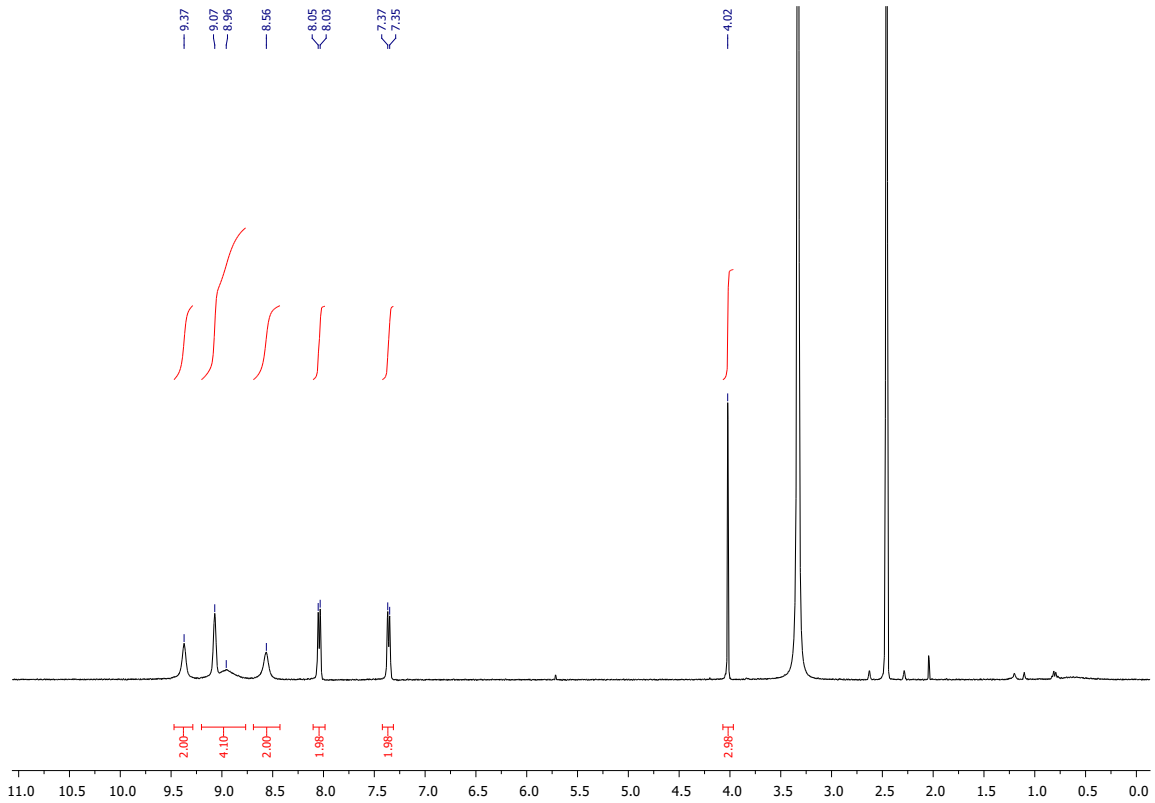

Figure S92: ^{1}H NMR spectrum of corrole **7f** (DMSO-d_6, 298 K).

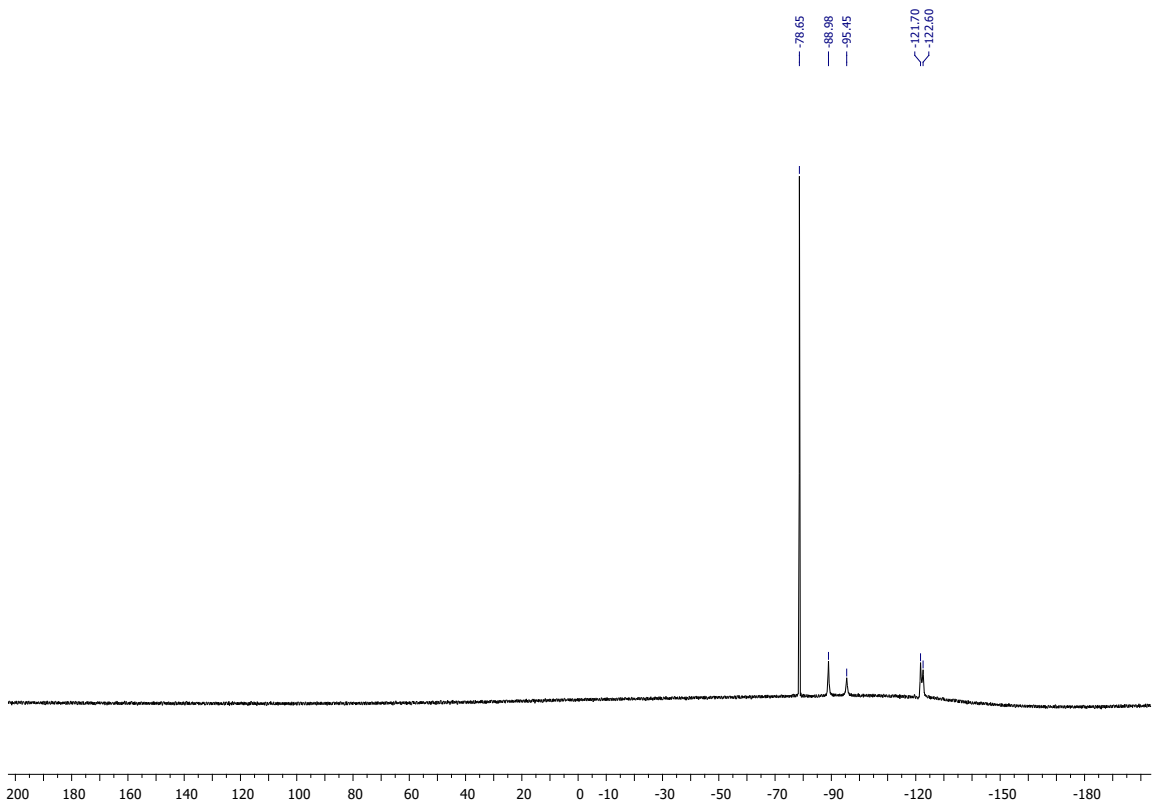

Figure S93: ^{19}F NMR spectrum of corrole **7f** (DMSO-d_6, 298 K).

5,15-perfluoroheptyl-10-(4-cyanophenyl)-corrole 7g

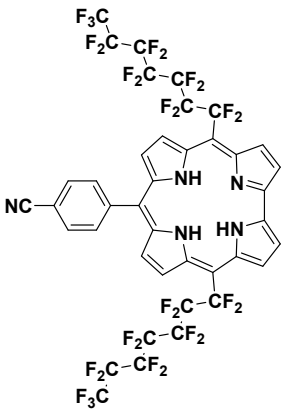

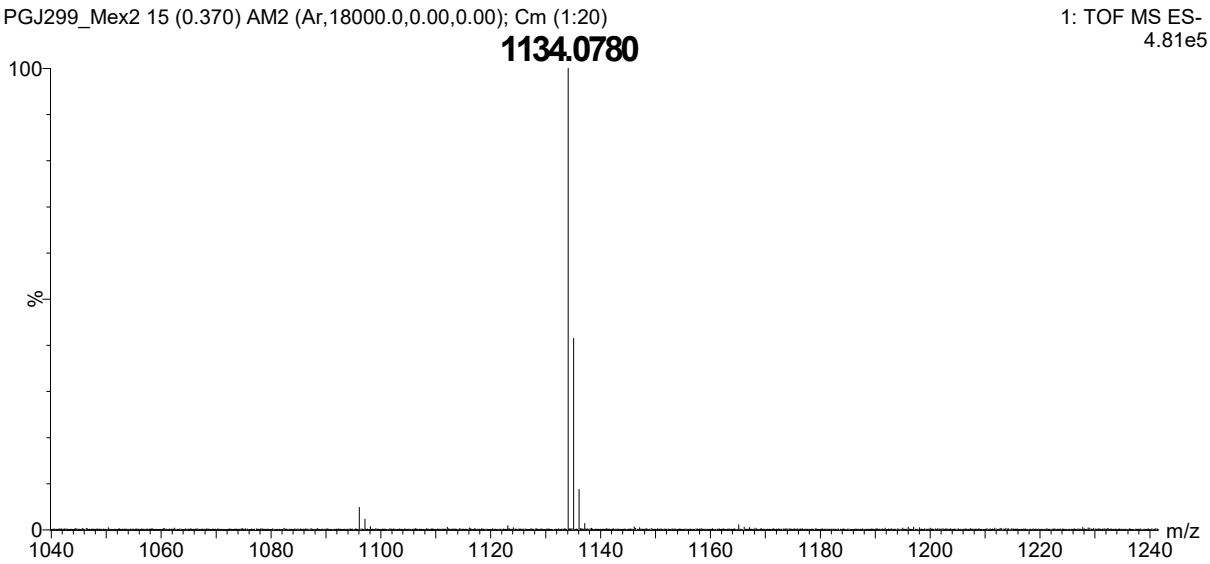

Figure S94: HRMS spectrum of corrole **7g**.

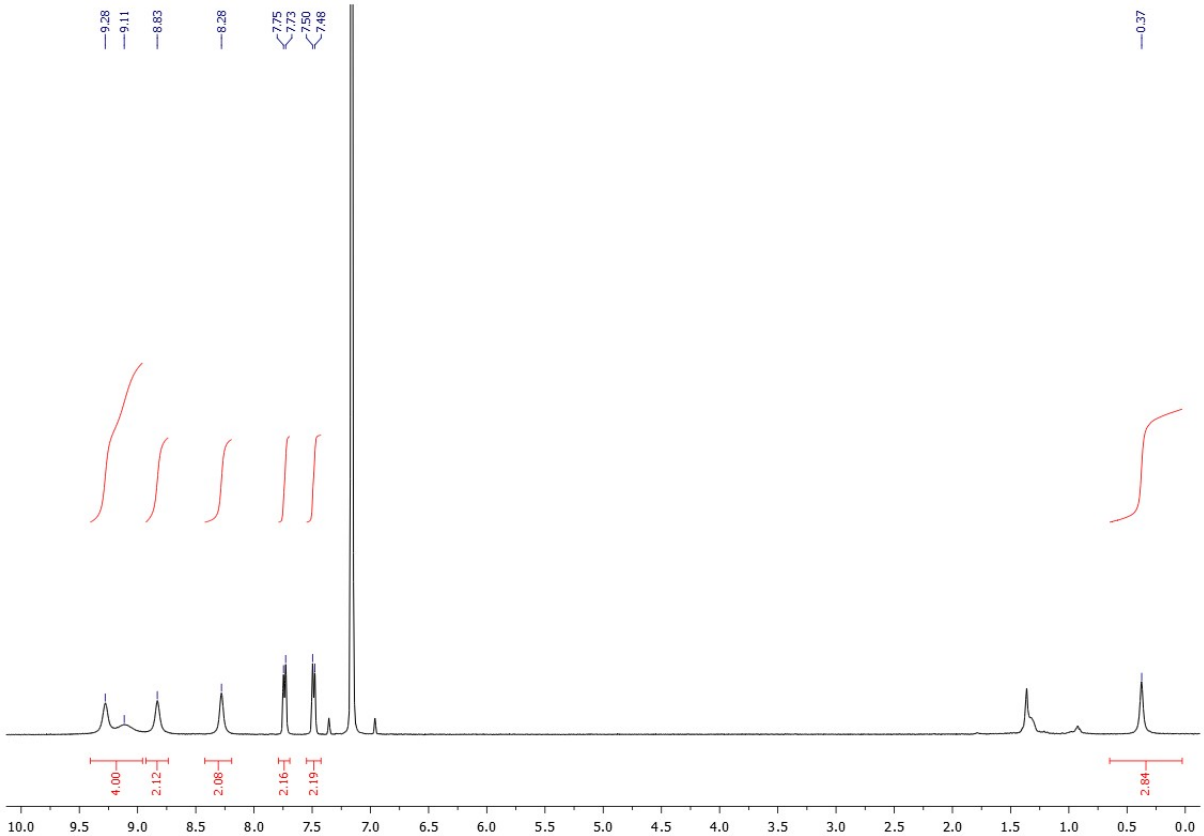

Figure S95: ^{1}H NMR spectrum of corrole **7g** (benzene-d_6, 298 K).

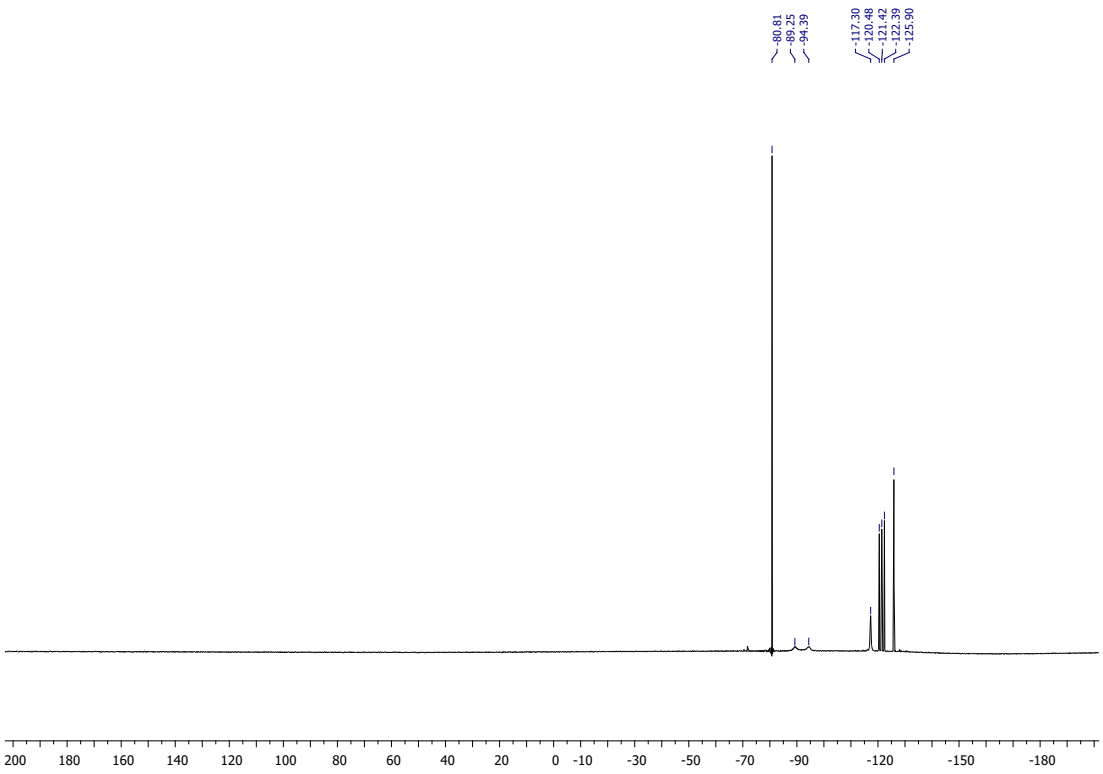

Figure S96: ^{19}F NMR spectrum of corrole **7g** (benzene-d_6, 298 K).

5,15-perfluoroheptyl-10-(*p*-tolyl)-corrole 7h

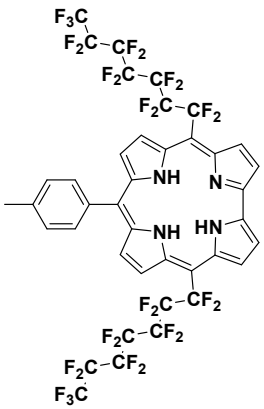

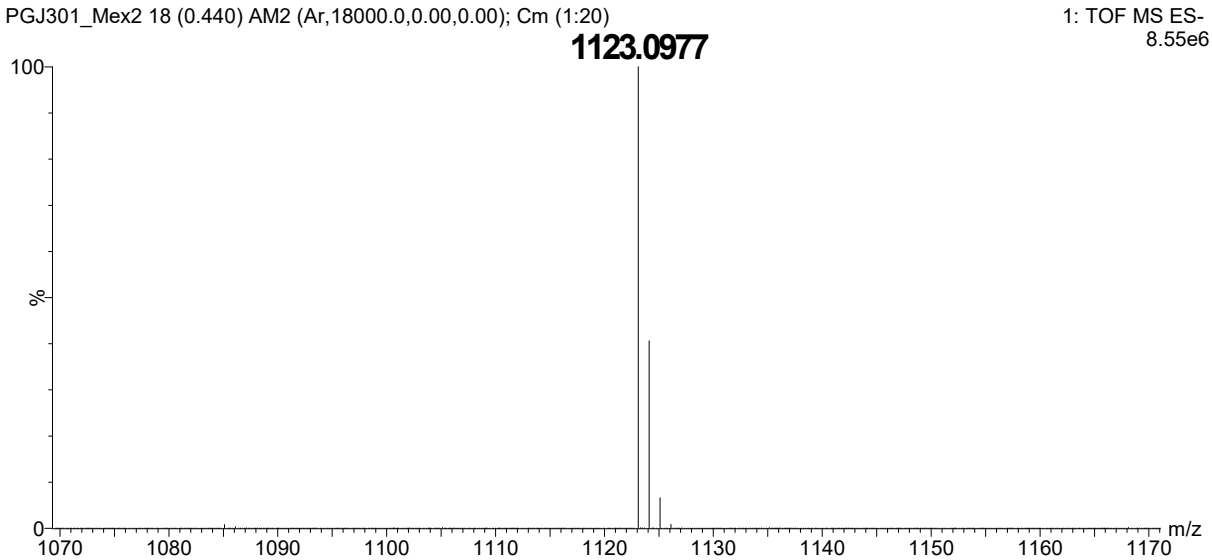

Figure S97: HRMS spectrum of corrole **7h**.

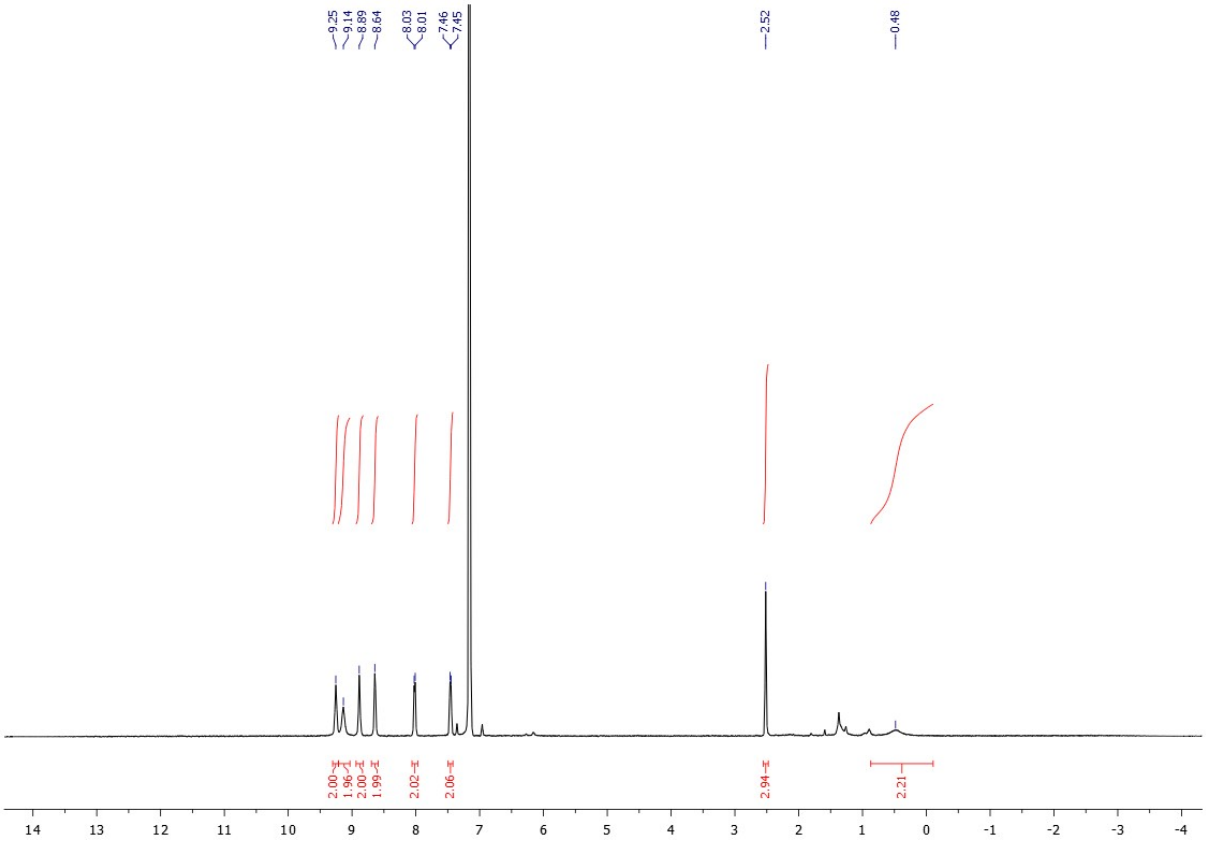

Figure S98: ^{1}H NMR spectrum of corrole **7h** (benzene-d_6, 333 K).

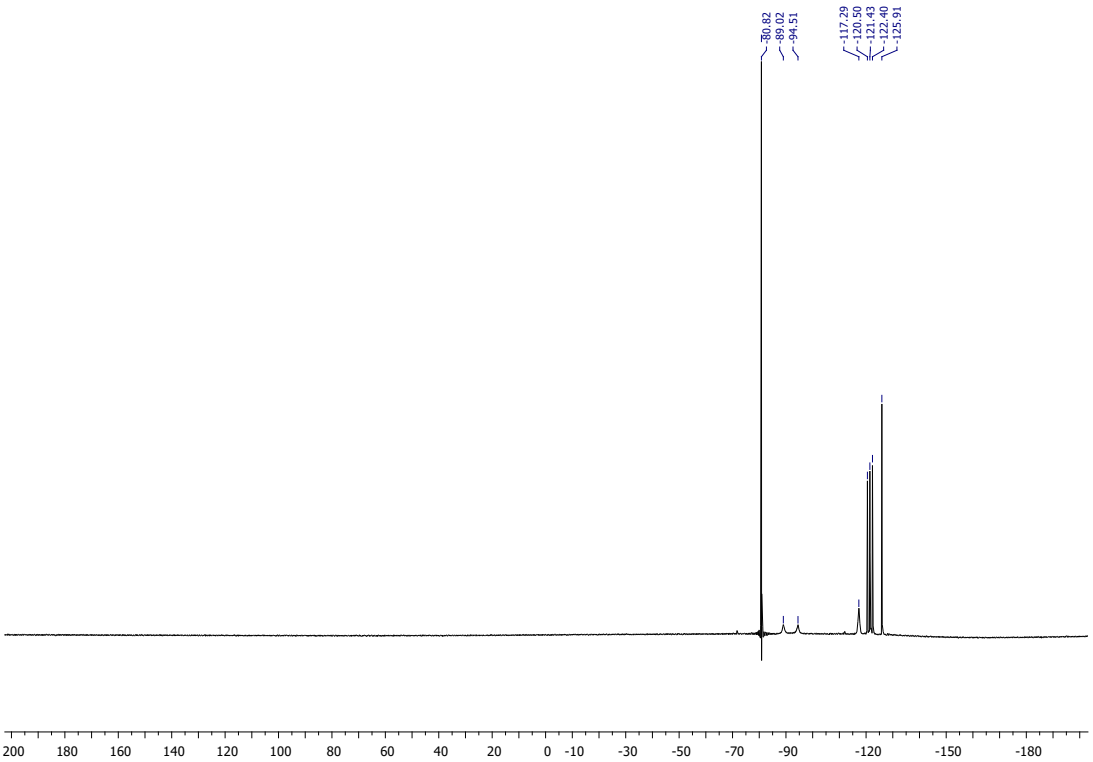

Figure S99: ^{19}F NMR spectrum of corrole **7h** (benzene-d_6, 298 K).

5,15-perfluoroheptyl-10-(*p*-anisyl)-corrole 7i

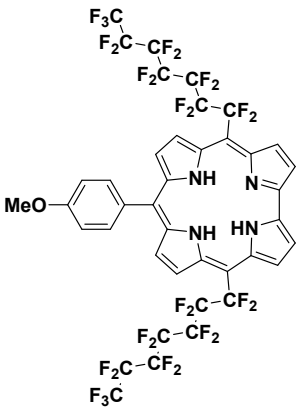

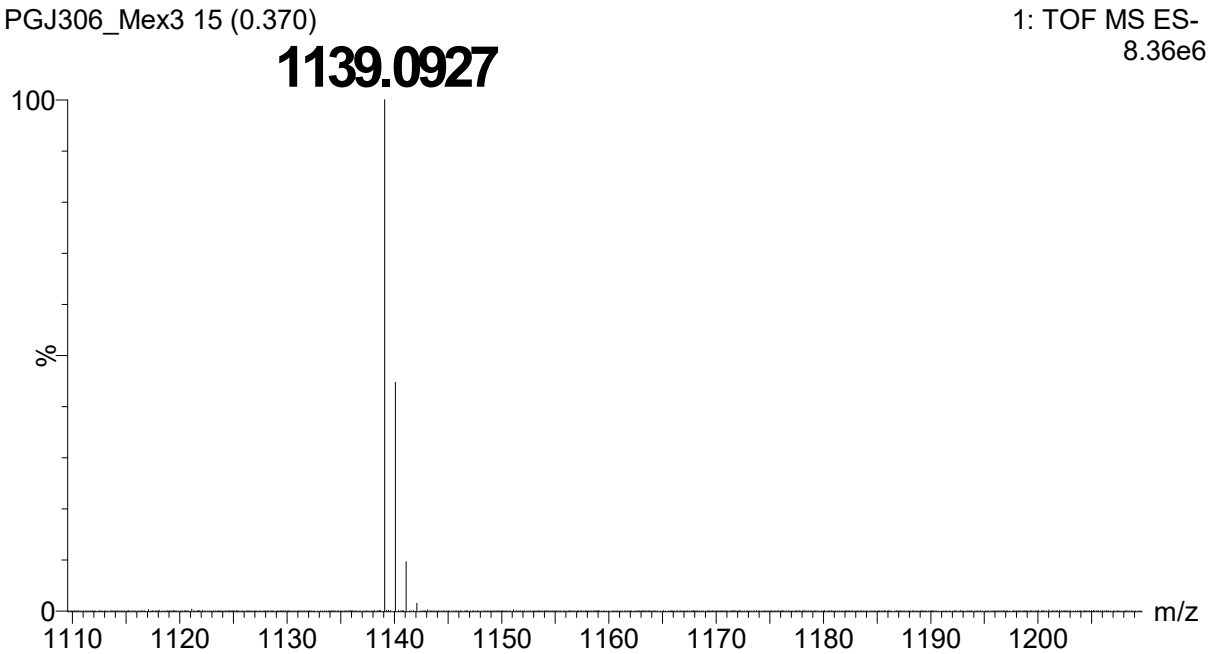

Figure S100: HRMS spectrum of corrole **7i**.

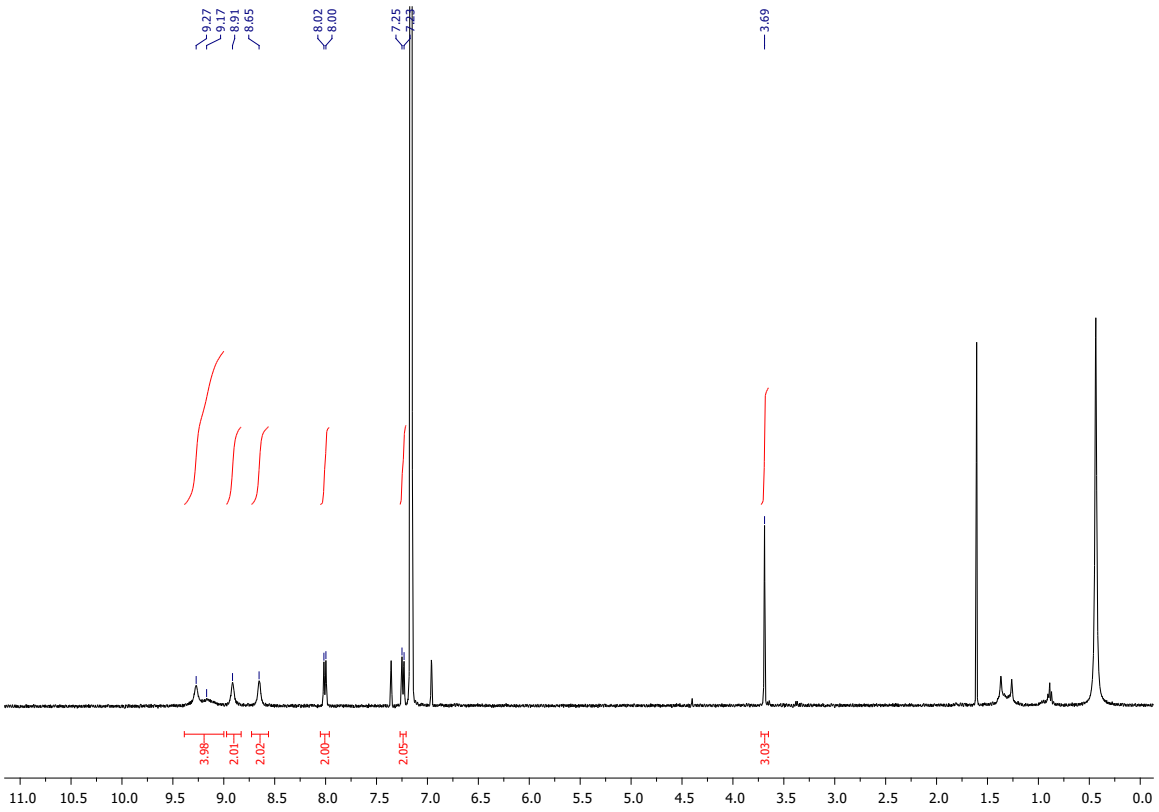

Figure S101: ^{1}H NMR spectrum of corrole **7i** (benzene-d_6, 333 K).

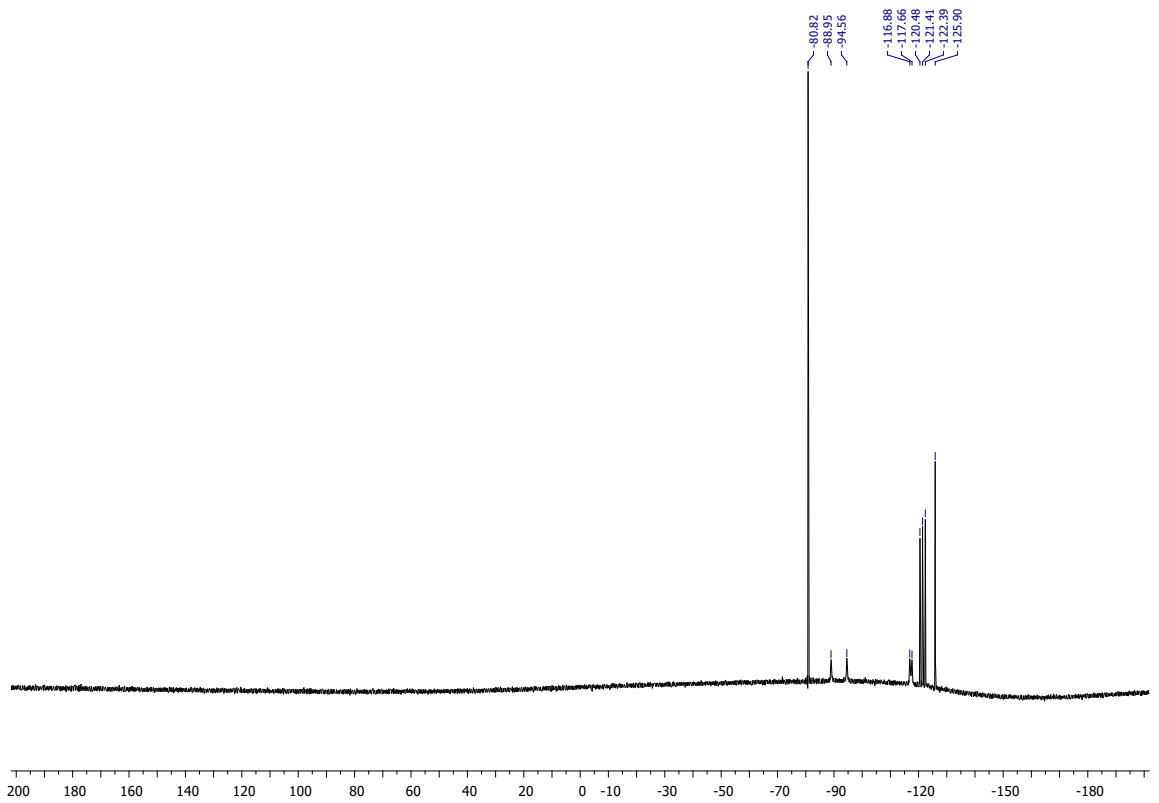

Figure S102: ^{19}F NMR spectrum of corrole **7i** (benzene-d_6, 298 K).

5-perfluoropropyl-10-(4-cyanophenyl)-15-perfluoropropionyl-corrole 8a

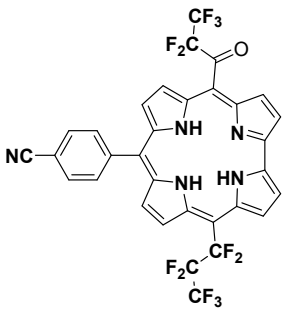

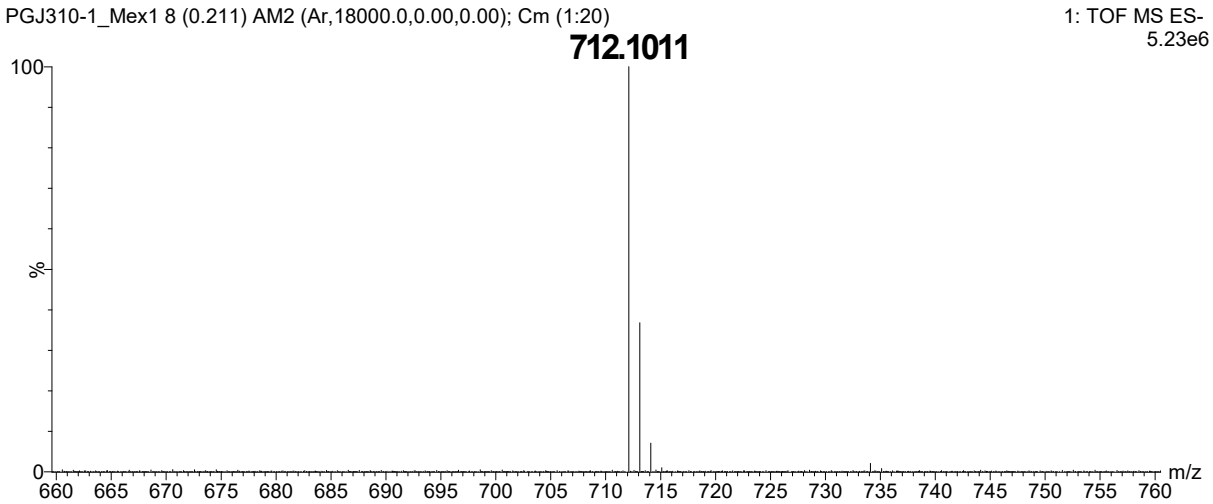

Figure S103: HRMS spectrum of corrole **8a**.

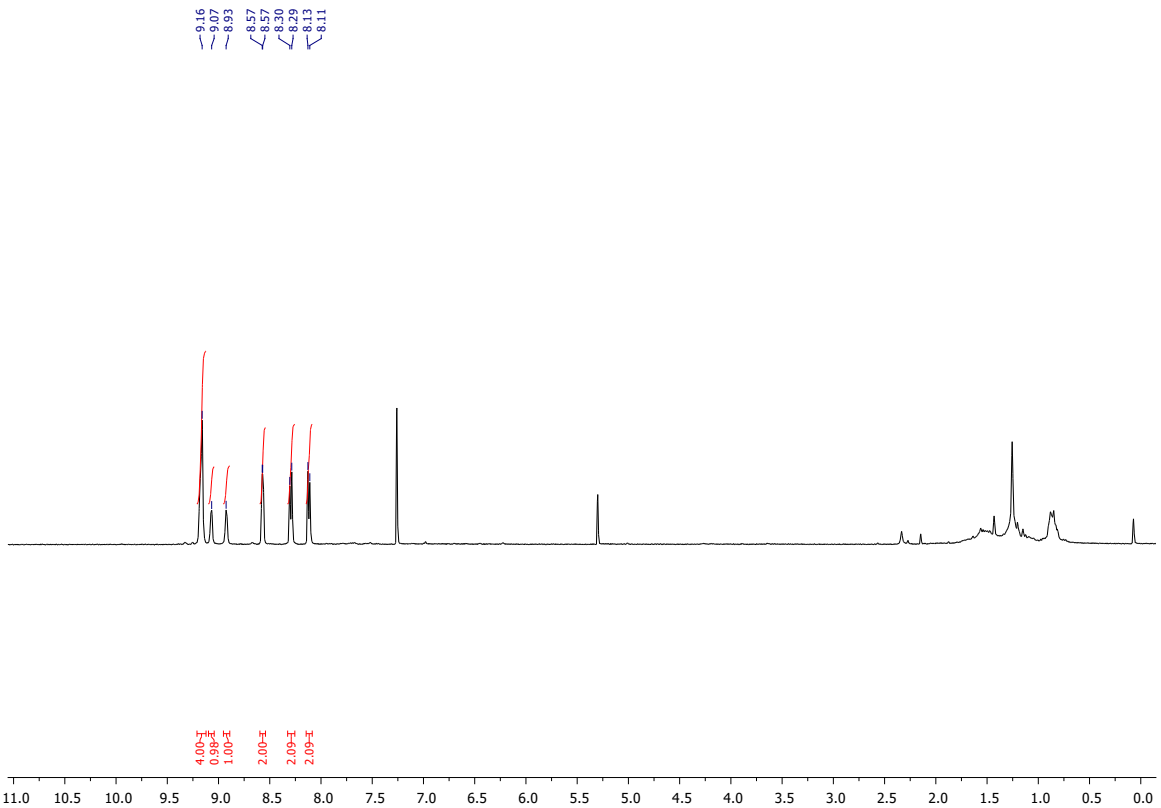

Figure S104: ^{1}H NMR spectrum of corrole **8a** ($CDCl_3$, 298 K).

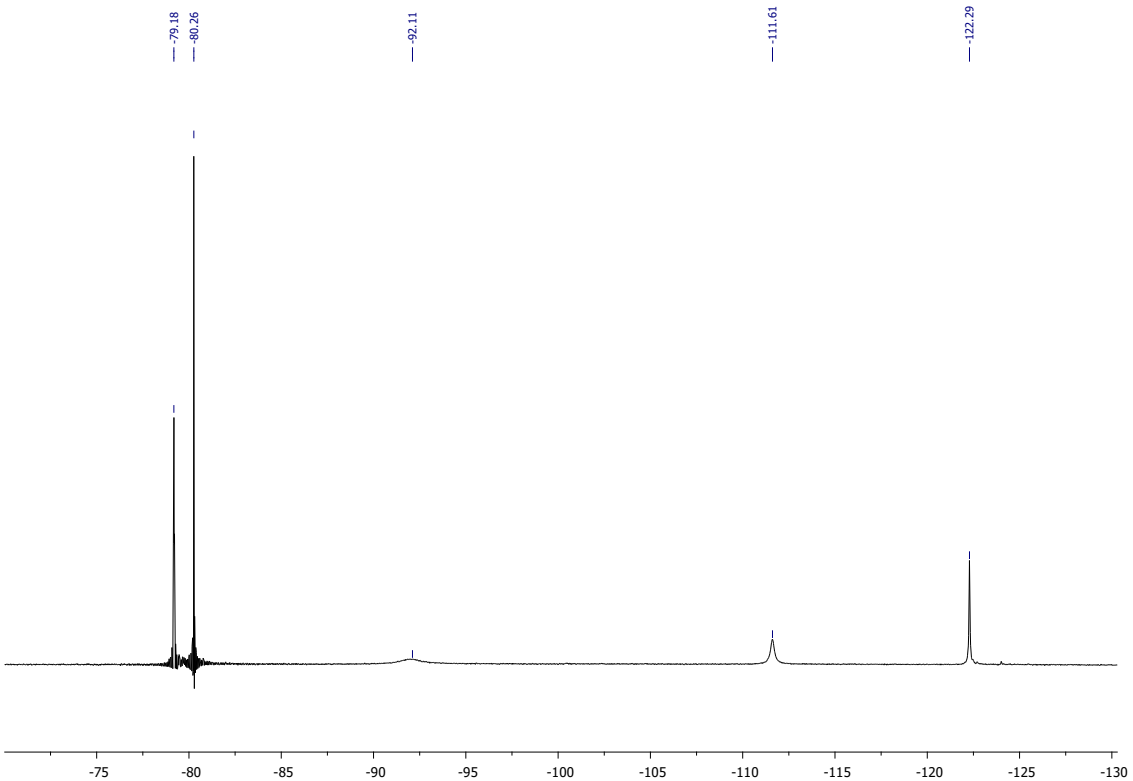

Figure S105: ^{19}F NMR spectrum of corrole **8a** ($CDCl_3$, 298 K).

5-perfluoroheptyl-10-(4-cyanophenyl)-15-perfluoroheptanoyl-corrole 8b

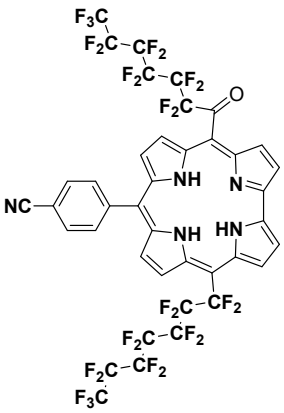

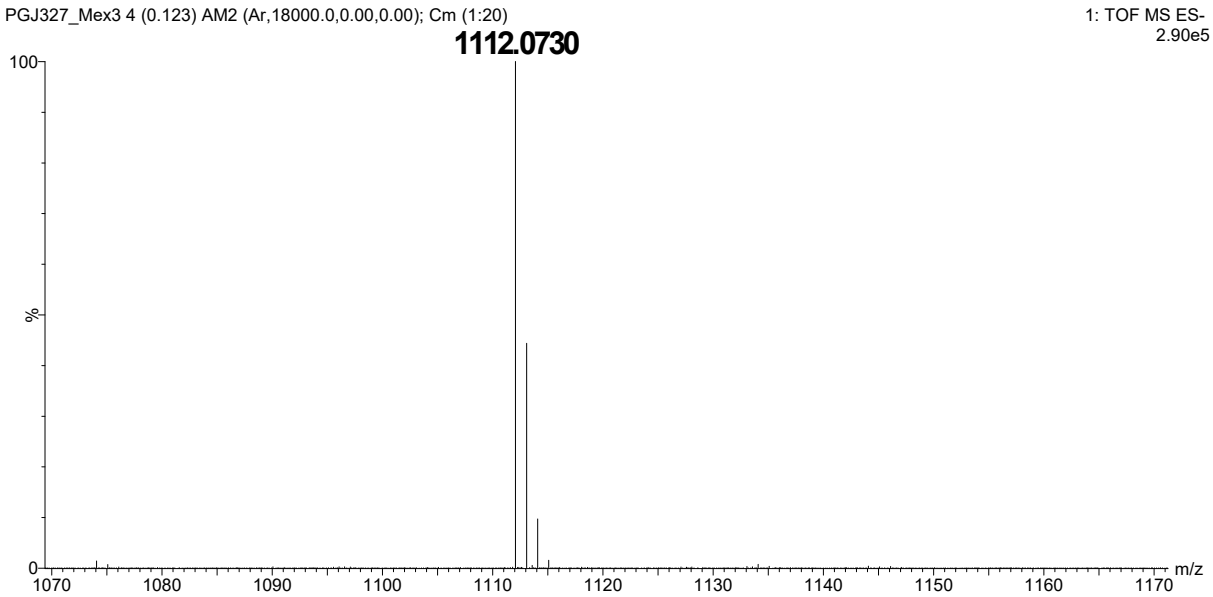

Figure S106: HRMS spectrum of corrole **8b**.

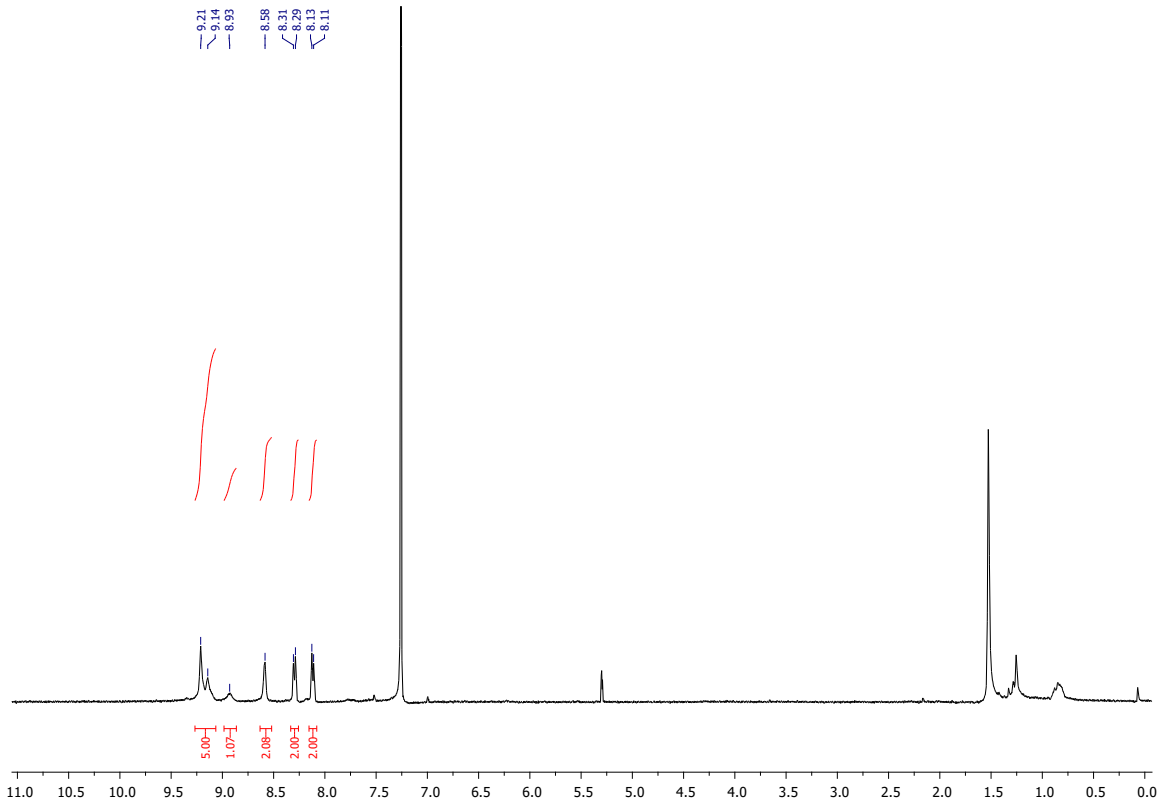

Figure S107: ^{1}H NMR spectrum of corrole **8b** ($CDCl_3$, 298 K).

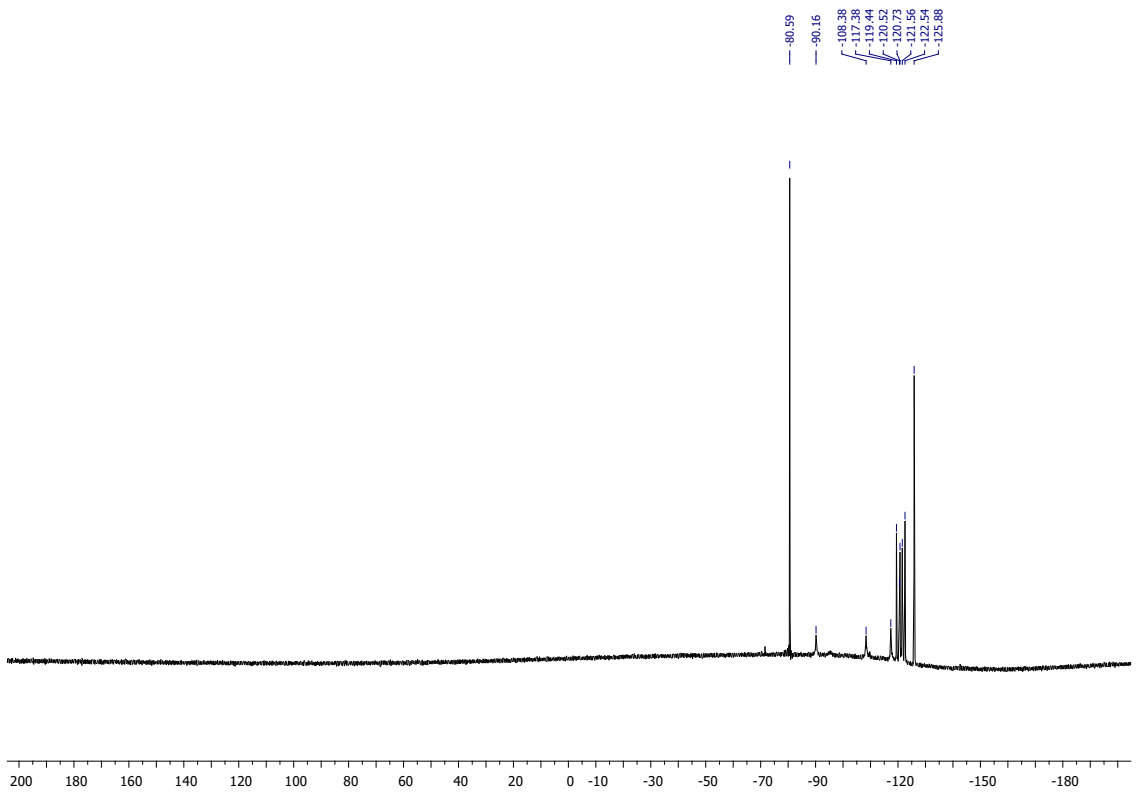

Figure S108: ^{19}F NMR spectrum of corrole **8b** ($CDCl_3$, 298 K).

5,15-carboxy-10-(4-carboxyphenyl)-corrole 9

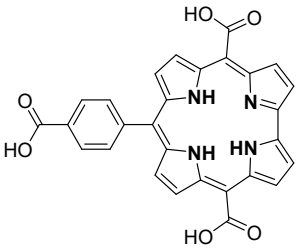

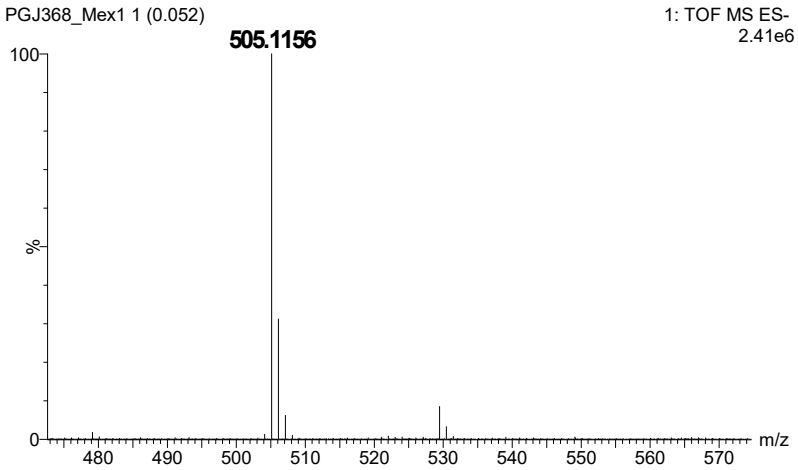

Figure S109: HRMS spectrum of corrole **9**.

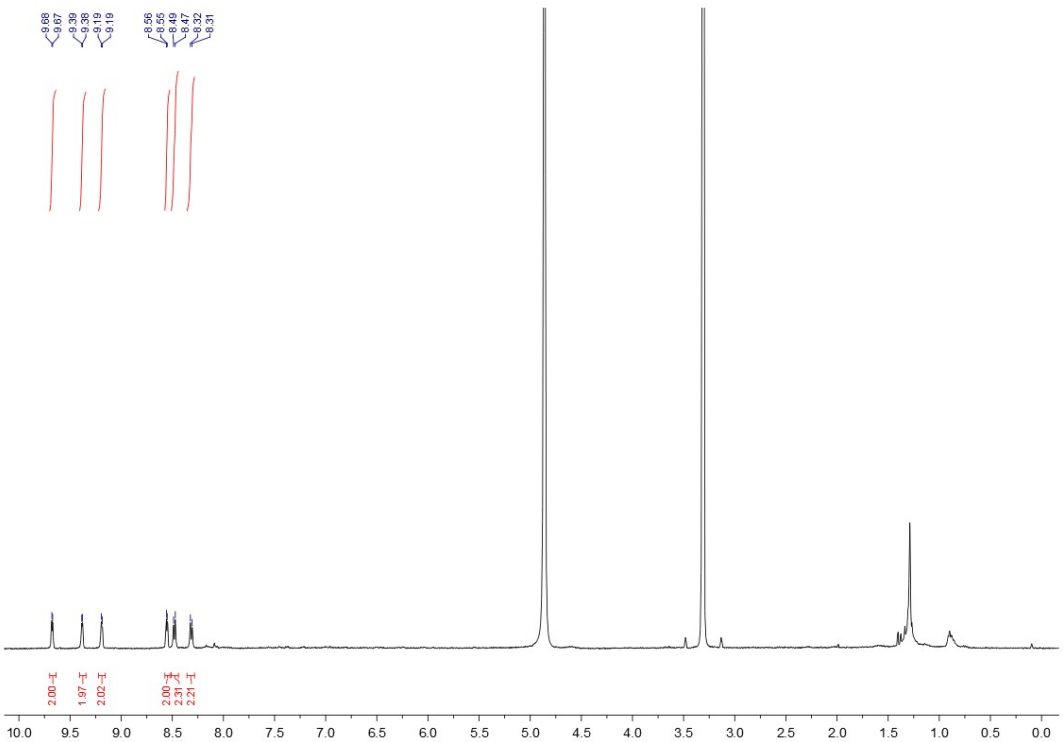

Figure S110: ^{1}H NMR spectrum of corrole **9** (methanol-d_4, 298 K).

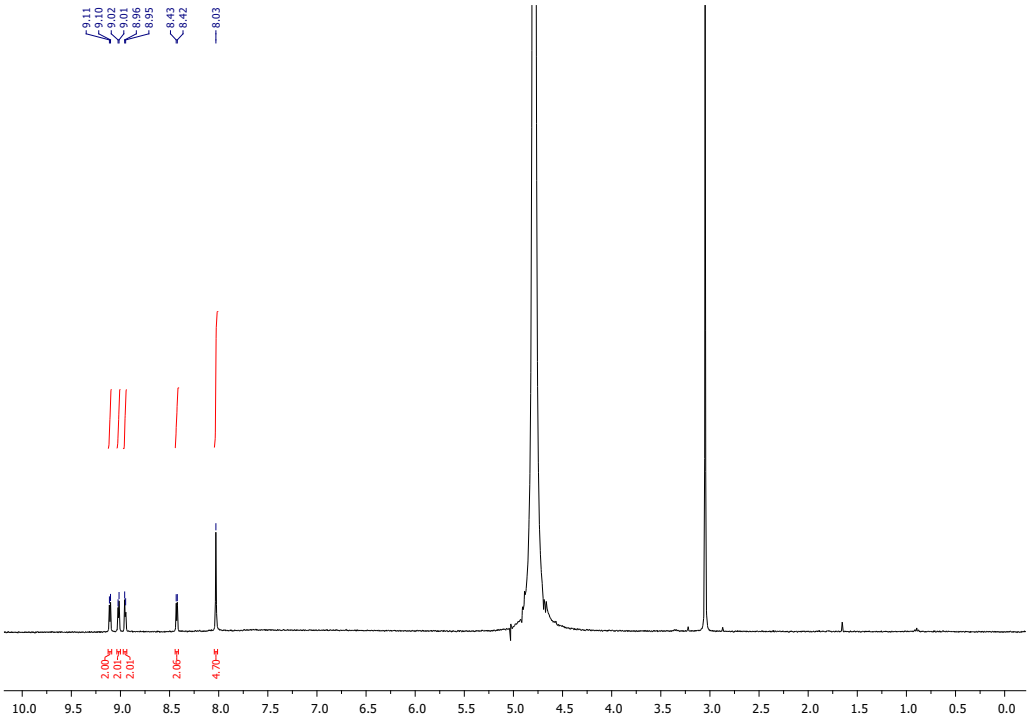

Figure S111: ^{1}H NMR spectrum of corrole **9** (D_2O + NaOD, 298 K).

Table S 5 : Crystal data and structure refinements of corroles **7a**, **7b**, **7c**, **7d** and **7i**.

Compound	**7a**	**7b**	**7c**	**7d**	**7i**
CCDC	2267225	2267226	2267223	2267227	2267224
Formula	$C_{28}H_{15}F_6N_5$	$C_{62}H_{42}F12N_8$	$C_{34}H_{24}F_6N_4O$	$C_{32.50}H_{16}ClF_{14}N_5$	$C_{40}H_{18}F_{30}N_4O$
M_w	535.45	1127.03	618.57	777.95	1140.58
Crystal system	triclinic	monoclinic	triclinic	triclinic	monoclinic
Temperature/ K	295	295	295	295	295
Space group	P -1	P 2/c	P -1	P -1	P 2_1/c
a/ Å	8.68015(18)	23.5597(4)	10.9445(10)	9.21263(19)	18.1959(7)
b/ Å	11.4089(3)	11.5589(2)	11.6383(9)	12.5354(2)	9.9152(4)
c/ Å	12.5860(3)	19.1588(3)	12.2119(9)	15.5289(3)	23.9000(9)
α/ °	80.6513(19)		102.813(7)	111.2842(18)	
β/ °	70.8233(19)	93.2727(13)	106.382(7)	103.5014(18)	101.141(4)
γ/ °	81.5848(18)		97.930(7)	95.1944(16)	
V/ Å^3	1155.82(5)	5208.88(14)	1421.4(2)	1594.14(6)	4230.7(3)
Z	2	4	2	2	4
Dc/g.cm^{-3}	1.539	1.437	1.445	1.621	1.791
Crystal colour	red	violet	violet	violet	red
Crystal size/mm^3	0.08*0.12*0.2	0.08*0.2*0.22	0.08*0.08*0.14	0.03*0.14*0.28	0.02*0.08*0.2
μ(Mo-Kα)/mm^{-1}	1.104	0.82355	0.8337	2.134	0.7686
N° of refl. measured	21228	48813	10539	28537	31602
N° of unique refl.	4510	9928	5291	6238	8688
N° of obs. refl.[$F^2 > 4\sigma F^2$]	4165	8305	3300	5676	4972
N° parameters refined	380	729	395	488	752
R_1 [$F^2>4\sigma F^2$]	0.0465	0.0765	0.0967	0.0728	0.0921
wR_1 [$F^2>4\sigma F^2$]	0.1286	0.2300	0.2826	0.2244	0.2365
R_2 [all refl.]	0.0491	0.0861	0.1320	0.0765	0.1331
wR_2 [all refl.]	0.1314	0.2463	0.3258	0.2292	0.2692
Goodness of fit [all refl.]	1.053	1.083	1.034	1.085	1.129
Residual Fourier/e. Å^{-3}	-0.434; 0.455	-0.419; 0.471	-0.404; 0.358	-0.764; 0.902	-0.526; 0.599

References

1 M. J. Frisch, G. W. Trucks, H. B. Schlegel, G. E. Scuseria, M. A. Robb, J. R. Cheeseman, G. Scalmani, V. Barone, G. A. Petersson, H. Nakatsuji, X. Li, M. Caricato, A. V. Marenich, J. Bloino, B. G. Janesko, R. Gomperts, B. Mennucci, H. P. Hratchian, J. V. Ortiz, A. F. Izmaylov, J. L. Sonnenberg, Williams, F. Ding, F. Lipparini, F. Egidi, J. Goings, B. Peng, A. Petrone, T. Henderson, D. Ranasinghe, V. G. Zakrzewski, J. Gao, N. Rega, G. Zheng, W. Liang, M. Hada, M. Ehara, K. Toyota, R. Fukuda, J. Hasegawa, M. Ishida, T. Nakajima, Y. Honda, O. Kitao, H. Nakai, T. Vreven, K. Throssell, J. A. Montgomery Jr., J. E. Peralta, F. Ogliaro, M. J. Bearpark, J. J. Heyd, E. N. Brothers, K. N. Kudin, V. N. Staroverov, T. A. Keith, R. Kobayashi, J. Normand, K. Raghavachari, A. P. Rendell, J. C. Burant, S. S. Iyengar, J. Tomasi, M. Cossi, J. M. Millam, M. Klene, C. Adamo, R. Cammi, J. W. Ochterski, R. L. Martin, K. Morokuma, O. Farkas, J. B. Foresman and D. J. Fox, Gaussian 16 2016.

2 M. Kruk, T. H. Ngo, P. Verstappen, A. Starukhin, J. Hofkens, W. Dehaen and W. Maes, *J. Phys. Chem. A*, 2012, **116**, 10695–10703.

3 T. Lu and F. Chen, *J. Comput. Chem.*, 2012, **33**, 580–592.

4 W. Dmowski, K. Piasecka-Maciejewska and Z. Urbanczyk-Lipkowska, *Synthesis*, 2003, 841–844.

5 W. Dmowski, K. Piasecka-Maciejewska and Z. Urbańczyk-Lipkowska, *Kem. U Ind.*, 2004, **53**, 339–341.

6 P.-G. Julliard, S. Pascal, O. Siri, D. Cortés-Arriagada, L. Sanhueza and G. Canard, *Comptes Rendus Chim.*, 2021, **24**, 27–45.

7 N. G. Connelly and W. E. Geiger, *Chem. Rev.*, 1996, **96**, 877–910.

8 A. M. Brouwer, *Pure Appl. Chem.*, 2011, **83**, 2213–2228.

9 O. V. Dolomanov, L. J. Bourhis, R. J. Gildea, J. A. K. Howard and H. Puschmann, *J. Appl. Crystallogr.*, 2009, **42**, 339–341.

10 G. Sheldrick, *Acta Crystallogr. Sect. A*, 2015, 71, 3–8.

11 G. M. Sheldrick, *Acta Crystallogr. Sect. C*, 2015, **C71**, 3–8.

12 R. Goldschmidt, I. Goldberg, Y. Balazs and Z. Gross, *J. Porphyrins Phthalocyanines*, 2006, **10**, 76–86.